Palaeobiodiversity and Palaeoenvironments (2022) 102:711–761
https://doi.org/10.1007/s12549-022-00537-z

SENCKENBERG

ORIGINAL ARTICLE

Refined conodont stratigraphy at Martenberg (Rhenish Massif, Germany) as base for a formal middle/upper Frasnian substage boundary

Felix Saupe[1] · Ralph Thomas Becker[1]

Received: 9 August 2021 / Revised: 15 February 2022 / Accepted: 3 May 2022 / Published online: 15 July 2022

Abstract

The famous Martenberg section of the eastern Rhenish Massif, Germany, type-section of classical Frasnian goniatite and conodont zonations, has been restudied in order to document the microfacies development and to refine the conodont stratigraphy around the global *semichatovae* Event/Transgression, the proposed level to define a future upper Frasnian substage. More than 8.000 platform elements were identified and include new taxa. *Palmatolepis jamieae* is subdivided into the subspecies *Pa. jamieae jamieae*, *Pa. jamieae savagei* n. ssp., *Pa. jamieae rosa* n. ssp., and *Pa. jamieae* ssp. δ. Another new species, *Pa. adorfensis* n. sp., was previously partly identified as *Pa. jamieae*, while *Pa. descendens* n. sp. has previously been described in open nomenclature from Inner Mongolia. Morphotypes are defined in *Icriodus symmetricus, Pa. ljaschenkoae*, and *Pa. proversa*. A global literature survey shows that the eustatic *semichatovae* Event can be recognised in more than 20 regions of all continents with (sub)tropical Upper Devonian outcrops. At Martenberg, the transgression is preceded by a thin but distinctive interval with unconformities, microbial mats, sheet cracks, and currents that brought in the regionally youngest volcaniclastics. The new conodont data confirm that no typical *Pa. jamieae* (sensu the holotype) occur in the two beds originally supposed to represent the *jamieae* Zone in its reference section. We fully support the conclusion of Ovnatanova and Kononova (2020) that the *jamieae* Zone should be abandoned. Early *Pa. jamieae* subspecies and the related new taxa enter at Martenberg and in a few other regions in the globally easily recognisable Frasnian Zone 10 (= *plana* Zone). Frasnian Zone 11 (*feisti* Zone) is subdivided into subzones FZ 11a (= *feisti* Subzone) and FZ 11b (= *nasuta* Subzone). The base of the latter coincides with the *semichatovae* Transgression, the *semichatovae* Subzone of more shallow shelf settings, and is proposed to define in future the upper Frasnian substage base. On a global scale, the Martenberg section is currently the best bed-by-bed documented section for facies changes, conodont and goniatite biostratigraphy at the middle/upper Frasnian transition. Therefore, it is a prime candidate for a future GSSP selection. A global literature survey identified more than 20 other pelagic conodont successions that have the potential for precise correlation and a better understanding of the environmental changes associated with the *semichatovae* Event.

Keywords Conodonts · Stratigraphy · Microfacies · Middle/upper Frasnian boundary · *Semichatovae* Event · Rhenish Massif

This article is a contribution to the special issue "The Rhenish Massif: More than 150 years of research in a Variscan mountain chain"

This article is registered in Zoobank under urn:lsid:zoobank.org:pub:BFBBF71D-8DFA-4A28-BE40-17AA62F0BCDD

✉ Felix Saupe
felix.saupe@uni-muenster.de

Ralph Thomas Becker
rbecker@uni-muenster.de

[1] Institut für Geologie und Paläontologie, Westfälische Wilhelms-Universität Münster, 48149 Münster, Germany

Introduction

The chronostratigraphic subdivision of the Devonian into series and stages was accomplished more than 20 years ago, although, some revisions are under way (see recent review by Becker et al. 2020a). For most of the stages, substage definitions have been proposed, but none of these have been ratified by the International Commission on Stratigraphy (ICS). Therefore, substages are widely used but are still informal. In the Frasnian, Ziegler and Sandberg (1997) proposed to use the eustatic *semichatovae* Transgression to define the base of a future upper Frasnian substage. It defines the originally poorly constrained base of global Depophase IId sensu Johnson et al. (1985; see

discussions by Becker and House 1998 and Sandberg and Ziegler 1998) and enabled a sudden spread of the name-giving *Palmatolepis semichatovae*, for example in shallow carbonate platforms. Since the *semichatovae* Transgression has been placed within the lower part of the "Early *rhenana* Zone" sensu Ziegler and Sandberg (1990) and within the MN Zone 11 of Klapper (1989), a subzone definition for a future formal substage is essential. Morrow and Sandberg (2008, p. 455) introduced a *semichatovae* Subzone, but it has hardly been used subsequently because its index species is very rare in pelagic facies. In this context, a refined correlation of the *semichatovae* Transgression into deeper-water successions of the *jamieae*-"Early *rhenana*" zones or in relation to the Frasnian (= Montagne Noire, MN) zones 10/11 is required. This has to be based on continuously (bed-by-bed) sampled sections, which, remarkably, has rarely been achieved on a global scale. It is logical to start this essential precondition for a future formal substage definition in the reference section of the *jamieae* and "Early *rhenana*" zones (from here on cited as Lower *rhenana* Zone), which is the Martenberg section of Germany.

The Martenberg section (Fig. 1) is an often studied, small outcrop in the eastern Rhenish Massif, from where Frasnian fossils (the goniatite *Trimanticoceras retrorsum*, crinoid fragments, and bivalves) were first described more than 180 years ago (von Buch 1832). For conodont workers, the section became well-known through Ziegler's (1962) "Standard Upper Devonian Conodont Zonation", the later conodont-goniatite correlation (House and Ziegler 1977), and the zonal revision by Ziegler and Sandberg (1990). The section was then used by Klapper and Becker (1998, 1999) to achieve a correlation between the "Standard" and Montagne Noire zonation of Klapper (1989), which led to a response (with some new data) by Ziegler and Sandberg (2000).

Becker and House (1998, p. 20) and Klapper and Becker (1999, p. 345) noted a previously neglected break in facies right before the level of *Pa. semichatovae* reported by Ziegler and Sandberg (1990). A thin intercalation of unconformities, volcaniclastics, and sheet cracks gives physical evidence of re-transgression pulses associated with the *semichatovae* Event. This stimulated us to re-investigate at Martenberg the middle/upper Frasnian transition combining macroscopic lithology, biostratigraphy, as well as bio- and microfacies. This involves the following research questions:

1. First documentation of changing carbonate microfacies at Martenberg, including the sedimentary expression of eustatic fluctuations at the proposed middle/upper Frasnian transition.
2. Refined local ranges of all conodont taxa based on revised, consistent taxonomic concepts (with subspecies and morphotype differentiation of zonally important taxa), especially of forms previously included in *Pa. jamieae.*
3. Development of a refined conodont zonation in pelagic facies, with subzones, and a focus on the disputed meaning and justification of a *jamieae* Zone (see Klapper and Becker 1999; Ovnatanova and Kononova 2020)
4. Proposal for a future, conodont-based upper Frasnian substage definition, including aspects of ammonoid bio- and sequence stratigraphy.

Abbreviations

Ad. = *Ancyrodella*, *Ag.* = *Ancyrognathus*, *I.* = *Icriodus*, *Pa.* = *Palmatolepis*, *Po.* = *Polygnathus*; EF = Early Form, LF = Late Form, FAD/FOD = first appearance (global) and (local) occurrence datum, LAD/LOD = last appearance/occurrence datum, * = new taxon, ? = assignment to the taxon is questionable, e.p. = *ex parte*, only a part of the material belongs to the mentioned taxon, non = specimen does not belong to the taxon.

Locality

The Martenberg section lies northeast of Diemelsee-Adorf in the Waldeck region at the eastern margin of the Rhenish Massif, Germany (GPS: 51°22'30.4"N, 8°48'46.1"E). It can be reached by following, from the eastern end of Adorf, the road towards Giershagen. After ca. one kilometre, the Martenberg "Klippe" (Figs. 1 and 2) is situated west of the road in a small depression. It is marked at a small parking area as a protected natural monument of the "Geopark Grenzwelten" (Mertmann 2017).

The outcrop was originally part of the Christiane Mine, which started from an open pit (e.g. Bernauer 1890; Masling 1911; Teeke 1953; Emde 1965). From the 13th century until 1963, it exploited a thick exhalative hematite ore body formed at the top of a basaltic volcanoe (Schlüter 1927; Paeckelmann 1928a, 1936; Bottke 1962, 1965), overlain by fossiliferous, condensed seamount limestones. The latter form the upper part of the Martenberg "Klippe" or "Rosenschlößchen" (Fig. 2), a monolith about 15 m in diameter and 10 m high (Sandberg et al. 1989a). The Martenberg section represents the axial dome of a second order anticline with smaller-scale special folding and a thrust zone (e.g. Schlüter 1927; Paeckelmann 1928a; Ree 1953; Becker 1984). It formed during the main Variscan orogeny as a subunit of the northeastwards branching, first order East Sauerland Anticline, due to the rheological resistance of the metabasalts in its core. The famous eastern face of the cliff (e.g. House and Ziegler 1977: fig. 1), which housed Ziegler´s lateral sections I, II, IV, and V, collapsed several years ago, which destroyed the formerly prominent, dense bed numbering. Fortunately, this did not affect the important section on the northern side (Figs. 2 and 3), which was the main section for Ziegler´s conodont sampling from 1958 to 1971, by Klapper and Becker (1998, 1999), and for this study.

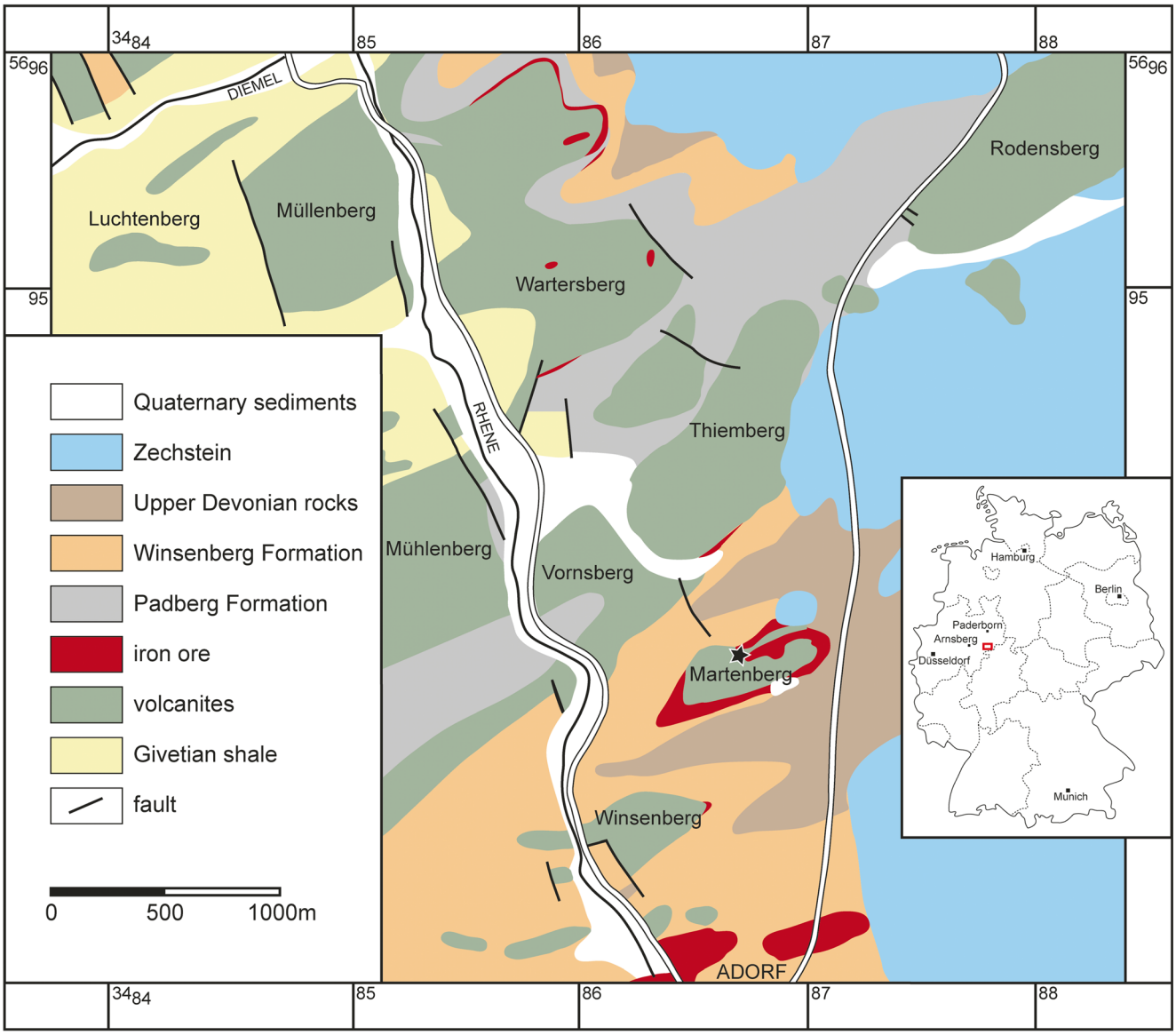

Fig. 1 Geographic location of the Martenberg north of Diemelsee-Adorf on a simplified geological map for the differentiated eastern part of the Ostsauerland Anticline (extracted from Becker 1984). The star marks the location of the section

Research history at Martenberg

Already more than 180 years ago, goniatites, crinoids, and bivalves were described from the Martenberg (von Buch 1832), followed by subsequent descriptions in Beyrich (1837), D'Archiac and De Verneuil (1842), and Sandberger and Sandberger (1850–1856). The diverse fauna was first monographed by Holzapfel (1882), who did not yet separate Givetian and Frasnian assemblages. Hematite-rich volcaniclastic limestones yielded the rich middle Givetian fauna described by Holzapfel (1895). At the same time, Denckmann (1895) coined the term "Adorfer Kalk", with the Martenberg as the type locality. This term now translates into Adorf Formation, which is defined by the onset of condensed, micritic cephalopod limestones above fossiliferous, metasomatically strongly iron impregnated, calcareous lapilli tuffites. The latter includes upper Givetian levels with pharciceratid faunas (Denckmann 1903, pl. 18; Kullmann and Ziegler 1970) and ranges to the lower/middle Franian transition (e.g. Ziegler 1958, 1971; Aboussalam 2003). The upper part of the micritic Adorf Limestone/Formation is characterised by strong dolomitisation. Thin-bedded dolomitic limestones range into the lower Famennian (Paeckelmann 1928a; Ziegler 1971), which results in a different time range of the terms Adorf Limestone/Formation and "Adorf-Stufe" (Matern 1929) or Adorfian, a regional chronostratigraphic unit that has been proposed to be harmonized with the Frasnian (Schindler et al. 2018, pp. 452–453).

Despite its small outcrop size and thickness, the Martenberg section became a key locality for Rhenish biostratigraphy when Wedekind (1913) used it to develop his lower Upper Devonian

Fig. 2 Overview of current outcrop conditions at Martenberg, eastern cliff, with the red arrow pointing to the refined north-eastern section. The small image in the lower right corner shows a close-up of the wider *semichatovae* Event interval between bed R-Q and Bed Q, characterised by thin-bedding (interval of "Sheet 1-3"). The ruler is folded out to a length of 30 cm. Bed P begins just above its top. (photos by T. Söte)

goniatite zonation of the "*Mantiococeras*-Stufe", which later became the "Adorfstufe". Wedekind (1918) added some goniatites and Matern (1929) suggested some revisions. When the stratigraphic significance of conodonts was realised in Germany, Devonian research concentrated on condensed limestones with goniatites, such as the Martenberg (Müller 1956). Bischoff and Ziegler (1957) revised the Middle/Upper Devonian transition with the help of conodonts and in a footnote (p. 35) they pointed out that the Martenberg section was systematically examined for conodonts by W. Ziegler. His results were published one year later (Ziegler 1958). He emphasised that the eastern cliff side was not very suitable for detailed investigations due to the rapid wedging out of layers. Therefore, he restricted himself to the north-western side, followed later (Ziegler 1971) by a numbered section at the northern side, which is also the section re-studied by us. Kullmann and Ziegler (1970) aimed to complete gaps in goniatite stratigraphy and its correlation with the developing conodont stratigraphy. However, as it later became clear (Becker et al. 1993; House and Kirchgasser 1993), the studies faced problems caused by the extreme condensation and local incompleteness of upper Givetian to lower middle Frasnian strata. House and Ziegler (1977) re-illustrated important goniatite type-material and were able to further refine the correlation between the goniatite and conodont succession. They re-established Wedekind´s (1913) distinction of do Iß and do Iγ faunas, which characterise the Frasnian zones UD I-I and UD I-J sensu Becker et al. (1993). However, it is important to note that the new faunas with *Stilleoceras retorquatum, Costamanticoceras nodulosum* and *Playfordites tripartitus* (generic assignments updated) came from a higher level than Wedekind´s very thin Iß interval, Denckmann´s "Webel Limestone". Based on the presence of *Beloceras*, the original Iß correlates with UD I-H. Becker and House (1993) and Becker (2002) documented some important Martenberg goniatite types and new records (e.g. the Australian *Trimanticoceras cinctum*), followed most recently by tornoceratid descriptions in Korn (2021a, 2021b).

Sandberg et al. (1989a) revised the conodont zonation at the Middle/Upper Devonian transition and established new

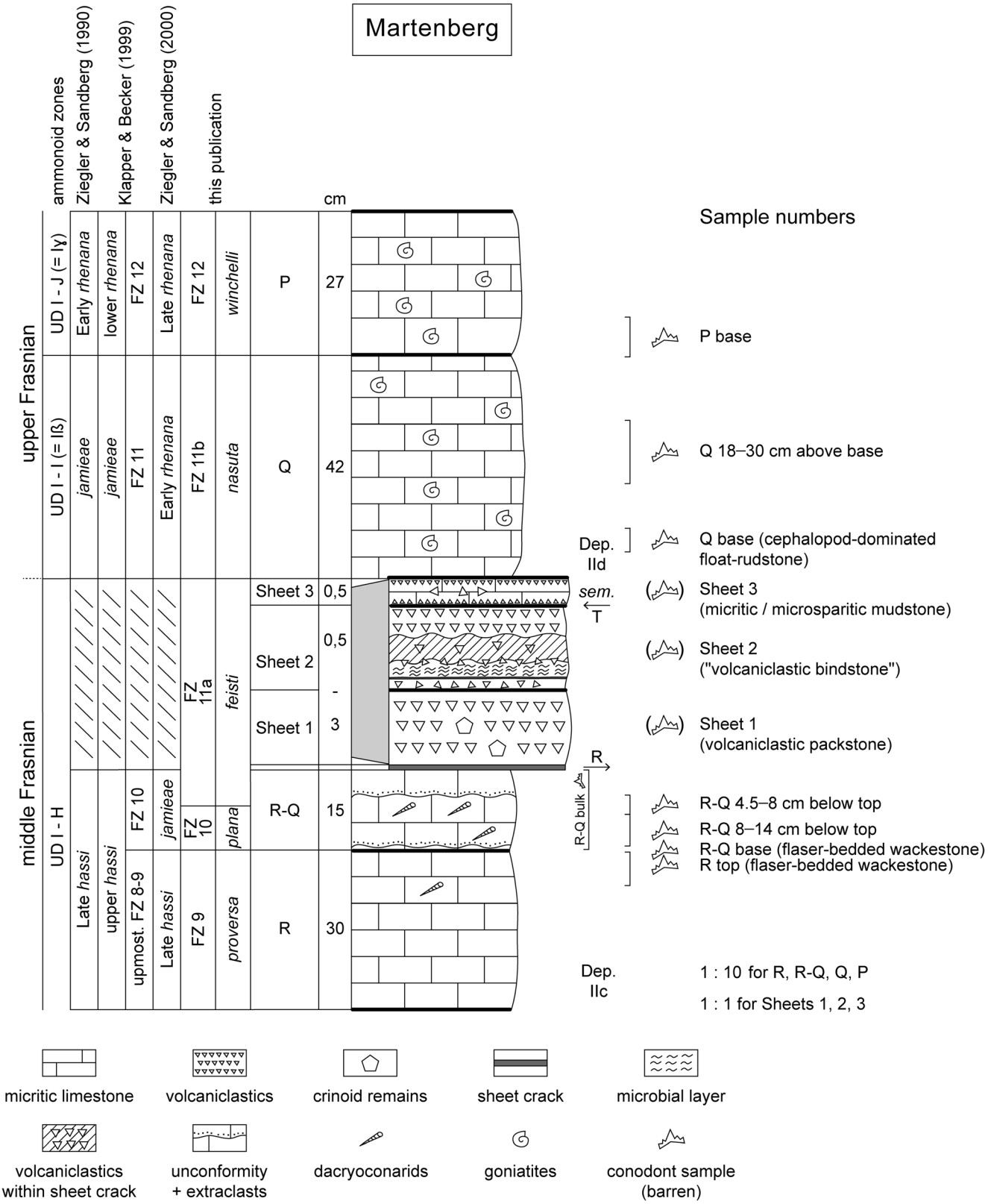

Fig. 3 Proposed Frasnian substage position, ammonoid zonal keys after Becker et al. (1993) and Wedekind (1913) (in brackets), conodont zone assignments of various authors, bed numbering, lithological log (scale 1 : 10), re-transgressive trends, position of depophases of Johnson et al. (1985), positions of new conodont samples, and microfacies data for Martenberg section NE. Between beds R-Q and Q lies the regressive interval, here exaggerated (scale 1 : 1) in order to show details, with previously neglected sheet cracks, unconformities, a microbial layer, and volcaniclastics (tuffites)

"standard zones", which partly used Martenberg as a reference section. This was followed by the major revision of the Frasnian and lower Famennian zonation by Ziegler and Sandberg (1990). Unfortunately, it was partly incompatible with the more detailed Montagne Noire Frasnian zonation established one year before by Klapper (1989). The schemes use several different zonal index species but also different taxonomic concepts of the same species, which prevented a simple correlation. Therefore, Klapper and Becker (1998, 1999) resampled the northern Martenberg section (which is "section q" of Ziegler and Sandberg 2000) in order to correlate the "Late Devonian Standard Conodont Zonation" and Montagne Noire Zonation based on data from the same section. This resulted in the recognition of problems at the middle/upper Frasnian transition, especially concerning the precise correlation between the Frasnian Zone 11 and *jamieae*/Lower *rhenana* zones, leading to discussions by Sandberg and Ziegler (1998) and Ziegler and Sandberg (2000). Ovnatanova and Kononova (2020) re-examined the Martenberg conodont collection of Willi Ziegler in 1994 and denied the justification of the *jamieae* Zone, a topic that is re-evaluated here based on new data.

Frasnian "Standard" and Montagne Noire zonations

Ziegler (1958, 1962) studied the biostratigraphic distribution of Upper Devonian conodonts and established a succession of zones based on the genera *Ancyrodella*, *Ancyrognathus*, *Palmatolepis*, *Polygnathus, Bispathodus*, and *Scaphignathus*. His work built on earlier results of Sannemann (1955), Müller (1956), Bischoff (1956), and Bischoff and Ziegler (1956, 1957). Following a revision of the middle/upper Famennian zonation (Ziegler and Sandberg 1984), the so-called "Standard Conodont Zonation" of the Frasnian and lower Famennian was refined and revised by Sandberg et al. (1989a) and Ziegler and Sandberg (1990). In the Frasnian, it is based on the supposed autochronologic phylogeny of *Palmatolepis* and its precursor *Mesotaxis*. Most Frasnian palmatolepids fall in *Manticolepis* Müller, 1956, a (sub)genus which rarely has been used by later authors (e.g. in Dzik 2002, who added the Frasnian genera *Kielcelepis* and *Lagovilepis*). We apply the traditional, wide generic concept but admit that a future dissolution of the "mega-genus" *Palmatolepis* into well-defined, monophyletic (sub)genera is desirable.

Based on the studies of several conodont-rich sections in the Montagne Noire, Klapper (1989) showed that the regional Frasnian deposits can be divided into thirteen conodont zones instead of only seven zones of the "Standard Zonation" of Ziegler (1958, 1962). Klapper´s Montagne Noire (MN) Zonation was based on iterative speciations in the genera *Ancyrodella*, *Ozarkodina* (s.l.), *Ancyrognathus,* and *Palmatolepis*. It considered the ranges of all species present in pelagic carbonate assemblages, if they were sufficiently short-ranging, as many show a consistent stratigraphic position in relation to *Palmatolepis*. He thus did not follow the "phylogenetic" (= autochronological) approach of Ziegler and Sandberg (1984), which was, anyway, not stringent since exceptions (e.g. "Uppermost *marginifera* Zone" defined by *Scaphignathus velifer velifer*) were allowed. Klapper (1989) intended the MN succession to be a regional zonation, which at that time had no claim to global application. This was underlined by the parallel introduction of a different regional zonation for the Canadian Rocky Mountains, published in the same Calgary Symposium volume by Klapper and Lane (1989). Klapper also referred to the preliminary results of graphic correlation, which could offer a finer resolution than conventional zoning and would thus probably replace it in the long term. From the data collected since the 1980s, Klapper et al. (1995) were able to present such an alternative to conventional zoning. Their "Frasnian Composite Standard" was based on the graphical correlation of 27 Frasnian sections from the Montagne Noire (France), western New York, and Western Australia. Values in CSUs (Composite Standard Units) provide either global or local (total) bases (= FADs/-FODs) and tops (= LADs/LODs) of species ranges, including marker taxa that define the bases of MN zones, some of which were used to fix the lines of correlation. The composite was later refined by data from the Timan-Pechora Basin in Russia (Klapper et al. 1996). Important data for ranges of Frasnian conodonts were published subsequently from the Cantabrian Mountains (García-López and Sanz-López 2002), NW Australia (Klapper 2007), the Pyrenees (e.g. Liao and Valenzuela-Ríos 2012), the Anti-Atlas of southern Morocco (e.g. Hartenfels et al. 2013; Aboussalam and Becker 2016; Becker et al., 2018), Algerian Sahara (Mahboubi et al. 2015), eastern North America (Klapper and Kirchgasser 2016), the Rhenish Massif (e.g. Becker et al. 2016a, 2016c; Hartenfels et al. 2016), the Iowa Basin (Day and Witzke 2017), South China (Zhang et al. 2019), and the Moroccan Meseta (Becker et al. 2020b; Aboussalam et al. 2020). Ranges of marker forms were combined in updated Frasnian composits (Klapper 1997; Klapper and Kirchgasser 2016). The latter study replaced the term "MN Zone" by "Frasnian Zone", but we prefer to name zones after their index species, because the names of fossils are easier to remember than simple numbers. Therefore, Frasnian Zone 10 is called *plana* Zone, Frasnian Zone 11 *feisti* Zone, and Frasnian Zone 12 *winchelli* Zone (see Becker et al. 2020a), but both are given in order to ease the stratigraphic understanding. Shallow-water Frasnian successions mostly lack the pelagic index species and require alternative regional zonations based mostly on polygnathids or icriodids (e.g. Matyja 1993; Kirilishina and Kononova 2004; Ovnatanova and Kononova 2008).

Due to the underlying disparate taxonomies, it was not possible to correlate the "Late Devonian Standard Conodont Zonation" and the Montagne Noire Zonation precisely until

Klapper and Becker (1998, 1999) resampled the Martenberg reference section and successfully applied the taxonomic concepts of the Montagne Noire zonation. As mentioned above (see Fig. 3), this raised problematical alignments of some of the "standard zones" by Ziegler and Sandberg (1990). This involved their original use of a generalised lithological log, which was corrected by Ziegler and Sandberg, 2000, fig. 2). More important was the uncertain correlation of the Frasnian Zone 11 found in Bed Q (= q, numbering of Ziegler 1971) either with the *jamieae* Zone, as suggested by the log of Ziegler and Sandberg, 1990, Fig. 3), or with the lower part of the "Early" *rhenana* Zone (see comments by Sandberg and Ziegler 1998). Ziegler and Sandberg (2000) restudied their samples (beds P, Q, R / samples VI'/6 to 12) from Martenberg and corrected their zonal identifications by re-assigning Bed Q (Sample VI/11b) to the "Early" *rhenana* Zone. In addition, they re-assigned the underlying upper part of Bed R (Sample VI'/10) to the *jamieae* Zone because of a supposed rare occurrence of *Pa. jamieae*. However, this did not clarify the situation and correlation problem, because Klapper and Becker (1999, p. 343) recognised that *Pa. jamieae* sensu Ziegler and Sandberg (1990) included different species (e.g. *Pa. jamieae* s.str. and *Palmatolepis* sp. B of Klapper and Foster Jr. 1986, now *Pa. feisti* Klapper, 2007). Since the holotype of *Pa. jamieae* came from higher strata at Schmidt Quarry in the Kellerwald region, and in the absence of an illustration of the oldest specimens of Ziegler and Sandberg (2000), the entry level of *Pa. jamieae* s. str. at Martenberg remained unclear. As a consequence, the justification for a *jamieae* Zone in its type locality was completely open. Recently, Ovnatanova and Kononova (2020) correlated the regional Timan-Pechora "conodont associations III-XI" of Ovnatanova et al. (1999) with the "Late Devonian Standard Conodont Zonation" and Frasnian zonation. This involved the re-examination of the Frasnian conodont collection of the Rhenish Massif in the laboratory of Willi Ziegler in 1994. They did not recognise any true *Pa. jamieae* in the Lower *rhenana* Zone at Martenberg, or below, and concluded that the *jamieae* Zone should not be considered as a separate biostratigraphic unit. Since the alleged *jamieae* specimens from Ziegler and Sandberg (2000) have not been revised, their true identity remained unsolved, a circumstance that we decided to overcome by new samples, which were partly exceedingly rich in conodonts.

Global *semichatovae* Transgression/Event

Sandberg et al. (1989b, 1992, 2002) and Sandberg and Ziegler (1998) established the *semichatovae* Transgression as a short-term, major eustatic deepening event. The expanded term *semichatovae* Event refers to the sudden sea-level rise combined with its effects on lithofacies and biota. It is recognisable as a lithological perturbation and bioevent, especially by migration pulses and radiations in several fossil groups, such as conodonts and ammonoids. The transgression and litho-/bioevent are named after *Pa. semichatovae*, a morphologically very distinctive species, which appeared as a cryptogenic taxon and spread fast pantropically, especially in shallower areas of carbonate platforms/ramps that were uninhabitable for most other palmatolepids. Sandberg et al. (1989b) pointed out that this opportunistic species may make up three-quarters of all *Palmatolepis* in neritic facies, while in deeper settings it only reached an abundance of 10% - or it is even rarer, as at Martenberg (Ziegler and Sandberg 2000) or other German seamount sections, such as Schmidt Quarry (Ziegler and Sandberg 1990; Ovnatanova and Kononova 2020). The *semichatovae* Transgression can be recognised pantropically (Fig. 4), but there is no published review of global distribution. Therefore, a comprehensive compilation is supplied here, roughly from west to east, giving the relevant regional lithological units, evidence for deepening/facies changes, some conodont information, and references for further reading (unclear localities are preceded by a question mark).

- **Southern Mackenzie District, Northwestern Canada**: Deepening trend with incoming of *Pa. semichatovae* in the reefal Upper Member of the Twin Falls Formation (McLean and Klapper 1998, p. 528) (Fig. 4: Point 1).
- **Alberta Rocky Mountains, Western Canada**: Spread of *Pa. semichatovae* in the poorly defined transition from the upper Pedrix to lower Mount Hawk formations (e.g. Klapper and Lane 1989: base of their regional Zone 5a; McLean and Klapper 1998) (Fig. 4: Point 1).
- **Great Basin, western USA** (17 localities of Nevada, Utah, Montana, Idaho, and Arizona): Onset and sudden spread of *Pa. semichatovae* associated with a major expansion (deepening) of the Pilot Basin (e.g. Sandberg et al. 1989b, 2003; Morrow and Sandberg 2008) (Fig. 4: Point 2).
- **?Michigan Basin, USA:** Sequence of radioactive black shales within the upper Norwood Member of the Antrim Shale (Gutschick and Sandberg 1991) (Fig. 4: Point 3).
- **Iowa Basin, USA**: Base of regional T-R cycle 7A at the base of the Lime Creek Formation (e.g. Day and Witzke 2017) (Fig. 4: Point 4).
- **Western New York, Appalachian Basin, eastern USA**: Upper tongue of thick black shales of the Rhinestreet Formation, with *Pa. semichatovae* occurring in the Relyea Creek Horizon (Klapper and Kirchgasser 2016) (Fig. 4: Point 5).
- **Boulonnais, northern France**: Deepening phase marked by the shaly Hydrequent Formation, enabling the sudden immigration of *Manticoceras* faunas (Becker 2002: recognised as *semichatovae* Event) (Fig. 4: Point 13).
- **Southern Dinant Sycline, southern Belgium**: Initial transgressive pulse marked by the shaly Boussou-en-Fagne Member of the Grand Breux Formation (*plana* Zone, Frasnian Zone 10), drowning the karstified Lion

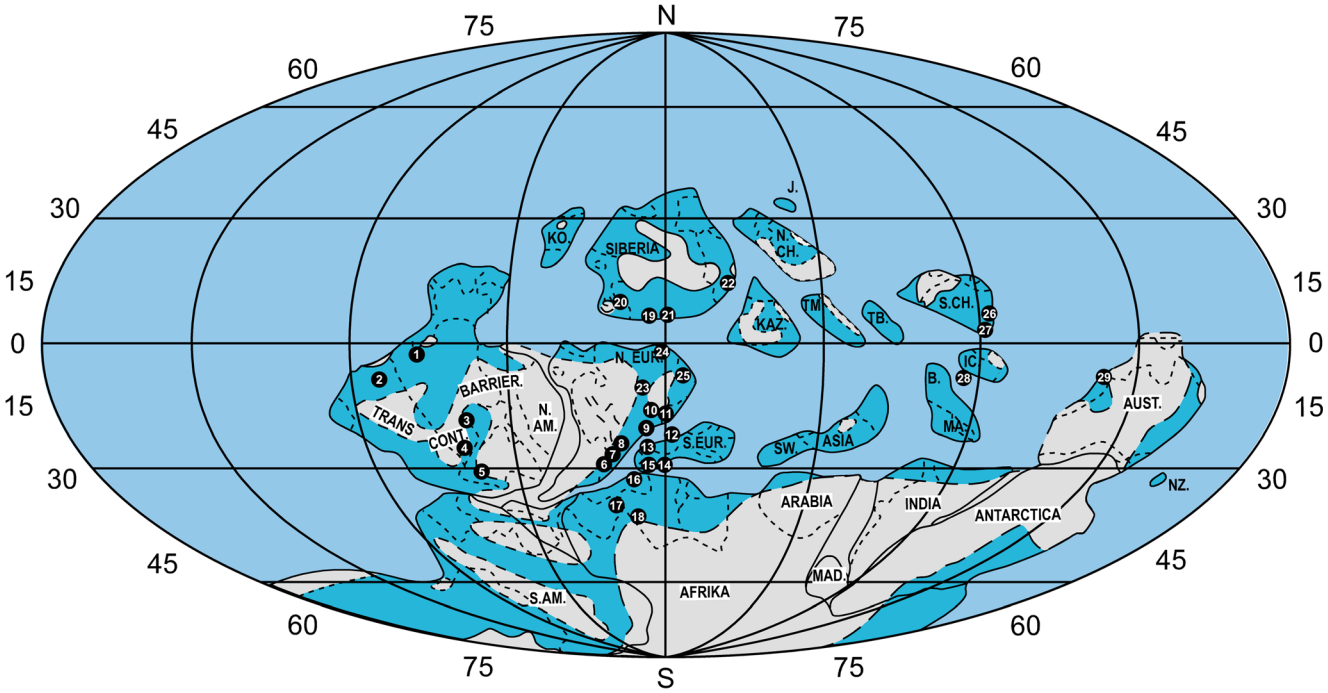

Fig. 4 Global records of the *semichatovae* Transgression positioned on an Upper Devonian plate tectonic reconstruction updated from Heckel and Witzke (1979) by Hartenfels and Becker (2016). *TRANS CONT. BARRIER* Trans Continental Barrier, *N. AM.* North America, *S. AM.* South America, *KO.* Kolyma, eastern Russia, *N. EUR* North Europe, *S. EUR* South Europe, *J.* Japan, *N. CH.* North China, *KAZ.* Kazakhstan, *TM.* Tarim (western China), *TB.* Tibet, *S. CH.* South China, *SW. ASIA* Southwest Asia, *B.* Burma, *MA.* Malaysia, *IC.* Indo-China, *AUST.* Australia, *MAD.* Madagascar. *1* Canadian Rocky Mountains, *2* Great Basin, western USA (Utah-Nevada), *3* Michigan Basin, *4* Iowa Basin, *5* western Appalachian Basin, *6* Ardennes, *7* Rhenish Massif, *8* Harz Mountains, *9* Saxothuringian Zone, *10* Pomerania, *11* Holy Cross Mountains, *12* Carnic Alps, *13* Boulonnais, northern France, *14* Montagne Noire, southern France, *15* Pyrenees, *16* Moroccan Meseta, *17* Anti-Atlas, southern Morocco, *18* southern Algeria, *19* Timan, *20* Polar Urals, *21* South Urals, *22* Rudny Altai, southern Siberia, *23* Lithuania, *24* Tatarstan, *25* Volgograd, Russian Platform *26* Hunan, South China, *27* Guangxi, South China, *28* Central Vietnam, *29* Canning Basin, Western Australia.

Mudmound, followed by the deeper-water, nodular Neuville Formation with *Ag. triangularis* and *Pa. semichatovae* and a sudden influx of goniatites (Streel et al. 1974; Sandberg et al. 1992; Boulvain et al. 1999; Da Silva et al. 2010: regional sea-level Event 7; Denayer and Poty 2010; Goolaerts and Gouwy 2015; Mottequin and Poty 2016: base of regional Aisemont Sequence) (Fig. 4: Point: 6).

- **Phillipville Massif, Belgium**: Drowning of the reefal platforms of the Phillipeville and Lustin formations leading to the deeper and open-water Neuville Formation, which includes small Petit-Mont reefs (e.g. Mottequin and Poty 2016) and proliferating goniatite faunas (Gatley 1983) (Fig. 4: Point: 6).
- **Namur Syncline, northern Belgium**: Drowning of the reefal Huccorne (in the north) and Rhisnes formations (in the south), leading to deposition of the deeper water, argillaceous Aisemont Formation, which yielded *Ag. triangularis* (Coen-Aubert and Lacroix 1979; Boulvain et al. 1999; Denayer and Poty 2010) (Fig. 4: Point: 6).
- **Vesdre Massif, eastern Belgium**: Drowning of the "First *Phillipsastrea* Biostrome", followed by maximum flooding in the middle Aisemont Formation (Bultynck et al. 1998; Poty and Chevalier 2007; Mottequin and Poty 2016) (Fig. 4: Point: 6).
- **Aachen region, western Rhenish Massif, Germany**: Drowning of the regionally youngest coral biostrome (Hahn Member of Walheim Formation), followed by deeper neritic nodular limestones (Schmithof Formation) with *Ag. triangularis* and an incursion of goniatites (Reissner 1990; Aboussalam and Becker 2016) (Fig. 4: Point: 7).
- **Eifel Mountains, western Rhenish Massif, Germany**: Intercalation of Oos Limestone facies by dark grey, pelagic marls and shales with goniatites and anaptychids at Wallersheim-Loch (Hauser and Hauser 2002) (Fig. 4: Point: 7).
- **Bergisch Gladbach-Paffrath Syncline, Rhenish Massif, Germany**: Change from platy limestones / marlstones with middle Frasnian conodonts of the Hombach Formation to hypoxic goniatite shales of the Sand Formation with upper Frasnian conodonts (Kleinebrinker 1992; Söte et al. 2021) (Fig. 4: Point: 7).
- **Northern Rhenish Massif, Germany**: Laminated black shale unit interrupting oxic, pelagic nodular limestones deposited on the top of the drowned Hönne Valley Reef Complex (Stichling et al., this vol.) (Fig. 4: Point: 7).

- **Burgberg Atoll, eastern Rhenish Massif, Germany**: Change from proximal reef debris of the Hoppecke Formation to pelagic flaserlimestone of the Grottenberg Member of the Burgberg Formation in the *plana* Zone (Frasnian Zone 10), followed by the onset of rich goniatite faunas of UD I-I (Hartenfels et al. 2016) (Fig. 4: Point: 7).
- **Dill Syncline, southern Rhenish Massif, Germany**: Change from massive to thin-bedded limestone with the oldest *Ag. triangularis* in seamount deposits of the Donsbach Quarry (Bender et al. 1988) (Fig. 4: Point: 7).
- **Western Harz Mountains, Germany**: Re-onset of sedimentation above the unconformity of the "Westharz Schwelle" in the basal upper Frasnian, with reworked Givetian to middle Frasnian conodonts at the base (Buchholz et al. 2001) (Fig. 4: Point: 8).
- **Unterharz, Germany**: Spread of pelagic carbonates with "*jamieae* Zone" conodonts (Schwab and Hüneke 2008) (Fig. 4: Point: 8).
- **?Saxothuringian Zone**: Onset of condensed pelagic limestone deposition with rich conodont faunas on drowned volcanic seamounts (e.g. Bartzsch et al. 2002) (Fig. 4: Point: 9).
- **?Montagne Noire, southern France**: Widening of a hypoxic shelf basin with goniatite shales with UD I-I/J faunas (Upper Member of Serre Formation) in the Cabrières sequence (Feist 1985; Becker and House 1994); *Pa. semichatovae* has not yet been found in faunas from lateral pelagic limestones. (Fig. 4: Point 14)
- **Benahmed region, central part of western Morrocan Meseta**: Sudden, transgressive onset of hypoxic goniatite shales (Boudouda Formation) with rich UD I-I/J faunas above a regional hiatus (Söte and Becker 2021) (Fig. 4: Point 16).
- **Middle Atlas Basement, Morocco**: Sudden onset of extremely condensed, upper Frasnian hypoxic goniatite shales with UD I-I/J faunas above a hiatus at Immouzer-du-Kandar (Aboussalam et al. 2020) (Fig. 4: Point 16).
- **Mrirt region, eastern part of western Morrocan Meseta**: Re-onset of condensed, pelagic limestones after a hiatus high in the *plana* Zone (Frasnian Zone 10), followed by continuing deepening marked by argillaceous, nodular limestones with *Pa. semichatovae* and a major change of water mass circulation evidenced by Nd isotopes (Lazreq 1999; Dopieralska et al. 2015; Becker et al. 2020b) (Fig. 4: Point 16).
- **Eastern Anti-Atlas, southern Morocco**: Transgressive onset of Kellwasser-type black goniatite limestones above unconformities on the Tafilalt and Maïder platforms, again associated with a major change in Nd isotopes (e.g. Wendt and Belka 1991; Becker et al. 1997, 2018; Dopieralska et al. 2015; Wendt 2021) (Fig. 4: Point 17).
- **Dra Valley, western Anti-Atlas, southern Morocco**: Sudden change from well-oxygenated, red nodular limestones with some corals and FZ 10 conodonts to hypoxic goniatite shales with rich UD I-I faunas (Becker et al. 2004) (Fig. 4: Point 17).
- **Algerian Sahara**: No distinctive *semichatovae* Transgression but a more continuous maximum of transgression within pelagic outer shelf facies (Mahboubi et al. 2019) (Fig. 4: Point 18).
- **Holy Cross Mountains, Poland**: Change from conodont-poor proximal reef debris limestones to condensed pelagic limestones with rich deep-water conodont faunas (Matyja and Narkiewicz 1995); the "Lower *gigas* Regressive Pulse" of Narkiewicz (1989) probably represents a regional tectonic pattern (Fig. 4: Point 11).
- **Western Pomerania, Poland**: Major "Early *rhenana* sealevel rise", which drowned a neritic carbonate platform and led to deposition of offshore shales (Matyja 1993: regional Event 2) (Fig. 4: Point 10).
- **?Northern Lithuania**: Interval of maximum transgression in the coastal to very shallow marine Frasnian succession of the middle part of the Stipinai Formation, based on palynostratigraphy suggested to correlate with the *semichatovae* Transgression (Jaglarz et al. 2021) (Fig. 4: Point 23).
- **Timan, northern Russian Platform**: Marked sea-level rise of the Syrachoy Formation above the Vetlasyan Infill stage (Lowstand System Tract), correlating laterally, in more basinal settings, with the boundary between Members 1 and 2 of the Lyaol Formation that contains *Pa. semichatovae* (e.g. House et al. 2000) (Fig. 4: Point 19).
- **(Sub)Polar Urals**: Level of argillaceous limestone sandwiched between brecciated and oolithic limestone at Malaya Usa River (Unit 8, Sobolev and Soboleva 2018) and change from massive limestones at the top of the Domanik Suite to thin-bedded, argillaceous limestones of the basal Mendym Suite in the Kozhim River section (Matveeva 2013) (Fig. 4: Point 20).
- **Western slope of South Urals**: Change from a pure limestone unit with conodonts of the *plana* Zone (Frasnian Zone 10) to argillaceous strata with supposed *Pa. jamieae* in the regionally expanded Domanik Formation of the Gabdyukovo section (Artyushkova et al. 2011) (Fig. 4: Point 21).
- **Guilin area, Guangxi, South China**: Joint entry of *Pa. semichatovae*, *Pa. nasuta*, and supposed *Pa. jamieae* (not figured) just above a change from thick- to thin-bedded limestones, as evidence for a minor deepening at the local base of the Liujiang Formation in the Dongcun section; entry of *Pa. semichatovae* above a chert intercalation within

the Liujiang Formation in the Longmen section (Wang 1994) (Fig. 4: Point 27).

- **SW Guangxi, South China:** Entry of *Pa. semichatovae* above a regressive, massive marker limestone within the Luijiang Formation (Sihongshan Section, Wang and Ziegler 1983; Wang 1994) (Fig. 4: Point 27).
- **Hunan, South China:** Change from neritic facies to pelagic beds with *Pa. semichatovae* and *Manticoceras* in the Shetianqiao section (Ma et al. 2004, 2009; Ma and Zong 2010). In a later review of South China Devonian sea level changes (Ma et al. 2017), the *semichatovae* Transgression is regionally named as "Qilijiang high stand" (Fig. 4: Point 26).
- **Central Vietnam**: Brief interruption of a middle/upper Frasnian carbonate sequence with pelagic conodont faunas by a single, thin shale just above the local first *Ag. triangularis* (Ta et al. 2021) (Fig. 4: Point 28).
- **Western Australia**: Onlap of condensed limestones with UD I-I manticoceratids and *Pa. semichatovae* on top of a conglomeratic reworking unit in the "Harpid Bed" of section "Windy Knolls" (Becker and House 1997, 2009) (Fig. 4: Point 29).

It is likely that the transgression is recognisable in further regions (e.g. Iran, Afghanistan, other parts of Central Asia), where biostratigraphic information is still too limited for precise international correlation.

Material and methods

Our reinvestigation at Martenberg concentrated in the northern section ("section q" of Ziegler and Sandberg 2000) on the critical interval that was established by the previous studies. It includes five samples for microfacies and eleven new samples for conodonts (R top = upper 7 cm of the bed, R-Q base, R-Q 8–14 cm below top, R-Q 4.5–8 cm below top, R-Q bulk = complete bed, Q base = 5–10 cm above base, Q 18–30 cm above base, "Sheet 1, 2, 3", P base = 0–8 cm above base), three of which (the "sheet samples") yielded no conodonts. Correlation of our samples (Fig. 3) with that in Klapper and Becker (1999) and Ovnatanova and Kononova (2020) is straight forward since they derived from the same section. The correlation with samples from sections VI and VI′in Ziegler and Sandberg (1990) is based on the lateral tracing of beds in House and Ziegler (1977) and in Ziegler and Sandberg (1990, 2000). Since thicknesses change along strike, the position of their samples within beds has to be approximated by interpolation, which did not result in any contradictions (e.g. different zonal assignments).

A total of 8575 Pa (= P1) elements were counted and identified; ramiform elements were picked but not identified, as many Upper Devonian multielement reconstructions are incomplete or doubtful. We give the number of *Nothognathella* elements, which are thought to represent Pb (= P2) elements of *Mesotaxis/Palmatolepis*, showing their strong underrepresentation although they are massive elements that should not have undergone different hydraulic sorting than the Pa (= P1) elements.

For the recovery of conodonts, each sample was dissolved in 10% formic acid. Washed residues were separated into >0.1, >0.315, and >0.63 mm fractions. As it is widespread standard practice, only the voluminous smallest fractions were treated before picking by heavy liquid separation, using diluted sodium polytungstate ($3Na_2WO_4 \times 9WO_3 \times H_20$). The light fraction was visually checked whether any significant amount of small-sized/juvenile conodonts finished accidently in that section, which was not the case. For each sample, the local alpha diversity was calcaluated, counting species and subspecies, not morphotypes.

The applied taxonomic concept distinguishes clearly between intraspecific morphotypes, subspecies, and species. Morphotypes are variants with distinctive morphological features that are part of populations but which intergrade. They are also used for forms with minor morphological differences when there is no clear evidence of different distributions in time, space, and biofacies in relation to the types of taxa. We recommend that the holotype/lectotype of a taxon should define Morphotype 1, although there have been divertions from this practice in the past. In subspecies, a few intermediate specimens may occur in relation to the nominate subspecies but both show different distributions in space, time, or biofacies, which suggests at least partial genetic separation. This definition is an essential part of present-day biological taxonomy and conservation biology. Subspecies are populations characterised by dominant factual genetical isolation and a key element towards speciation. In full species, there should be no intermediates between populations after speciation was complete; intermediates are restricted to the mostly short time intervals of the gradually evolving lineage, which is not preserved in cryptogenic taxa. We are aware that we can apply this concept currently only to the Pa elements. There could be species with common or very similar Pa but more different other elements. It is notable that subspecies have not been used in Frasnian palmatolepids while they are long established and very successfully applied in biostratigraphy in Famennian lineages of the genus. This difference has no logical base and led us to recognise Frasnian subspecies.

Carbonate microfacies analysis and classification follow the nomenclature by Dunham (1962), the standard microfacies

Table 1 Total conodont record combined with previously published data at Martenberg

	Martenberg										
Zone	FZ 9	FZ 10		FZ 11a		FZ 11b			FZ 12		
	proversa	*plana*		*feisti*		*nasuta*			*winchelli*		
new samples	R	R-Q				Q			P		
	top	base	8-14 b. t.	4.5-8 b. t.	bulk	base	18-30 a. b.		base		
Ziegler and Sandberg (1990)	VI'/ 11 | VI/ 12a	-	-	-	VI'/ 10 | VI/ 12a	VI' 9 | VI/ 11b	VI´/8	VI'/ 6, 7 | VI/ 11a | IV/ 1b	-	-	VI'/ 5 | VI/ 10e
Klapper and Becker (1998)	R upp. 7, 10	-	-	-	R-Q	-	Q 20-25 a. b.	Q 3-13 b. t.	P 0-8	P 8-18	-
Ziegler and Sandberg (2000)	-	-	-	-	upper part Bed r	Q = VI/ 11b	-	-	-	-	P
Ovnatanova and Kononova (2020)	VI' 11	-	-	-	VI' 10	VI' 9 | VI 11b	"q"/ Q (22 a. b.)	-	"q"/ P (l. p.)	-	-
Ad. nodosa (= *gigas* M1)	2	132	24	100	18	ZS1|OK	87	ZS1|KB	12	KB	ZS1
Ad. gigas (= *gigas* M3)	6	70	44	57	29	ZS1/OK					
Ag. amplicavus	KB	11	1	-	1						
Ag. barbus	1										
Ag. coeni	1	7	13	18	6						
Ag. iowaensis	OK										
Ag. leonis (= *tsiensi* auct.)	ZS1|KB|OK	10	5	8	3	-	1				
Ag. triangularis	ZS1*	**4**	-	4	2	ZS1|OK	60	ZS1|KB	42	KB	ZS1
I. symmetricus (M1)	7	428	43	17	24	1	6				
Nothognathella sp.	6	40	9	87	21	-	17				
Pa. amplificata	3	5|1 cf.	3|1cf.	15	2						
Pa. domanicensis	OK	-	-	-	1						
Pa. hassi	7	95	106	460	96	2 cf.|ZS1|OK	642	ZS1	176	-	ZS1
Pa. housei (= aff. *proversa*)	KB										
Pa. ljaschenkoae (M1)	(?KB)	9		1	6	-	(OK)				
Pa. ljaschenkoae (M2)	1	102	34	113	53	-	(OK)				
Pa. ljaschenkoae (M3)	(?KB)	64	21	27	18	-	(OK)				
Pa. mucronata	KB	19	1	4	20	-	3				
Pa. plana	ZS1*	**41**	9	28	15	ZS1|OK	-	ZS1	-	-	ZS1
Pa. punctata martenbergensis	1	6	-	-	(ZS1|KB|OK)	(ZS1)	(OK)	(ZS1)	-	-	(ZS1)
Pa. proversa (M1)	**(ZS1|OK)**	21	6	10	14	(ZS1|OK)	-	(ZS1)	-	-	(ZS1)
Pa. proversa (M2)	**(ZS1|OK)**	47	24	73	34	(ZS1|OK)	-	(ZS1)	-	-	(ZS1)
Pa. "transitans"	OK*	-	-	-	OK*	OK*	OK*				
Po. paradecorosus	34	902	200	1736	157	1	400	(ZS1)	-	-	-
Po. webbi	1	46	23	77	18	OK	139	KB	8	KB	-
Ad. curvata (EF)		7	-	-	2	ZS1|(OK)	43	KB	-	-	-
Ad. hamata		1cf.	2								
I. symmetricus (M2 = *curvatus*)		131	20	21	8						
Pa. adorfensis n. sp.		**3**	2								
Pa. aff. *feisti*		2	-	-	2						
Pa. jamieae savagei n. ssp. (M1)		**2**	-	3							
Pa. kireevae		17	-	-	7	-	-	-	OK		
Pa. punctata bohemica (*sepkoskii* M.)		1									
Pa. jamieae rosa n. ssp.		1	1	-	-	-	-	-	1		
Pa. simpla		11	-	-	2	-	-	ZS1	-	-	ZS1
Palmatolepis sp. juv.		16	4	-	6	-	-	-	42		
Po. aequalis		3									
Po. praepolitus		3	-	22	7	-	1	ZS1|KB			
Po. robustus		37									
Ag. guangxiensis			1								
Pa. manzuri			2	11							
Pa. hassi to *feisti* (transitional)				**2**							
Pa. descendens n. sp.				1	-	-	2				
Pa. feisti				**9**	-	-	343	KB|(ZS1)			
Pa. jamieae savagei n. ssp. (M2)				1?	-	-	-	-	3		
Icriodus sp. 1 (with offset denticle)					1						
Pa. jamieae auct.					ZS2*	ZS1*	-	ZS1*	-	-	ZS1
Pa. cf. *domanicensis*					1						
Ad. lobata						OK	-	ZS1	-	-	ZS1
I. praealternatus praealternatus						**ZS1**	-	(KB)	17	-	-
Pa. nasuta						**ZS2**	14	(ZS1)	13	-	ZS1
Pa. semichatovae						**ZS2**					
Pa. ederi						**OK**	OK	ZS1			
Po. dubius						OK					
Po. lodinensis						OK	OK	-	OK		
Po. politus						OK	OK	KB	OK	-	-
Po. uchtensis						OK	OK				
Ad. curvata (LF)							4	KB	-	-	(ZS1)
I. alternatus cf. *helmsi*							1				
Pa. uyenoi							KB	-	-	-	-
Ad. ioides									**23**	KB	ZS1
Ad. ioides (M1)									**1**		
Pa. brevis									**4**	-	-
Pa. jamieae jamieae									1		
Pa. rhenana									**15**	-	ZS2
Pa. winchelli									**7**	KB	-
recorded taxa	18	28	19	19	(24)	20	21	17	16	-	22
local Lazerus Taxa	-	1	9	7	2	8	6	2	7	-	-
specimen (bed)	70	2295	599	2905	574	4	1763	-	365	-	-
specimen (total)	8575										

ZS1=Ziegler and Sandberg (1990)

ZS2=Ziegler and Sandberg (2000)

KB=Klapper and Becker (1998)

OK=Ovnatanova and Kononova (2020)

()=cf.

?=questionable

*identification rejected/doubtful

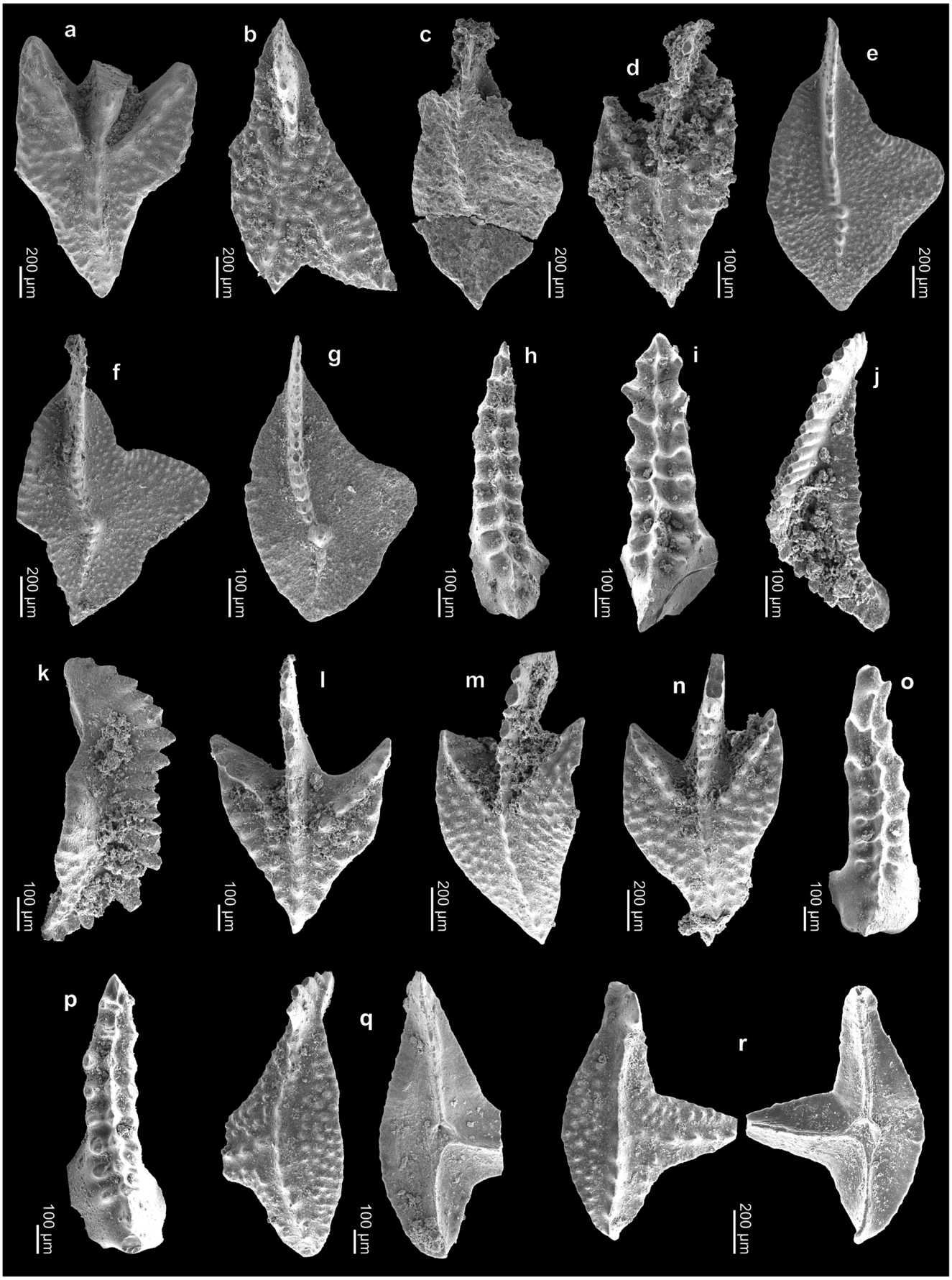
a
200 µm
b
200 µm
c
200 µm
d
100 µm
e
200 µm
f
200 µm
g
100 µm
h
100 µm
i
100 µm
j
100 µm
k
100 µm
l
100 µm
m
200 µm
n
200 µm
o
100 µm
p
100 µm
q
100 µm
r
200 µm

◀ **Fig. 5** Conodonts from Martenberg, part 1. **a** *Ad. gigas* (= M3) Youngquist, 1947, GMM B9A.13-1, Sample R top. **b** *Ag. coeni* Klapper, 1990, GMM B9A.13-2, Sample R top. **c** *Pa. ljaschenkoae* (M2) Ovnatanova, 1976, GMM B9A.13-3, Sample R top. **d** *Ad. nodosa* (= *gigas* M1) Ulrich and Bassler, 1926, GMM B9A.13-4, Sample R top. **e** *Pa. punctata martenbergensis* Müller, 1956, GMM B9A.13-5, Sample R top. **f** *Pa. amplificata* Klapper, Kuz'min and Ovnatanova, 1996, GMM B9A.13-6, Sample R top. **g** *Pa. hassi* juv. Müller and Müller, 1957, GMM B9A.13-7, Sample R top. **h** *I. symmetricus* (M1) Branson and Mehl, 1934, GMM B9A.13-8, Sample R top. **i** *I. symmetricus* (M1) Branson and Mehl, 1934, GMM B9A.13-9, Sample R top. **j** *Nothognathella* sp., GMM B9A.13-10, Sample R top. **k** *Nothognathella* sp., GMM B9A.13-11, Sample R top. **l** *Ad. nodosa* (= *gigas* M1) Ulrich and Bassler, 1926, GMM B9A.13-12, Sample R-Q base. **m** *Ad. gigas* (= M3) Youngquist, 1947, GMM B9A.13-13, Sample R-Q base. **n** *Ad. gigas* (= M3) Youngquist, 1947, GMM B9A.13-14, Sample R-Q base. **o** *I. symmetricus* (M1) Branson and Mehl, 1934, GMM B9A.13-15, Sample R-Q base. **p** *I. symmetricus* (M2) Branson and Mehl, 1934, GMM B9A.13-16, Sample R-Q base. **q** *Ag. amplicavus* Klapper, Kuz'min and Ovnatanova, 1996, GMM B9A.13-17, Sample R-Q base. **r** *Ag. amplicavus* Klapper, Kuz'min and Ovnatanova, 1996, GMM B9A.13-18, Sample R-Q base.

models by Flügel (2004), and the modified facies types of Hartenfels (2011).

Conodont succession

The section log (Fig. 3) shows the positions of old and new conodont samples, three of which were barren. The complete faunal records supplemented by the data of Ziegler and Sandberg (1990, 2000), Klapper and Becker (1998), and Ovnatanova and Kononova (2020) are given in Table 1. All taxa from resampled beds are illustrated based on a representative selection and in stratigraphic order (Figs. 5, 6, 7, 8, 9, 10, 11, and 12).

The top of Bed R yielded a total of 11 taxa (70 specimens), including *Ad. nodosa* (= *gigas* M1) (Fig. 5d), *Ad. gigas* (= M3) (Fig. 5a), *Ag. coeni* (Fig. 5b), *I. symmetricus* M1 (Figs. 5h, i), *Nothognathella* sp. (Figs. 5j, k), *Pa. amplificata* (Fig. 5f, morphotype without rostrum), *Pa. hassi* (Fig. 5g), *Pa. ljaschenkoae* (M2) (Fig. 5c), *Pa. punctata martenbergensis* (Fig. 5e), *Po. paradecorosus,* and *Po. webbi*. *Palmatolepis martenbergensis* Müller, 1956 is used by us as a subspecies of *Pa. punctata* differing from the nominate form by a marked anterior platform sinus before the lateral lobe and a short offset of the carina at the marked central node.

Our fauna agrees roughly with records of Klapper and Becker (1999), who took samples from the upper 7 cm and 10 cm, respectively, of Bed R. They found in addition *Ag. leonis* (= *tsiensi* auct.), *Ag. amplicavus*, *Ag. barbus, Pa. proversa,* and *Pa. housei* (= aff. *proversa*). The correlation with the data of Ziegler and Sandberg (1990) is not straight forward since their Table 1 combines records from their samples Ma VI/11 and VI/12a; the latter corresponds to our Beds R plus R-Q. Their record of *Ag. triangularis* is doubtful due to their wide taxonomic concept of the species and since a representative was not illustrated. Ovnatanova and Kononova (2020) suggested that the record refers to *Ag. iowaensis*. They confirmed the presence of *Ag. leonis* (= *tsiensi* auct.) as well as *Pa. proversa,* and additionally recorded *Pa. domanicensis* and *Pa. transitans*. We doubt the latter identification, as for higher beds, since *Pa. transitans* normally does not range above the lower half of the middle Frasnian (Klapper 1997). In the absence of illustrations, we do not know which palmatolepid was locally identified as *Pa. transitans* but *Pa. punctata martenbergensis* is an option. In *Pa. transitans*, there may be an anterior platform sinus but no carina offset and no posterior platform sini. An important note in Ovnatanova and Kononova (2020) is the observation that, in Ziegler´s collection, *Pa. plana* occurs only in Sample MA VI´/10 (Bed R-Q), not in the two samples that represent Bed R. The combined alpha diversity (not counting morphotypes) for the upper part of Bed R is 18.

Bed R-Q was sampled with very high stratigraphic resolution due to the existing uncertainties concerning its precise age. It was divided into three segments: R-Q base, R-Q 8–14 cm below top, and R-Q 4.5–8 cm below top. The results of Sample R-Q bulk, taken initially, are presented as well and can be easily correlated with the samples of previous authors. The rich Sample R-Q base yielded a total of 28 taxa (2295 specimens), with a record gap for *Pa. domanicensis*. Compared to our preceding Sample R top, the following conodonts were additionally found: *Ag. amplicavus* (Figs. 5q, r), *Ag. leonis* (Figs. 6a, b), *Ag. triangularis* (Figs. 6c, e, f), *Ad.* cf. *hamata* (= *gigas* M2) (Fig. 7h), *Ad. curvata* (Early Form) (Figs. 7i, j), *Pa. ljaschenkoae* (M1) (Fig. 6g), *Pa. ljaschenkoae* (M3) (Fig. 6j), *Pa. mucronata* (Fig. 6l), *Pa. plana* (Figs. 6m, n), *Pa. proversa* (M1) (Fig. 6p), *Pa. proversa* (M2) (Fig. 6o), *Pa. adorfensis* n. sp. (Figs. 7b, r, s, 9i, j), *Pa.* aff. *feisti* (Fig. 7q), *Pa. jamieae savagei* n. ssp. (M1) (Figs. 8d, e), *Pa. kireevae* (Fig. 7m, juvenile), *Pa. punctata bohemica* (*sepkoskii* Morphotype) (Fig. 7a), *Pa. jamieae rosa* n. ssp. (Fig. 8a), *Pa. simpla* (Fig. 8f), *Pa. manzuri* (Fig. 6k), *Palmatolepis* sp. juv. with smooth platforms (Figs. 7n-p), *I. symmetricus* (M2 = *curvatus*) (Figs. 8b, c), *Po. praepolitus* (Figs. 7e, f), *Po. aequalis* (Figs. 8g, h), and *Po. robustus* (Figs. 8i, j). It is a matter of subjective judgement to recognise *Pa. bohemica* as full species or subspecies of *Pa. punctata*. We think that the differences of *Pa. sepkoskii* Bardashev and Bardasheva (2012), the slight angle of the fine posterior carina and slightly more sinuous posterior platform margin in the holotype, are not significant enough to warrant distinction beyond the morphotype level, the taxonomic concept applied here.

Sample R-Q 8–14 cm below top yielded only 19 taxa (599 specimens), with a record gap of nine further taxa, probably due to the reduced specimen number. Compared to Bed R-Q base, only *Ag. guanxiensis*, represented by a weakly ribbed variant (Fig. 9k), is a new addition. The rich Sample R-Q 4.5–8 cm below top yielded a total of 19 taxa (2905 specimens), with a local record gap for further seven taxa. New forms, compared to Sample R-Q 8–14 cm below top, are *Pa. hassi*

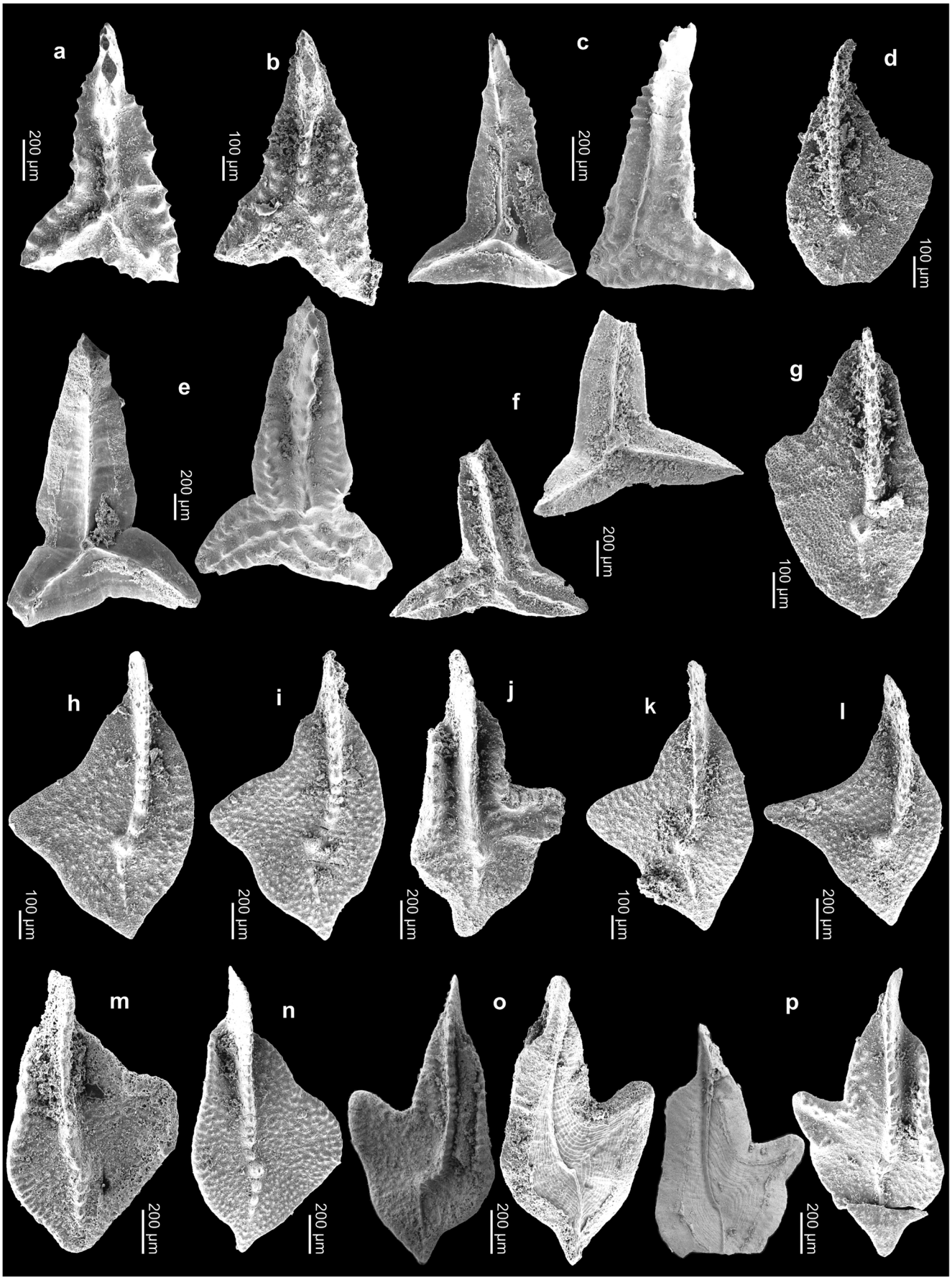
a
200 µm
b
100 µm
c
200 µm
d
100 µm
e
200 µm
f
200 µm
g
100 µm
h
100 µm
i
200 µm
j
200 µm
k
100 µm
l
200 µm
m
200 µm
n
200 µm
o
200 µm
p
200 µm

◀ **Fig. 6** Conodonts from Martenberg, part 2. **a** *Ag. leonis* Sandberg, Ziegler and Dreesen, 1992, GMM B9A.13-19, Sample R-Q base. **b** *Ag. leonis* Sandberg, Ziegler and Dreesen, 1992, GMM B9A.13-20, Sample R-Q base. **c** *Ag. triangularis* Youngquist, 1945, GMM B9A.13-21, Sample R-Q base. **d** *Pa. ljaschenkoae* (M1) Ovnatanova, 1976, GMM B9A.13-22, Sample R-Q base. **e** *Ag. triangularis* Youngquist, 1945, GMM B9A.13-23, Sample R-Q base. **f** *Ag. triangularis* Youngquist, 1945, GMM B9A.13-24, Sample R-Q base. **g** *Pa. ljaschenkoae* (M1) Ovnatanova, 1976, GMM B9A.13-25, Sample R-Q base. **h** *Pa. hassi* Müller and Müller, 1957, GMM B9A.13-26, Sample R-Q base. **i** *Pa. hassi* Müller and Müller, 1957, GMM B9A.13-27, Sample R-Q base. **j** *Pa. ljaschenkoae* (M3) Ovnatanova, 1976, GMM B9A.13-28, Sample R-Q base. **k** *Pa. manzuri*, Bardashev, 2009, GMM B9A.13-29, Sample R-Q base. **l** *Pa. mucronata* Klapper, Kuz'min and Ovnatanova, 1996, GMM B9A.13-30, Sample R-Q base. **m** *Pa. plana* Ziegler and Sandberg, 1990, GMM B9A.13-31, Sample R-Q base. **n** *Pa. plana* Ziegler and Sandberg, 1990, GMM B9A.13-32, Sample R-Q base. **o** *Pa. proversa* (M2) Ziegler, 1958, GMM B9A.13-33, Sample R-Q base. **p** *Pa. proversa* (M1) Ziegler, 1958, GMM B9A.13-35, Sample R-Q base

transitional to *Pa. feisti*, *Pa. feisti* (Figs. 10l-s and 11a-c), *Pa. descendens* n. sp. (Fig. 10k), and *Pa. jamieae savagei* n. ssp. (M2, Fig. 10j). A flood of *Pa. paradecorosus* and dominance of *Pa. hassi* among the palmatolepids are characteristic.

The moderately rich Sample R-Q bulk yielded, combined with previous records, 24 taxa (574 specimens), with a record lack for further two species known from the subunits. Compared to the other samples from the bed, *Pa. domanicensis* (Fig. 11j), *Pa.* cf. *domanicensis*, with a rather narrow, lappet-like side lobe (Fig. 12f), and *Icriodus* sp. 1 with an offset denticle on the cusp (Fig. 12e) are additions. Unusually, the bulk sample did not contain *Pa. feisti*, which may mean that it did not include much material from the upper part of the bed. Ziegler and Sandberg (2000) recorded *Pa. jamieae* from the "upper part of Bed r", which probably is equivalent to our Bed R-Q. Since no specimen was illustrated, and with respect to the wide taxonomic concept applied in Ziegler and Sandberg (1990), which included, e.g. *Pa. feisti* specimens (see Klapper 2007), this record remains doubtful; such records are quoted in the following as "*Pa. jamieae* auct.".

As noted above, the thin volcaniclastics and tuffite layers between beds R-Q and Q yielded no conodonts at all. Sample sizes are normally smaller than in the other cases, but the complete lack of conodonts, even in micritic layers with subordinate volcanic clasts, is surprising. Bed Q was previously divided into several segments (Ziegler and Sandberg 1990; Klapper and Becker 1999). Aiming at high stratigraphic resolution, we separated a sample from the base (Q base, correlating with samples VI′/9 and VI/11b of Ziegler and Sandberg 1990) and from the middle part (Q 18–30 above base), which includes roughly Sample VI′/8 of Ziegler and Sandberg (1990: 15–24 cm above base at a laterally reduced thickness of only 33 cm) and Sample Q 20–25 above base of Klapper and Becker (1999); the first and third are combined here (Table 1). For the upper part of the bed, there are Sample Q 3–13 cm below top of Klapper and Becker (1999) and the samples of Ziegler and Sandberg (1990: VI′/6, 7 = upper 13 cm and IV/1b, which was shown at ca. the level of VI/7).

Sample Q base yielded just four specimens, the long-ranging *I. symmetricus* (M1), *Pa.* cf. *hassi*, and *Po. paradecorosus*. First occurrences of *Pa. nasuta* and a single, encrusted *Pa. semichatovae* were described by Ziegler and Sandberg (2000) from Sample VI/11b. In the absence of illustrations, we cannot re-assign the supposedly associated "*Pa. gigas gigas*". Records of Ziegler and Sandberg (1990) included *Ad. lobata*, *Ad. gigas, Ad. nodosa*, *Ad. curvata, Ag. triangularis* (confirmed by Ovnatanova and Kononova 2020), *Pa. proversa, Pa. punctata* (possibly *punctata martenbergensis*), *Pa. plana,* "*Pa. jamieae* auct." (identification as *jamieae* rejected by Ovnatanova and Kononova 2020), and *I. praealternatus* (= cf. *alternatus*, see Sandberg et al. 1992, p. 61). The revision of material by Ovnatanova and Kononova (2020) added supposed *Pa. transitans* (possibly *punctata martenbergensis*), *Pa. ederi, Po. politus*, *Po. webbi, Po. dubius* (including *Po. foliatus*, see Huddle 1970), *Po. lodinensis,* and *Po. uchtensis*. The combined alpha diversity for the lower part of Bed Q is 20, with record gaps of further eight taxa, such as *Ag. leonis, Pa. ljaschenkoae, Pa. feisti, Pa. simpla, Pa. mucronata*, *Pa. kireevae, Pa. descendens* n. sp., and *Po. praepolitus*.

The new Sample Q 18–30 cm above base yielded a total of 21 taxa (1763 specimens), with six new forms compared to the combined record for the base of the bed: *Ad. curvata* (Late Form) (Fig. 12l) and an unusual, single *I. alternatus* cf. *helmsi*, a specimen with inner longitudinal row of nodes turned into irregular ribs (Fig. 12i). It is the type-level of the rare *Po. descendens* n. sp. (Figs. 12g, h). We could confirm the presence of *Pa. nasuta* (Figs. 12j, k) and found the last local *Pa. mucronata.* Additionally, *Pa. uyenoi* was described by Klapper and Becker (1998) from their Sample Q 20–25 cm above base. Ziegler and Sandberg (1990) found in the middle of Bed Q, in addition, *Ad. gigas*, *Ad. lobata, Pa. punctata* (probably *punctata martenbergensis*), and *Pa. proversa*. Ovnatanova and Kononova (2020) added *Pa. kireevae, Pa. ljaschenkoae, Pa. "transitans", Pa. ederi*, *Po. politus, Po. lodinensis,* and *Po. uchtensis*. The combined alpha diversity for the middle of Bed Q is 21, with six further record gaps.

For the upper part of Bed Q, we summarise data from the literature, which include Samples VI′/6, 7 (upper 9 of 33 cm), parts of Sample VI/11a, Sample IV/1b of Ziegler and Sandberg (1990), and Sample Q 3–13 cm below top of Klapper and Becker (1999). There are no newcomers in relation to the middle part of the bed. *Palmatolepis feisti* is still present and includes specimens identified by Ziegler and Sandberg (1990) as *Pa. jamieae* (see Klapper 2007, p. 523). *Palmatolepis jamieae jamieae* does not occur (Ovnatanova and Kononova, 2020). Klapper and Becker (1999) reported *Pa. uyenoi* as *Pa.* aff. *Pa. winchelli* and *Pa. feisti* as *Palmatolepis* sp. B. The combined alpha diversity is only


a
200 µm
b
200 µm
c
200 µm
d
200 µm
e
100 µm
f
100 µm
g
200 µm
h
200 µm
i
200 µm
j
200 µm
k
100 µm
l
200 µm
m
100 µm
n
100 µm
o
100 µm
p
100 µm
q
100 µm
r
200 µm
s
200 µm

◀ **Fig. 7** Conodonts from Martenberg, part 3. **a** *Pa. punctate bohemica* (*sepkoskii* Morphotype) Klapper and Foster Jr., 1993, GMM B9A.13-37, Sample R-Q base. **b** *Pa. adorfensis* n. sp., slightly atypical, GMM B9A.13-38, Sample R-Q base. **c** *Po. paradecorosus* Ji and Ziegler, 1993, GMM B9A.13-39, Sample R-Q base. **d** *Po. paradecorosus* Ji and Ziegler, 1993, GMM B9A.13-40, Sample R-Q base. **e** *Po. praepolitus* Kononova, Alekseev and Barskov, 1996, GMM B9A.13-41, Sample R-Q base. **f** *Po. praepolitus* Kononova, Alekseev and Barskov, 1996, GMM B9A.13-42, Sample R-Q base. **g** *Nothognathella* sp., GMM B9A.13-42, Sample R-Q base. **h** *Ad.* cf. *hamata* Ulrich and Bassler, 1926, *hamata* sensu Klapper (2021) with nodes only, GMM B9A.13-43, Sample R-Q base. **i** *Ad. curvata* (Early Form) (Branson and Mehl, 1934), GMM B9A.13-44, Sample R-Q base. **j** *Ad. curvata* (Early Form) (Branson and Mehl, 1934), GMM B9A.13-45, Sample R-Q base. **k** *Po. webbi* Stauffer, 1938, GMM B9A.13-46, Sample R-Q base. **l** *Pa.* cf. *amplificata* Klapper, Kuz'min and Ovnatanova, 1996, GMM B9A.13-47, Sample R-Q base. **m** *Pa. kireevae* juv. Ovnatanova, 1976, GMM B9A.13-48, Sample R-Q base. **n** *Palmatolepis* sp. juv., GMM B9A.13-49, Sample R-Q base. **o** *Palmatolepis* sp. juv., GMM B9A.13-50, Sample R-Q base. **p** *Palmatolepis* sp. juv., GMM B9A.13-51, Sample R-Q base. **q** *Pa.* aff. *feisti* Klapper, 2007, GMM B9A.13-52, Sample R-Q base. **r** *Pa. adorfensis* n. sp., GMM B9A.13-53, Sample R-Q base (holotype). **s** *Pa. adorfensis* n. sp., GMM B9A.13-54, Sample R-Q base (paratype)

17, with additional record gaps for two species, *Pa. kireevae* and *Po. lodinensis*. Notable are the youngest local records of *Ad. curvata* (Early Form) and *Pa. ederi*.

Bed P was divided by Klapper and Becker (1999) into two segments (0–8 cm and 8–18 cm). We re-sampled the lower part (Sample P base) and confirmed in comparison to the combined evidence of all previous papers the FODs of *Pa. winchelli* (Fig. 12n), *Pa. brevis* (Fig. 12p), *Pa. rhenana* (Fig. 12m), *Pa. jamieae jamieae* (Fig. 12o), *Ad. ioides* (M1, Fig. 12t), and *Ad. ioides* (s.str.). There is a single *Pa. jamieae rosa* n. ssp., three *Pa. jamieae savagei* n. ssp. (M2, Figs. 12q–s), and *Pa. jamieae jamieae* is represented by only one specimen. As in older beds, *Pa. hassi* is dominant. In Samples VI′/5 and VI/10e of Ziegler and Sandberg (1990) from the lower part of Bed P, the locally youngest *Pa. proversa* were recorded, which meant an upper range extension in relation to the composite range of Klapper et al. (1996). We have reservations concerning Bed P records in Ziegler and Sandberg (1990) of *Pa. punctata* and *Pa. plana*.

The following taxa constitute the known Martenberg conodont faunas around the middle/upper Frasnian boundary (see Table 1):

- *Ad. curvata* (Early Form of Klapper 1989) (Branson and Mehl, 1934), Figs. 7i, j, 11p, 52 specimens
- *Ad. curvata* (Late Form of Klapper 1989) (Branson and Mehl, 1934), Fig. 12q, four specimens
- *Ad. gigas* (= M3 of Klapper 1989) Youngquist, 1947, Figs. 5a, m, n, 8o, p, 206 specimens
- *Ad. hamata* Ulrich and Bassler, 1926, sensu its type, Figs. 9g, h, two specimens
- *Ad.* cf. *hamata* Ulrich and Bassler, 1926, *hamata* sensu Klapper (2021) with nodes only, Fig. 7h, one specimen
- *Ad. ioides* Ziegler, 1958, 23 specimens
- *Ad. ioides* (M1 of Klapper 2021) Ziegler, 1958, Figs. 12t, 1 specimen
- *Ad. lobata* Branson and Mehl, 1934 (records of Ziegler and Sandberg 1990 and Ovnatanova and Kononova 2020)
- *Ad. nodosa* (= *gigas* M1 of Klapper 1989) Ulrich and Bassler, 1926, Figs. 5d, l, 8k, l, 11h, i, 375 specimens
- *Ag. amplicavus* Klapper, Kuz'min and Ovnatanova, 1996, Figs. 5q, s, 11g, 13 specimens
- *Ag. coeni* Klapper, 1990, Fig. 5b, 45 specimens
- *Ag. guangxiensis* Wang, 1994, Fig. 9k, one specimen
- *Ag. iowaensis* Youngquist, 1947 (record of Ovnatanova and Kononova 2020)
- *Ag. leonis* (= "*tsiensi*" auct. of Mouravieff 1982) Sandberg, Ziegler and Dreesen, 1992, Figs. 6a, b, 8m, n, 11f, 27 specimens
- *Ag. triangularis* Youngquist, 1945, Figs. 6c, e, f, 9o, p, q, 11k, l, 112 specimens
- *I. prealternatus prealternatus* Sandberg, Ziegler and Dreesen, 1992, 17 specimens
- *I. alternatus* cf. *helmsi* Sandberg and Dreesen, 1984, Fig. 12i, one specimen
- *I. symmetricus* (M1 of this study) Branson and Mehl, 1934, Figs. 5h, i, o, 526 specimens
- *I. symmetricus* (M2 of this study = *curvatus*) Branson and Mehl, 1934, Figs. 5p, 8b, c, 180 specimens
- *Nothognathella* sp., Figs. 5j, k, 7g, 180 specimens
- *Pa. adorfensis* n. sp., Figs. 7b, r, s, 9i, j, five specimens
- *Pa. amplificata* Klapper, Kuz'min and Ovnatanova, 1996, Figs. 5f, 7l (cf.), 9m (cf.), 9n, 11d-e, r, 30 specimens
- *Pa. brevis* Ziegler and Sandberg, 1990, Fig. 12p, four specimens
- *Pa. descendens* n. sp., Figs. 10k, 12g, h, three specimens
- *Pa. domanicensis* Ovnatanova, 1976, Fig. 11j, one specimen
- *Pa.* cf. *domanicensis* Ovnatanova, 1976, Fig. 12f, one specimen
- *Pa. ederi* Ziegler and Sandberg, 1990 (records of Ziegler and Sandberg 1990 and Ovnatanova and Kononova 2020)
- *Pa. feisti* Klapper, 2007, Figs. 10l-s, 11a-c, 352 specimens
- *Pa.* aff. *feisti* Klapper, 2007, Figs. 7q, 12a, b, four specimens
- *Pa. hassi* Müller and Müller, 1957, Figs. 5g, 6h, i, 8r, s, 10c, d, 1582 specimens
- *Pa. housei* Klapper, 2007 (record of Klapper and Becker 1999: recorded as *Pa.* aff. *proversa*)
- *Pa. jamieae jamieae* Ziegler and Sandberg, 1990, Fig. 12o, one specimen, platform rather narrow
- *Pa. jamieae savagei* n. ssp. (M1), Figs. 8d, e, 10g, h, i, five specimens
- *Pa. jamieae savagei* n. ssp. (M2), Figs. 12q, s, three specimens, Fig. 12r, one questionable specimen intermediate towards *jamieae savagei* n. ssp. (M1), Fig. 10j, one questionable specimen intermediate towards *jamieae jamieae*


a
b
c
d
e
f
g
h
i
j
k
l
m
n
o
p
q
r
s
t
u
100 µm
200 µm

◀ **Fig. 8** Conodonts from Martenberg, part 4. **a** *Pa. jamieae rosa* n. ssp., GMM B9A.13-55, Sample R-Q base (paratype). **b** *I. symmetricus* (M2) Branson and Mehl, 1934, GMM B9A.13-56, Sample R-Q base. **c** *I. symmetricus* (M2) Branson and Mehl, 1934, GMM B9A.13-57, Sample R-Q base. **d** *Pa. jamieae savagei* n. ssp. (M1), GMM B9A.13-58, Sample R-Q base (paratype). **e** *Pa. jamieae savagei* n. ssp. (M1), GMM B9A.13-59, Sample R-Q base (holotype). **f** *Pa. simpla* Ziegler and Sandberg, 1990, GMM B9A.13-60, Sample R-Q base. **g** *Po. aequalis* Klapper and Lane, 1985, GMM B9A.13-61, Sample R-Q base. **h** *Po. aequalis* Klapper and Lane, 1985, GMM B9A.13-62, Sample R-Q base. **i** *Po. robustus* Klapper and Lane, 1985, GMM B9A.13-63, Sample R-Q base. **j** *Po. robustus* Klapper and Lane, 1985, GMM B9A.13-64, Sample R-Q base. **k** *Ad. nodosa* (= *gigas* M1) Ulrich and Bassler, 1926, GMM B9A.13-65, Sample R-Q 8-14 cm below top. **l** *Ad. nodosa* (= *gigas* M1) Ulrich and Bassler, 1926, GMM B9A.13-66, Sample R-Q 8-14 cm below top. **m** *Ag. leonis* Sandberg, Ziegler and Dreesen, 1992, GMM B9A.13-67, Sample R-Q 8-14 cm below top. **n** *Ag. leonis* Sandberg, Ziegler and Dreesen, 1992, GMM B9A.13-68, Sample R-Q 8-14 cm below top. **o** *Ad. gigas* (= M3) Youngquist, 1947, GMM B9A.13-69, Sample R-Q 8-14 cm below top. **p** *Ad. gigas* (= M3) Youngquist, 1947, GMM B9A.13-70, Sample R-Q 8-14 cm below top. **q** *Ag. leonis* Sandberg, Ziegler and Dreesen, 1992, GMM B9A.13-71, Sample R-Q 8-14 cm below top. **r** *Pa. hassi* Müller and Müller, 1957, GMM B9A.13-72, Sample R-Q 8-14 cm below top. **s** *Pa. hassi* Müller and Müller, 1957, GMM B9A.13-73, Sample R-Q 8-14 cm below top. **t** *Pa. ljaschenkoae* (M2) Ovnatanova, 1976, GMM B9A.13-74, Sample R-Q 8-14 cm below top. **u** *Pa. ljaschenkoae* (M2) Ovnatanova, 1976, GMM B9A.13-75, Sample R-Q 8-14 cm below top

- *Pa. jamieae rosa* n. ssp., Figs. 8a, 9l, three specimens
- *Pa. kireevae* Ovnatanova, 1976, Figs. 7m, 11s, 24 specimens
- *Pa. ljaschenkoae* (M1 of this study) Ovnatanova, 1976, Figs. 6d, g, 9r, 11m, 16 specimens
- *Pa. ljaschenkoae* (M2 of this study) Ovnatanova, 1976, Figs. 5c, 8t, u, 11n, 303 specimens
- *Pa. ljaschenkoae* (M3 of this study) Ovnatanova, 1976, Figs. 6j, 9d, 10a, b, 11o, 130 specimens
- *Pa. manzuri* Bardashev, 2009, Fig. 6k, 13 specimens
- *Pa. mucronata* Klapper, Kuz'min and Ovnatanova, 1996, Figs. 6l, 9c, 10e, 47 specimens
- *Pa. nasuta* Müller, 1956, Figs. 12j, k, 27 specimens
- *Pa. plana* Ziegler and Sandberg, 1990, Figs. 6m, n, 9a, b, 10f, 93 specimens
- *Pa. proversa* (M1 of this study) Ziegler, 1958, Figs. 6p, 9e, f, 51 specimens
- *Pa. proversa* (M2 of this study) Ziegler, 1958, Figs. 6o, 11q, 178 specimens
- *Pa. punctata bohemica* (*sepkoskii* Morphotype of this study) Klapper and Foster Jr., 1993, Fig. 7a, one specimen
- *Pa. punctata martenbergensis* Müller, 1956, Fig. 5e, seven specimens
- *Pa. rhenana* Bischoff, 1956, Fig. 12m, 15 specimens
- *Pa. semichatovae* Ovnatanova, 1976 (one specimen recorded by Ziegler and Sandberg 1990)
- *Pa. simpla* Ziegler and Sandberg, 1990, Figs. 8f, 12c, d, 13 specimens
- *Pa. uyenoi* Klapper, 2007 (record of Klapper and Becker 1999)
- *Pa. winchelli* (Stauffer, 1938) (senior synonym of *Pa. subrecta* Klapper and Foster Jr., 1993), Fig. 12n, seven specimens
- *Po. aequalis* Klapper and Lane, 1985, Figs. 8g, h, three specimens
- *Po. lodinensis* Pölsler, 1969 (record of Ovnatanova and Kononova 2020)
- *Po. paradecorosus* Ji and Ziegler, 1993, Figs. 7c, d, 3430 specimens
- *Po. politus* Ovnatanova, 1969 (record of Ovnatanova and Kononova 2020)
- *Po. praepolitus* Kononova, Alekseev and Barskov, 1996, Figs. 7e, f, 33 specimens
- *Po. robustus* Klapper and Lane, 1985, Figs. 8i, j, 37 specimens
- *Po. uchtensis* Ovnatanova and Kuz'min, 1991 (record of Ovnatanova and Kononova 2020)
- *Po. webbi* Stauffer, 1938, Fig. 7k, 312 specimens

Stratigraphic interpretation and diversity trends of Martenberg succession

No zonal marker was found in Sample R top by our re-sampling, but Ziegler and Sandberg (1990), confirmed by Ovnatanova and Kononova (2020), found *Pa. proversa*, the index fossil of Frasnian Zone 9 (*proversa* Zone) in Bed R and much further below. Ziegler and Sandberg (1990) recorded in addition *Pa. plana*, index fossil of Frasnian Zone 10 (*plana* Zone), but this was rejected for the detailed succession of Section VI′ by the revision of samples by Ovnatanova and Kononova (2020, p. 116). Typical *Pa. amplificata* enter, after Klapper et al. (1996), in the higher part of Frasnian Zone 10 while Bardashev (2009) gave a lower range for the closely related *Pa. manzuri*. We collected specimens that are intermediate between the types of the two species, which are, therefore, in accord with the published ages. Ovnatanova and Kononova (2020) showed, for the Timan, a joint entry of *Pa. amplificata* with *Pa. proversa*. *Ancyrognathus amplicavus* enters already at the base of Frasnian Zone 7 (Klapper et al. 1996), *Ag. iowaensis* at the base of Frasnian Zone 9 (Klapper and Kirchgasser 2016), *Pa. ljaschenkoae* near the top of Frasnian Zone 8 (Klapper 1997), and *Pa. mucronata* in the upper part of Frasnian Zone 9. The co-occurrence of *Ag. barbus* and *Pa. mucronata* found by Klapper and Becker (1999) meant an upper range extension for the first taxon; previously (Klapper 1997), *Ag. barbus* was thought to range only into the middle of Frasnian Zone 8. In

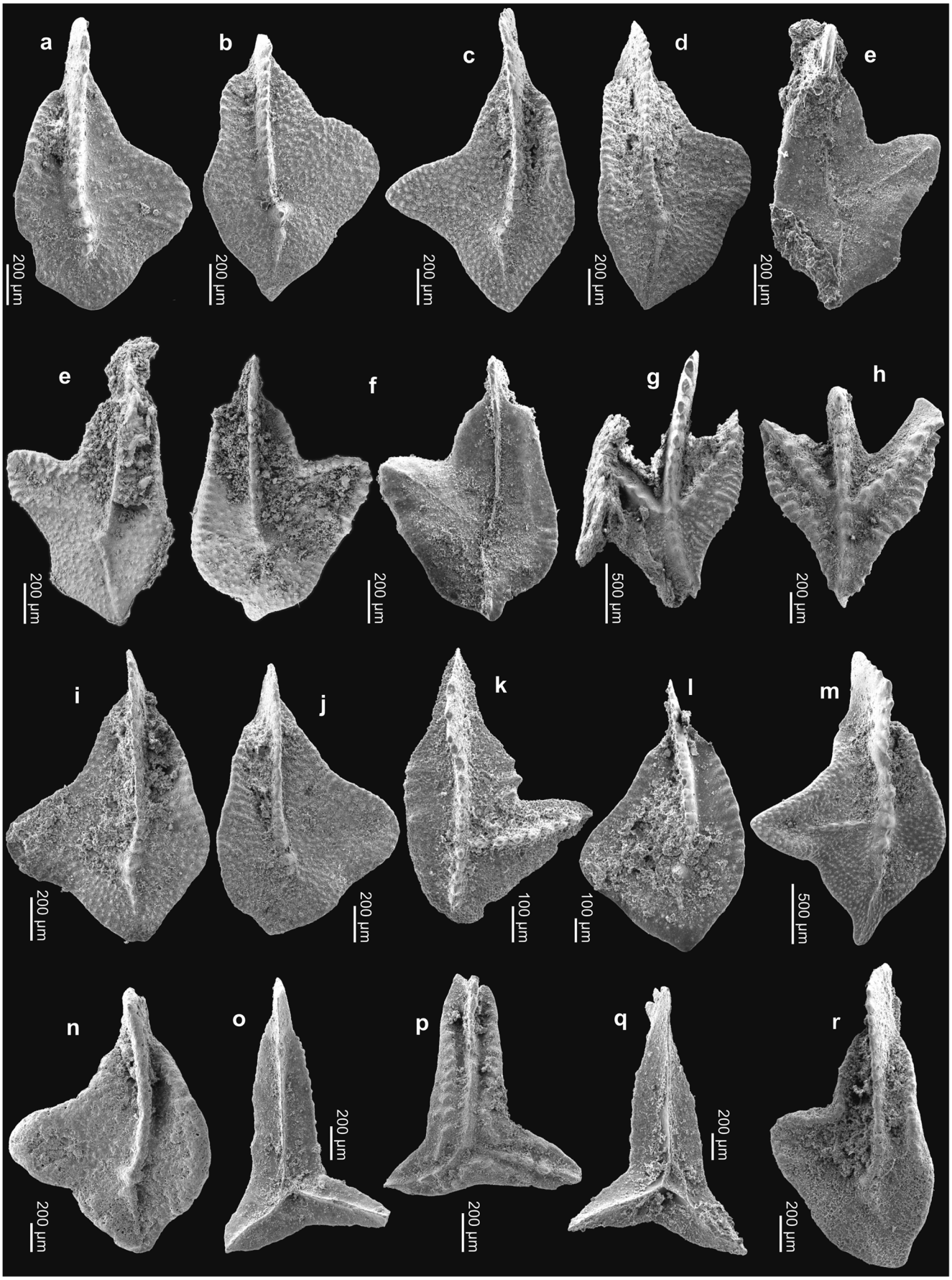
a
200 µm
b
200 µm
c
200 µm
d
200 µm
e
200 µm
e
200 µm
f
200 µm
g
500 µm
h
200 µm
i
200 µm
j
200 µm
k
100 µm
l
100 µm
m
500 µm
n
200 µm
o
200 µm
p
200 µm
q
200 µm
r
200 µm

◀ **Fig. 9** Conodonts from Martenberg, part 5. **a** *Pa. plana* Ziegler and Sandberg, 1990, GMM B9A.13-76, Sample R-Q 8-14 cm below top. **b** *Pa. plana* Ziegler and Sandberg, 1990, GMM B9A.13-77, Sample R-Q 8-14 cm below top. **c** *Pa. mucronata* Klapper, Kuz'min and Ovnatanova, 1996, GMM B9A.13-78, Sample R-Q 8-14 cm below top. **d** *Pa. ljaschenkoae* (M3) Ovnatanova, 1976, GMM B9A.13-79, Sample R-Q 8-14 cm below top. **e** *Pa. proversa* (M1) Ziegler, 1958, GMM B9A.13-80, Sample R-Q 8-14 cm below top. **f** *Pa. proversa* (M1) Ziegler, 1958, GMM B9A.13-83, Sample R-Q 8-14 cm below top. **g** *Ad. hamata* Ulrich and Bassler, 1926, typical form, GMM B9A.13-84, Sample R-Q 8-14 cm below top. **h** *Ad. hamata* Ulrich and Bassler, 1926, typical form, GMM B9A.13-85, Sample R-Q 8-14 cm below top. **i** *Pa. adorfensis* n. sp., GMM B9A.13-86, Sample R-Q 8-14 cm below top (paratype). **j** *Pa. adorfensis* n. sp., GMM B9A.13-87, Sample R-Q 8-14 cm below top (paratype). **k** *Ag. guanxiensis* Wang, 1994, GMM B9A.13-88, Sample R-Q 8-14 cm below top. **l** *Pa. jamieae rosa* n. ssp., GMM B9A.13-89, Sample R-Q 8-14 cm below top (holotype). **m** *Pa.* cf. *amplificata* Ulrich and Bassler, 1926, GMM B9A.13-90, Sample R-Q 8-14 cm below top. **n** *Pa. amplificata* Ulrich and Bassler, 1926, GMM B9A.13-91, Sample R-Q 8-14 cm below top. **o** *Ag. triangularis* Youngquist, 1945, GMM B9A.13-92, Sample R-Q 4.5-8 cm below top. **p** *Ag. triangularis* Youngquist, 1945, GMM B9A.13-93, Sample R-Q 4.5-8 cm below top. **q** *Ag. triangularis* Youngquist, 1945, GMM B9A.13-94, Sample R-Q 4.5-8 cm below top. **r** *Pa. ljaschenkoae* (M1) Ovnatanova, 1976, GMM B9A.13-95, Sample R-Q 4.5-8 cm below top

summary, it seems that the top of Bed R is not younger than the upper Frasnian Zone 9 (*proversa* Zone).

Due to the first occurrence of *Pa. plana* (Figs. 6m, n) in our re-sampling, Sample R-Q base can be assigned to Frasnian Zone 10 (*plana* Zone). Previously, Bed R-Q has not been studied with our stratigraphic precision. *Palmatolepis plana* is found in all three segments (R-Q base, R-Q 8–14 cm below top, R-Q 4.5–8 cm below top) as well as in Sample R-Q bulk. Therefore, the boundary between Frasnian zones 9/10 is placed at the base of Bed R-Q. In addition, Sample R-Q base includes *Pa. jamieae savagei* n. ssp. (M1) (Figs. 8d, e), *Pa. adorfensis* n. sp. (Figs. 7b, r, s, 9i, j), and *Pa. jamieae rosa* n.ssp. (Fig. 8a), which become accessory Frasnian Zone 10 indicators. "*Palmatolepis jamieae*" specimens of Ziegler and Sandberg (2000) were probably based on one or some of these taxa. This provides a correlation of the base of the Frasnian Zone 10 (*plana* Zone) with the *jamieae* Zone sensu Ziegler and Sandberg (2000), but all early forms resembling, to some extent, *Pa. jamieae* are too rare to be used as zonal index taxa. The strong increase of alpha diversity in Frasnian Zone 10 (*plana* Zone) is probably an artefact of the strong increase of available specimens; most newcomers occur in small numbers.

Unexpected was the early entry of *Ag. triangularis* (Figs. 6c, e, f), which has not been verified in Frasnian Zone 10 (*plana* Zone) until now (see composite ranges in Klapper 1997 and Klapper and Kirchgasser 2016). The diagnostic free blade of these early representatives is partly preserved (Fig. 6c). The basal pit becomes relatively smaller with growth. As a consequence, *Ag. triangularis* loses its status as auxiliary Frasnian Zone 11 (*feisti* Zone) indicator, but becomes important to recognise levels from Frasnian Zone 10 (*plana* Zone) upwards. This has implications for the precise dating of reef extinctions and the separation of the two deepening pulses in the middle/upper Frasnian transition.

The single *Ag. guangxiensis* from Sample R-Q 8–14 below top is of some stratigraphic value. The species was originally described from the middle of the Lower *rhenana* Zone of Sihongshan, Guangxi (Wang and Ziegler 1983), but a slightly older, weakly ribbed representative was found above the entries of *Pa. plana* and *Ag. triangularis* at Longmen (Wang 1994). This gives a perfect match with our weakly ribbed Martenberg specimen from the higher Frasnian 10 Zone (*plana* Zone), which at the same time means a new record for Europe. The Montagne Noire record of *Ag. guangxiensis* (Klapper 1989) belongs to the related *Ag. barbus* (see Sandberg et al. 1992, p. 52, and Klapper 1997, p. 124). In comparison to the base of the zone, the alpha diversity stagnated when the sample-size related record gaps are taken into consideration.

Sample R-Q 4.5–8 cm below top yielded *Pa. feisti* (Figs. 10l-s, 11a-c), the Frasnian Zone 11 (*feisti* Zone) index species. Since we divide this zone (see below), it also marks the base of the Frasnian 11a Subzone (*feisti* Subzone). Associated are oldest *Pa. descendens* n. sp. (Fig. 10k) and a *Pa. jamieae savagei* n. ssp. (M2) that approaches *Pa. jamieae jamieae* (Fig. 10j). The rare *Icriodus* sp. 1 is distinctive, but perhaps pathological. In relation to the preceding zone, there is no significant change of alpha diversity.

Because of *Pa. nasuta* and rare *Pa. semichatovae* found by Ziegler and Sandberg (2000), the lower part of Bed Q can be assigned to a distinctive subdivision of the Frasnian Zone 11, the new Frasnian Subzone 11b or *nasuta* Subzone. The base correlates straight with the base of the Lower *rhenana* Zone sensu Ziegler and Sandberg (1990) and with the base of the *semichatovae* Subzone sensu Morrow and Sandberg (2008) that is typical for more shallow-water successions. The entry of *Po. lodinensis* adds to the subzone distinction; the species enters in the composite range of Klapper et al. (1996) slightly above the base of Frasnian Zone 11. The record of *Po. uchtensis* at this level is somewhat unusual since the species does not overlap with *Pa. semichatovae* in its Timan type region (Ovnatanova and Kononova 2020, Fig. 3). *Palmatolepis semichatovae* is very rare in the Rhenish Massif. Apart from the occurrence at Martenberg and from four specimens from the Schmidt Quarry (Ziegler and Sandberg 1990, Bed 21), the only other record is a single specimen from the Hölloch Valley of the Lahn Syncline (Gereke 2007, p. 58).

The local decline, not necessarily their final extinction, of some previously characteristic species seems typical for the transition from Bed R-Q to Bed Q: *Ag. coeni, Ag. leonis, Pa. amplificata, Pa. domanicensis,* and *Pa. kireevae*. Frasnian Subzones 11a and 11b are physically separated at Martenberg by an interval with unconformities and current-induced sedimentation immediately preceding the *semichatovae* Transgression (see microfacies analyses below). This sedimentary break did not result in a reduction of total alpha diversity. The

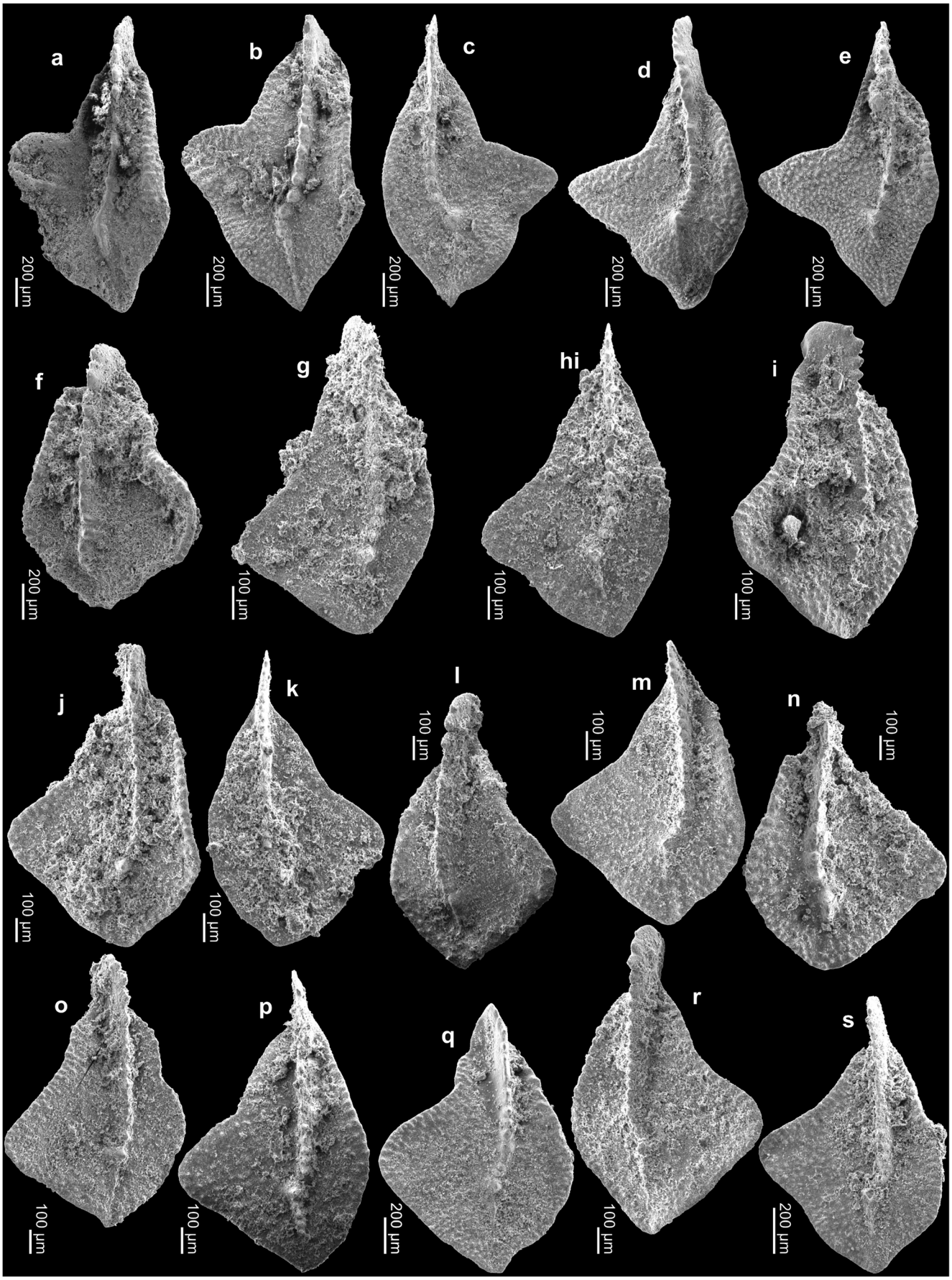
a
200 µm
b
200 µm
c
200 µm
d
200 µm
e
200 µm
f
200 µm
g
100 µm
hi
100 µm
i
100 µm
j
100 µm
k
100 µm
l
100 µm
m
100 µm
n
100 µm
o
100 µm
p
100 µm
q
200 µm
r
100 µm
s
200 µm

◀ **Fig. 10** Conodonts from Martenberg, part 6. **a** *Pa. ljaschenkoae* (M3) Ovnatanova, 1976, GMM B9A.13-96, Sample R-Q 4.5-8 cm below top. **b** *Pa. ljaschenkoae* (M3) Ovnatanova, 1976, GMM B9A.13-97, Sample R-Q 4.5-8 cm below top. **c** *Pa. hassi* Müller and Müller, 1957, GMM B9A.13-98, Sample R-Q 4.5-8 cm below top. **d** *Pa. hassi* Müller and Müller, 1957, GMM B9A.13-99, Sample R-Q 4.5-8 cm below top. **e** *Pa. mucronata* Klapper, Kuz'min and Ovnatanova, 1996, GMM B9A.13-100, Sample R-Q 4.5-8 cm below top. **f** *Pa. plana* Ziegler and Sandberg, 1990, GMM B9A.13-101, Sample R-Q 4.5-8 cm below top. **g** *Pa. jamieae savagei* n. ssp. (M1), GMM B9A.13-103, Sample R-Q 4.5-8 cm below top (paratype). **h** *Pa. jamieae savagei* n. ssp. (M1), GMM B9A.13-104, Sample R-Q 4.5-8 cm below top (paratype). **i** *Pa. jamieae savagei* n. ssp. (M1), GMM B9A.13-105, Sample R-Q 4.5-8 cm below top (paratype). **j** *Pa. jamieae savagei* n. ssp. (M2), GMM B9A.13-106, Sample R-Q 4.5-8 cm below top (paratype), specimen intermediate towards *Pa. jamieae jamieae*. **k** *Pa. descendens* n. sp., GMM B9A.13-107, Sample R-Q 4.5-8 cm below top (holotype). **l** *Pa. feisti* Klapper, 2007, GMM B9A.13-108, Sample R-Q 4.5-8 cm below top. **m** *Pa. feisti* Klapper, 2007, GMM B9A.13-109, Sample R-Q 4.5-8 cm below top. **n** *Pa. feisti* Klapper, 2007, GMM B9A.13-110, Sample R-Q 4.5-8 cm below top. **o** *Pa. feisti* Klapper, 2007, GMM B9A.13-111, Sample R-Q 4.5-8 cm below top. **p** *Pa. feisti* Klapper, 2007, GMM B9A.13-112, Sample R-Q 4.5-8 cm below top. **q** *Pa. feisti* Klapper, 2007, GMM B9A.13-113, Sample R-Q 4.5-8 cm below top. **r** *Pa. feisti* Klapper, 2007, GMM B9A.13-114, Sample R-Q 4.5-8 cm below top. **s** *Pa. feisti* Klapper, 2007, GMM B9A.13-115, Sample R-Q 4.5-8 cm below top

disappearance of taxa was balanced by newcomers; the *semichatovae* Event is locally characterised by faunal turnover, with continuing high levels of episodic record gaps.

The middle and upper parts of Bed Q represent the middle and upper Frasnian Subzone 11b (*nasuta* Subzone). The local entry of *Ad. curvata* Late Form (new records) is interesting but the morphotype has a lower range, starting at the base of the Frasnian Zone 10 (*plana* Zone) in the Frasnian composite (Klapper and Kirchgasser 2016). The entry of *Palmatolepis uyenoi* recorded by Klapper and Becker (1999) seems suitable to characterise a higher level of the Frasnian 11b Subzone (see composite range in Klapper 2007, p. 529: CSU 113.1–124.4). The restriction of *Pa. ederi* to Frasnian Subzone 11b (*nasuta* Subzone) at Martenberg agrees with the upper composite range of Klapper et al. (1996) but Ziegler and Sandberg (1990) reported younger specimens from other sections. Following the original illustrations of Ziegler and Sandberg (1990) (compare synonymy of Klapper 1997), revisions of Ovnatanova and Kononova (2020), and our re-sampling, there are no *Pa. jamieae* s.str. (= *jamieae jamieae*) in the Martenberg Frasnian Subzone 11b (*nasuta* Zone). At Schmidt Quarry in the Kellerwald region, the type-level of *Pa. jamieae jamieae* coincides with the local FOD of *Pa. nasuta* (Ziegler and Sandberg 1990, Table 2, Sample 84-GER-1 = Bed 23), but associated *Ad. ioides* indicate a level above Frasnian Zone 11, which is supported by the position of the *Pa. semichatovae* level, indicating Frasnian Subzone 11b (*nasuta* Subzone) well below (Bed 21). However, there may be Frasnian Zone 11 records of *Pa. jamieae jamieae* from other regions (see stratigraphic range in taxonomic chapter).

Because of the first occurrences of *Pa. winchelli* and *Ad. ioides*, the lower part of Bed P falls in the basal Frasnian Zone 12 (*winchelli* Zone). Based on the revised Martenberg record of Ovnatanova and Kononova (2020, p. 117), on our two new specimens, and because of the association of the holotype with *Ad. ioides* at Schmidt Quarry, this is the type and main level of *Pa. jamieae jamieae*. We confirm the upper range extension of Ovnatanova and Kononova (2020) for *Pa. brevis*, which Ziegler and Sandberg (1990) regarded as typical for the Lower *rhenana* Zone. The local downwards range extension of *Pa. rhenana* (= *rhenana rhenana*) by Ziegler and Sandberg (2000) and Ovnatanova and Kononova (2020, p. 117) is also confirmed by our new sample from the base of Bed P. It means that the index species of the Upper *rhenana* Zone enters near the base of Frasnian 12 Zone (*winchelli* Zone). In the Frasnian composite of Klapper (1997), its FAD is at CSU 124.3, higher in the Frasnian Zone 12, and only slightly below the Lower Kellwasser level (compare FOD at Steinbruch Schmidt, Ziegler and Sandberg 1990). We prefer *Pa. winchelli* (= *subrecta*) as zonal index species but are pleased about the improved precision in the correlation of Frasnian Zonation and "Standard Zones".

The literature data (see Table 1) suggest a decline of alpha diversity in Frasnian Subzone 11b (*nasuta* Subzone) and Frasnian Zone 12 (*winchelli* Zone), down to 19–23 taxa (from 26–28, local Lazarus Taxa included). The proven alpha diversity of only 16 recorded taxa in the lower part of Bed P probably reflects the much smaller number of recovered specimens (365, Table 1) in relation to the middle part of Bed Q (with 1763 specimens). When we consider all previous faunas, the alpha diversities of the upper part of Bed Q and of Bed P do not differ. Above our study interval, a distinctive upper subdivision of the Frasnian Zone 12 (*winchelli* Zone) is marked by the successive entries of *Po. kirchgasseri* (= *Polygnathus* n. sp. BT, lower part of Bed M, Klapper and Becker 1999) and, elsewhere, of *Ag. asymmetricus* in the Lower Kellwasser Limestone (upper part of Bed M).

Systematic palaeontology

Icriodus symmetricus Branson and Mehl, 1934
(M1: Figs. 5h, i, o; M2: Figs. 5p, 8b, c)

* 1934 .*Icriodus symmetricus* - Branson and Mehl: p. 226, pl. 13, figs. 1–3 [= M1].

* 1938 *Icriodus curvatus* - Branson and Mehl: p. 162, pl. 26, figs. 23–26 [= M2].

1984 *Icriodus symmetricus* - Sandberg and Dreesen: p. 157, pl. 1, figs. 2–6 [figs. 2–4 = M2, fig. 5 = juv., fig. 6 = M1].

1993 *Icriodus symmetricus* - Ji and Ziegler: p. 57, pl. 5, figs. 11–13 [= M2].

1994 *Icriodus symmetricus* - Wang: pl. 8, figs. 2–3, 9 [fig. 2 = M1, figs. 3, 9 = M2].

1998 *Icriodus symmetricus* - Bultynck et al.: p. 57, pl. 8, figs. 24–25 [fig. 24 = M1, fig. 25 = M1].

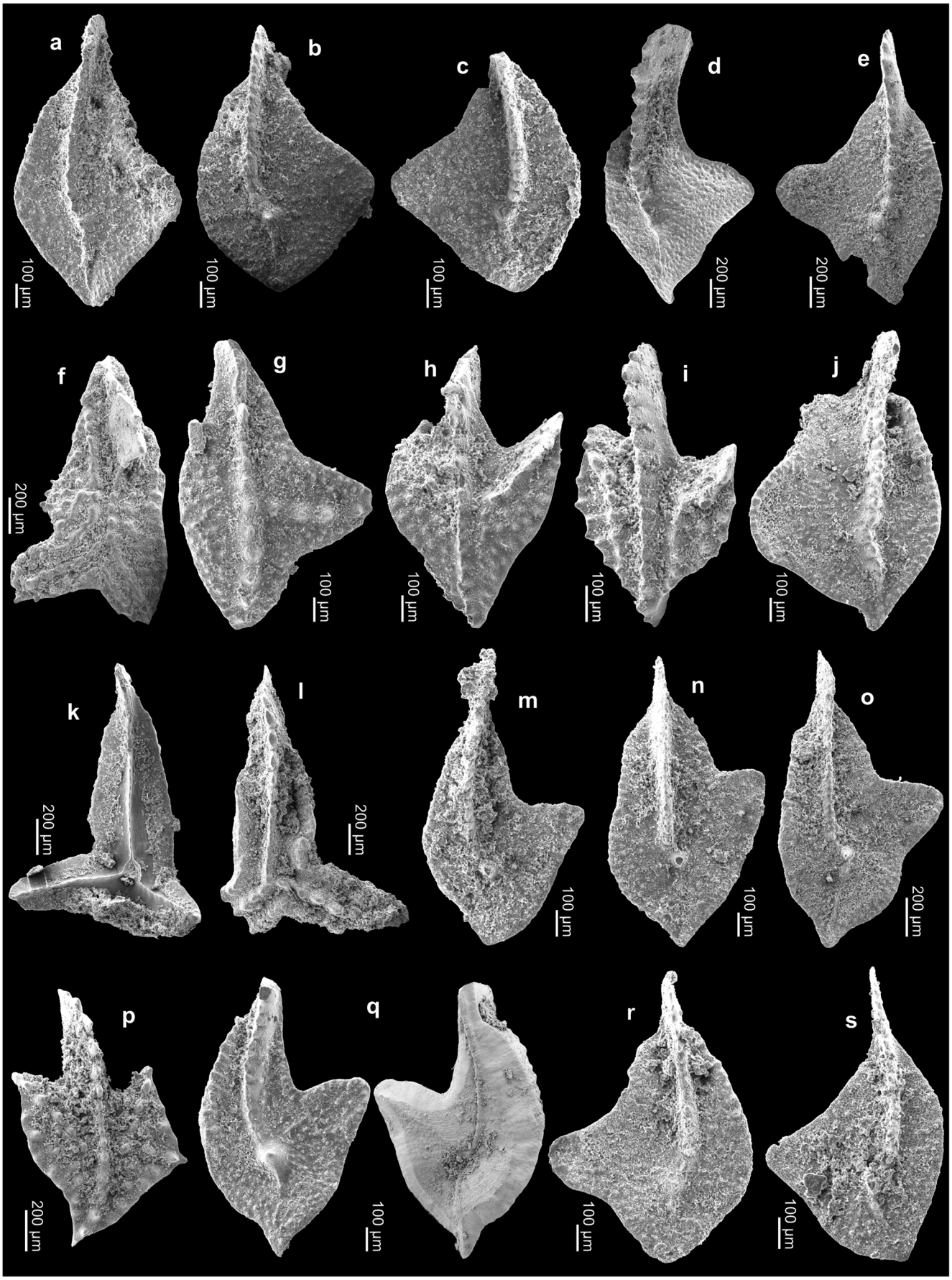
a
100 µm
b
100 µm
c
100 µm
d
200 µm
e
200 µm
f
200 µm
g
100 µm
h
100 µm
i
100 µm
j
100 µm
k
200 µm
l
200 µm
m
100 µm
n
100 µm
o
200 µm
p
200 µm
q
100 µm
r
100 µm
s
100 µm

◀ **Fig. 11** Conodonts from Martenberg, part 7. **a** *Pa. feisti* Klapper, 2007, GMM B9A.13-116, Sample R-Q 4.5-8 cm below top. **b** *Pa. feisti* Klapper, 2007, B9A.13-117, Sample R-Q 4.5-8 cm below top. **c** *Pa. feisti* Klapper, 2007, B9A.13-118, Sample R-Q 4.5-8 cm below top. **d** *Pa. amplificata* Ulrich and Bassler, 1926, GMM B9A.13-119, Sample R-Q 4.5-8 cm below top. **e** *Pa. amplificata* Ulrich and Bassler, 1926, GMM B9A.13-120, Sample R-Q 4.5-8 cm below top. **f** *Ag. leonis* Sandberg, Ziegler and Dreesen, 1992, GMM B9A.13-121, Sample R-Q bulk. **g** *Ag. amplicavus* Klapper, Kuz'min and Ovnatanova, 1996, GMM B9A.13-122, Sample R-Q bulk. **h** *Ad. nodosa* (= *gigas* M1) Ulrich and Bassler, 1926, GMM B9A.13-123, Sample R-Q bulk. **i** *Ad. nodosa* (= *gigas* M1) Ulrich and Bassler, 1926, GMM B9A.13-124, Sample R-Q bulk. **j** *Pa. domanicensis* Ovnatanova, 1976, GMM B9A.13-125, Sample R-Q bulk. **k** *Ag. triangularis* Youngquist, 1945, GMM B9A.13-126, Sample R-Q bulk. **l** *Ag. triangularis* Youngquist, 1945, GMM B9A.13-127, Sample R-Q bulk. **m** *Pa. ljaschenkoae* (M1) Ovnatanova, 1976, GMM B9A.13-128, Sample R-Q bulk. **n** *Pa. ljaschenkoae* (M2) Ovnatanova, 1976, GMM B9A.13-129, Sample R-Q bulk. **o** *Pa. ljaschenkoae* (M3) Ovnatanova, 1976, GMM B9A.13-130, Sample R-Q bulk. **p** *Ad. curvata* (Early Form) (Branson and Mehl, 1934), GMM B9A.13-131, Sample R-Q bulk. **q** *Pa. proversa* (M2) Ziegler, 1958, GMM B9A.13-132, Sample R-Q bulk. **r** *Pa. amplificata* Klapper, Kuz'min and Ovnatanova, 1996, GMM B9A.13-134, Sample R-Q bulk. **s** *Pa. kireevae* Ovnatanova, 1976, GMM B9A.13-135, Sample R-Q bulk

Revised diagnosis: Narrow platform, which can be straight (M1) to slightly curved (M2), with 5–9 transverse rows of denticles from median stages on; posterior half of the median row distinctly higher than lateral rows; it may extend posteriorly by two to four denticles beyond the lateral rows; denticles of the median row somewhat laterally compressed, connected by a thin, longitudinal ridge; denticles of lateral rows pointed, subcircular and isolated; narrow part of the basal cavity extents posteriorly to a subcircular outline.

Discussion: Two main morphotypes are distinguished based on the curvature of the middle and posterior part of the platform, excluding the anterior apex. Morphotype 1 is more or less straight, with a curvature < 10°, Morphotype 2 is markedly curved (> 10°). Some variance can be observed in the two morphotypes.

There are median to adult stages with five to six transverse rows and posteriorly two or more denticles beyond the lateral rows and median to adult stages with seven to nine transverse rows and posteriorly normally one or two (Fig. 5h), rarely up to four small denticles (Figs. 5i, o) beyond the lateral rows in Morphotype 1.

In Morphotype 2, median to adult stages with five to six transverse rows and posteriorly three to four denticles beyond the lateral rows and median to adult stages with seven to nine transverse rows and posteriorly one to three denticles beyond the lateral rows (Figs. 5p, 8b, c) can be observed.

Morphotype 1 corresponds to the lectotype of *I. symmetricus* and Morphotype 2 to the holotype of *I. curvatus*. Morphotypes are assigned in order to provide a base to establish in future possible different distributions in time, space, and facies (possible ecomorphotype patterns).

Ziegler (1975) mentioned that originally the asymmetrical outline of the basal cavity was thought to be the characteristic of *I. curvatus*, but that it is encompassed within the variability range of *I. symmetricus*. In his opinion, if *I. curvatus* was to be treated separately, this should be done on the basis of its long middle row that extends posteriorly three to four denticles beyond the lateral rows. However, he also mentioned that this feature has not been found in later described curved specimens.

Stratigraphic and geographic range: The species ranges throughout the Frasnian and can be found pantropically. Narkiewicz and Bultynck (2010, p. 609) excluded supposed older (upper Givetian) forms (*I. tafilaltenis* vs. *I. symmetricus*).

Icriodus sp. 1
(Fig. 12e)

non 2006 *Latericriodus* (or *Anthognathus*) *rarus* - Dzik: p. 32, fig. 10b.

Description: The platform is curved (ca. 20°) with six transverse rows. The posterior half of the median row is distinctly higher than the lateral rows. The denticles of the median row are laterally compressed. They continue posteriorly as a ridge with three denticles, the second of which is developed as a short transverse ridge. The denticles of the lateral rows are pointed. Prominent is an offset, large denticle on the right side of the widened cusp at the level of the most posterior transverse row, where the normal right side denticle is missing.

Discussion: Our single specimen is kept in open nomenclature since we cannot exclude that the irregular denticulation is pathological. Dzik (2006) published similar but more straight specimens from the upper Famennian *styriacus* Zone of the Holy Cross Mountains as "*Latericriodus* (or *Antognathus*) *rarus*". We do not think that our specimen is conspecific. Two different icriodids with marginal ridges and single small nodes of the upper cusp were illustrated by Lys and Serre (1957, pl. IX) from the Frasnian of the Montagne Noire as *I.* cf. *nodosus* and *Icriodus* sp. Wang (1994) illustrated as *I. symmetricus* from the lower Frasnian of the Sihongshan section, Guangxi, a straight specimen with only five rows of denticles, with the median row merged to a complete longitudinal ridge, and with an additional prominent denticle on the right side of the upper cusp.

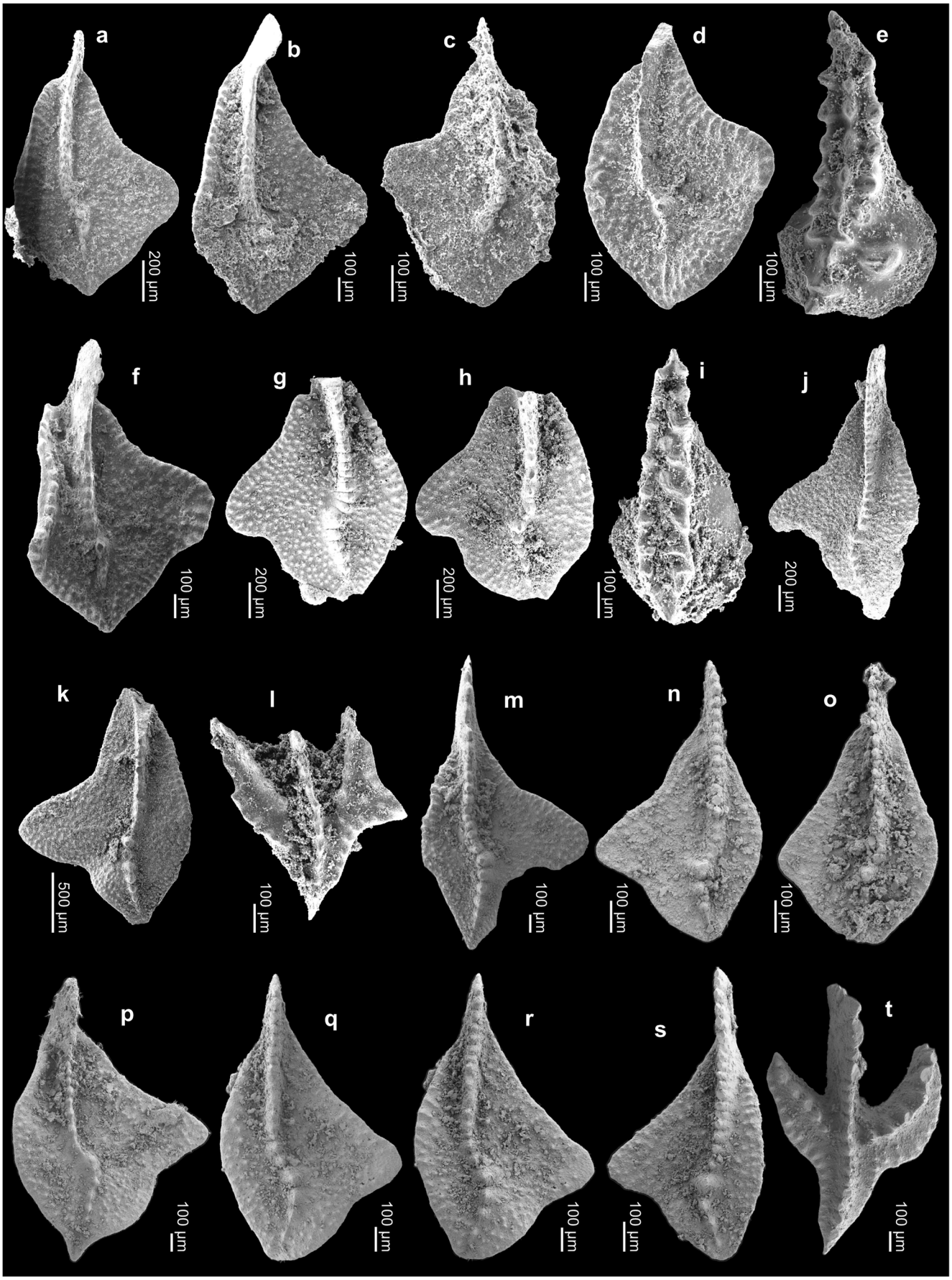
a
200 µm
b
100 µm
c
100 µm
d
100 µm
e
100 µm
f
100 µm
g
200 µm
h
200 µm
i
100 µm
j
200 µm
k
500 µm
l
100 µm
m
100 µm
n
100 µm
o
100 µm
p
100 µm
q
100 µm
r
100 µm
s
100 µm
t
100 µm

◀ **Fig. 12** Conodonts from Martenberg, part 8. **a** *Pa.* aff. *feisti* Klapper, 2007, GMM B9A.13-136, Sample R-Q bulk. **b** *Pa.* aff. *feisti* Klapper, 2007, GMM B9A.13-137, Sample R-Q bulk. **c** *Pa. simpla* Ziegler and Sandberg, 1990, GMM B9A.13-138, Sample R-Q bulk. **d** *Pa. simpla* Ziegler and Sandberg, 1990, GMM B9A.13-139, Sample R-Q bulk. **e** *Icriodus* sp. 1, possibly pathological, GMM B9A.13-140, Sample R-Q bulk. **f** *Pa.* cf. *domanicensis* Ovnatanova, 1976, GMM B9A.13-146, Sample R-Q bulk. **g** *Pa. descendens* n. sp., GMM B9A.13-147, Sample Q 18 - 30 cm above base (paratype). **h** *Pa. descendens* n. sp., GMM B9A.13-148, Sample Q 18 - 30 cm above base (paratype). **i** *I. alternatus* cf. *helmsi* Sandberg and Dreesen, 1984, GMM B9A.13-149, Sample Q 18 - 30 cm above base. **j** *Pa. nasuta* Müller, 1956, GMM B9A.13-150, Sample Q 18 - 30 cm above base. **k** *Pa. nasuta* Müller, 1956, B9A.13-151, Sample Q 18 - 30 cm above base. **l** *Ad. curvata* (Late Form) (Branson and Mehl, 1934), GMM B9A.13-152, Sample Q 18 - 30 cm above base. **m** *Pa. rhenana* Bischoff, 1956, GMM B9A.13-153, Sample P base. **n** *Pa. winchelli* (Stauffer, 1938), GMM B9A.13-154, Sample P base. **o** *Pa. jamieae jamieae* Ziegler and Sandberg, 1990, GMM B9A.13-155, Sample P base. **p** *Pa. brevis* Ziegler and Sandberg, 1990, GMM B9A.13-156, Sample P base. **q** *Pa. jamieae savagei* n. ssp. (M2), GMM B9A.13-157, Sample P base (paratype). **r** *Pa. jamieae savagei* n. ssp. (M2), GMM B9A.13-158, Sample P base (paratype), specimen intermediate towards *Pa. jamieae savagei* n. ssp. (M1). **s** *Pa. jamieae savagei* n. ssp. (M2), GMM B9A.13-159, Sample P base (paratype). **t** *Ad. ioides* (M1) Ziegler, 1958, GMM B9A.13-160, Sample P base

Stratigraphic and geographic range: Restricted to the Frasnian Subzone 11a (*feisti* Subzone) of Martenberg.

Palmatolepis jamieae jamieae Ziegler and Sandberg, 1990 (Fig. 12o)

*e.p.	1990	*Palmatolepis jamieae* - Ziegler and Sandberg: p. 50, pl. 6, figs. 1–3, 9, 10 [figs. 4–7 = *Pa. feisti*, fig. 8 = *Pa.* cf. *uyenoi*, pl. 11, figs. 4–6 = *Pa. uyenoi* fide Klapper, 2007].
non	1992	*Palmatolepis jamieae* - Helsen and Bultynck: pl. 3, figs. 6, 7 [fig. 6 = *Pa. wildungensis*, fig. 7 = *Pa. jamieae rosa* n. ssp.].
e.p.	1992	*Palmatolepis jamieae* - Sandberg et al.: pl. 3, fig. 3 [non fig. 5 = *Pa. feisti*].
non	1992	*Palmatolepis jamieae* - Lazreq: pl. 1, figs. 14, 15 [fig. 14 = *Palmatolepis* ?n. sp., fig. 15 = *Pa. adorfensis* n. sp.].
	1993	*Palmatolepis jamieae* - Matyja: pl. 21, fig. 7.
non	1993	*Palmatolepis jamieae* - Ji and Ziegler: pl. 27, figs. 1-3 [fig. 1 = *Pa. jamieae savagei* n. ssp. M2, fig. 2 = *Pa. jamieae* ssp. δ, fig. 3 = *Pa. winchelli*].
non	1993	*Palmatolepis jamieae* - Ji: pl. 13, fig. 10–12 [figs. 10–11 = *Pa. jamieae savagei* n. ssp. M1, fig. 12 = *Pa. jamieae* ssp. δ].
non	1994	*Palmatolepis jamieae* - Wang: p. 102, pl. 6, figs. 11–14 [non pl. 2, fig. 10 = *Pa. plana*, pl. 6, figs. 11–12= *Pa. uyenoi* (narrow form), fig. 13 = *Pa. plana*, fig. 14 = *Pa. jamieae savagei* n. ssp. M2]
non	1994	*Palmatolepis jamieae* - Bai et al.: p. 172, pl. 7, figs. 10, 17, 18 [= *Pa. jamieae rosa* n. ssp.].
non	1995	*Palmatolepis jamieae* - Matyja and Narkiewicz: pl. 1, fig. 3 [= *Pa. jamieae* ssp. δ].
non	1998	*Palmatolepis jamieae* - Bultynck et al.: p. 58. pl. 1, fig. 13 [= *Pa. adorfensis* n. sp.].
non	1999	*Palmatolepis jamieae* - Lazreq: pl. 8, figs. 4, 5 [fig. 4 = *Pa. adorfensis* n. sp., fig. 5 = *Pa. feisti*].
	1999	*Palmatolepis jamieae* – Ovnatanova et al.: pl. 2, fig. 13.
non	2001	*Palmatolepis jamieae* - Savage and Yudina: p. 291, pl. 8, figs. 5–6 [= *Pa. feisti*].
non	2001	*Palmatolepis* cf. *jamieae* - Savage and Yudina: p. 291, pl. 10, figs. 11–13 [fig. 11 = *Pa. nasuta*, figs. 12–13 = *Pa.* ?*hassi*].
non	2002	*Palmatolepis jamieae* - Levman and Bitter: pl. 1, fig. 10 [= a younger homeomorph of *Pa. feisti*, perhaps related to Lazreq, 1992, pl. 1, fig. 14].
non	2002	*Kielcelepis*? (or *Lagovilepis*) *jamieae* - Dzik: p. 593, figs. 34.A, B, D, K, M [= *Pa. hassi*], fig. 34, L [= *Palmatolepis* sp. juv.], figs. 34.C, E, F, G, H, I, J, N–P [= other elements].
	2004	*Palmatolepis jamieae* – Izokh et al., p. 94, pl. 1, figs. 7, 8, 10.
?e.p.	2004	*Palmatolepis jamieae* – Galushin and Kononova, p. 38, 40 [non fig. 8.5 = *Pa. jamieae savagei* n. ssp. M1, with smooth outer platform, giving a slight trend towards ssp. δ].
non	2005	*Palmatolepis jamieae* - Çapkınoğlu: p. 228, figs. 5.15–16 [fig. 15 = *Pa. jamieae* ssp. δ, fig. 16 = juvenile].
non	2007	*Palmatolepis jamieae* - Erina in Kim et al.: p. 270, pl. 130, fig. 8 [transitional between *Pa. jamieae* and *Pa. foliacea*].
	2007	*Palmatolepis jamieae* - Klapper: p. 523, figs. 4.5-9.
e.p.	2008	*Palmatolepis jamieae* - Ovnatanova and Kononova: p. 1092, pl. 11, figs. 1–2 [fig. 1 = re-illustration of holotype; non pl. 10, figs. 16–18 = *Pa. jamieae* ssp. δ, pl. 11, fig. 3 = *Pa. jamieae* ssp. δ, fig. 4 = *Pa.* cf. *plana*, fig. 5 = *?Pa. nasuta*, fig. 6 = *Pa. jamieae* ssp. δ, fig. 7 = *Pa. jamieae savagei* n. ssp. M1, variant with reduced posterior sinus, figs. 8–9 = *Pa.* cf. *foliacea,* transitional from *Pa. jamieae*, pl. 14, fig. 10 = *Pa. jamieae savagei* n. ssp. M1, variant without posterior sinus].
	2009	*Palmatolepis jamieae* - Klapper: fig. 1.3.16 [re-illustration from 2007].
non	2010	*Palmatolepis jamieae* - Lang and Wang: p. 25, pl. 1, figs. 12–13 [= *Pa. jamieae savagei* n. ssp. M1, fig. 12 = variant without posterior sinus].
	2013	*Palmatolepis jamieae* - Savage: p. 17, figs. 5.20–22.
non	2014	*Palmatolepis jamieae* – Bardashev and Bardasheva, tab. 1.3, pl. 4, fig. 8 [= *Pa. adorfensis* n. sp.].
	2015	*Palmatolepis* cf. *rotunda* - Malec: pl. 5, fig. 1.
non	2015	*Palmatolepis jamieae* - Malec: pl. 5, figs. 2, 3 [fig. 2 = *Pa. kireevae*, fig. 3 = *Pa.* cf. *kireevae*].
non	2016	*Palmatolepis jamieae* - Huang and Gong: fig. 4.14 [?variant of *Pa. jamieae* ssp. δ], fig. 6.20 [smooth variant of *Pa. jamieae rosa* n. ssp.]
non	2016	*Palmatolepis jamieae* - Wang: p. 194, pl. D-5, figs. 8, 11 [fig. 8 = *Pa. jamieae savagei* n. ssp. M2, fig. 11 = *Pa. plana*; re-illustrations from 1994].
non	2016c	*Palmatolepis jamieae* – Becker et al., p. 226 [= narrow form of *Pa. uyenoi* and one specimen of *Pa. adorfensis* n. sp.].
non	2017	*Palmatolepis jamieae* - Ovnatanova et al.: p. 1084, pl. 35, figs. 3–4, pl. 41, fig. 1 [pl. 35, fig. 3 = *Pa. jamieae rosa* n. ssp., fig. 4 = *Palmatolepis* sp. ε, pl. 41, fig. 1 = *Pa. jamieae* ssp. δ].
non	2018	

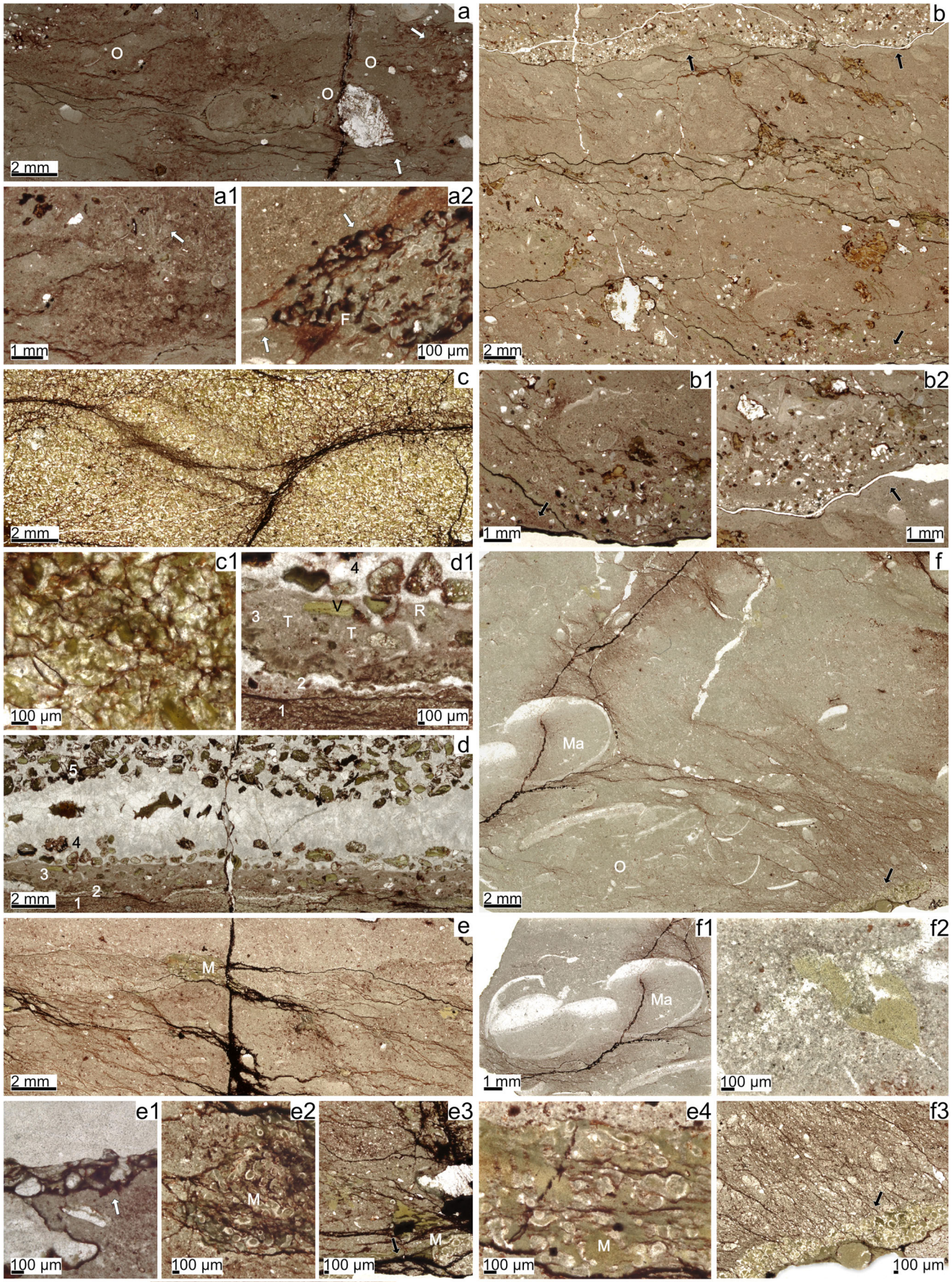
a
O
O
O
2 mm
a1
1 mm
a2
F
100 µm
b
2 mm
c
2 mm
b1
1 mm
b2
1 mm
c1
100 µm
d1
4
V
3
T
R
T
2
1
100 µm
f
Ma
O
2 mm
d
5
4
3
2 mm
1
2
e
M
2 mm
f1
Ma
1 mm
f2
100 µm
e1
100 µm
e2
M
100 µm
e3
M
100 µm
e4
M
100 µm
f3
100 µm

◀ **Fig. 13** Microfacies of sampled beds **a** Top of Bed R: flaser-bedded, bioturbated bioclastic wackestone with micritic to microsparitic matrix, isolated styliolines, stylioline nests (*arrows*), ostracods (*O*), and red-brownish iron enrichments. **a1** Detail of the top of Bed R, showing a stylioline nest (arrow). **a2** Detail of the top of Bed R, showing a lump of small, *Frutexites*-type microstromatolites surrounding small stylioline shells (*arrows*). **b** Bed R-Q base: flaser-bedded, bioturbated bioclastic wackestone with micritic to microsparitic, partly nodular matrix and two levels of fine-grained, angular to subangular, partly iron-mineralized extraclast enrichments (crinoid debris/volcaniclasts) at the base and top. Note that a very thin sparite seam follows the sharp base of the upper level on the right side but not in the middle, where the underlying fine micrite is truncated by extraclast packstone. **b1** Detail of the base of Bed R-Q, showing fine extraclast enrichments above the iron-stained basal surface (*arrow*). **b2** Detail of the base of Bed R-Q, showing the sharp base of the upper extraclast interval. **c** "Sheet 1": flaser-bedded, chloritized and carbonatic tuff (volcaniclastic packstone) with diagenetic iron and clay mineralizations. **c1** Detail of "Sheet 1", showing the chloritization of rather well-sorted angular clasts, as typical for recrystallized tuff. **d** "Sheet 2": very fine-grained, recrystallized (chloritic), calcareous tuffite at the base (*1* Layer 1), followed above an undulating unconformity and a very thin, sparitic sheet crack (*2* Layer 2) by a grey band of microbialite with clotted micrite fabric (*3* Layer 3), in the upper part with embedded, partly coated, subrounded to angular clasts derived from the basal layer plus irregular and chloritized microlapilli, then, above a rippled unconformity by a thicker sheet crack with floating, cavernous, chloritic volcaniclasts in the lower part of Layer 4 (*4*), becoming increasingly abundant towards the top (*5* Layer 5). **d1** Details of "Sheet 2", showing the fine, clastic nature of Layer 1 at the base (*1*), the thin sparite sheet of Layer 2 (*2*), diffuse micrite clotting and tube-like meandering internal structures (*T*) in the microbial Layer 3, with chloritized volcaniclasts (*V*) at the rippled (*R*) top, and partly iron-coated, size-sorted extraclasts at the base of Layer 4 (*4*). **e** "Sheet 3": flaser-bedded, unfossiliferous, reddish, micritic to microsparitic mudstone with some isolated, chloritized, lumped microlapilli (*M*) within the middle part. **e1** Details of "Sheet 3", showing the thin, iron-coated extraclastic layer (*arrow*) at the top. **e2** Details of "Sheet 3", showing an isolated, lumped microlapilli (*M*) with internal spherical aggregates. **e3** Details of "Sheet 3", showing the thin, chloritized volcaniclastic layer with fine spherical aggregates at the base (*arrow*). **e4** Details of "Sheet 3", showing a chloritized, lumped microlapilli (*M*) with internal spherical aggregates from the middle of the unit. **f** Lower part of Bed Q: flaser-bedded, cephalopod-dominated floatstone with goniatites (*Manticoceras*; Ma), ostracods that partly show geopetal filling (*O*), fragmented, partly ribbed bivalves, other shell debris, and micrite matrix. **f1** Details of the lower part of Bed Q, showing the cross-section of a *Manticoceras* (*Ma*) with geopetal filling. **f2** Details of the lower part of Bed Q, showing one of the rare, last, greenish, chloritized microlappilli from within the middle part. **f3** Details of the base of Bed Q, showing the greenish, volcaniclastic layer (*arrow*) with spherical aggregates, overlain by microsparitic mudstone

		Palmatolepis jamieae - Komatsu et al.: fig. 7l [?extreme variant of *Pa. jamieae savagei* n. ssp. M1].
non	2018	*Palmatolepis jamieae* – Bardashev, pl. 9, fig. 8 [= *Pa. adorfensis* n. sp.; re-illustration from 2014].
	2019	*Palmatolepis jamieae* - Savage: p. 486, figs. 12.13–15 [re-illustrations from 2013].
e.p.	2020	*Palmatolepis jamieae* - Ovnatanova and Kononova: figs. 5.1–3 [re-illustrations of holo- and topotypes], 5.7 [re--illustration from 2008], 5.9–12 [re-illustrations from Klapper 2007]; non figs. 4–6, 8 = *Pa. jamieae* ssp. δ, re-illustrations from 2008].

Type locality and level: Schmidt Quarry, Kellerwald, eastern Rhenish Massif, level with *Ad. ioides*, therefore, *winchelli* Zone (Frasnian Zone 12), upper Frasnian.

Material: One specimen from Sample P base (Fig. 12o).

Revised diagnosis of Klapper, 2007: Outline of platform roughly triangular to pyriform; outer lobe relatively narrow, midline of lobe directed laterally; outer posterior sinus commonly distinct; blade-carina sigmoidal but straight anteriorly, curving towards lobe just anterior of central node; posterior carina short, reaching or almost reaching posterior tip, curved inwardly; rim of marginal nodes on inner side of platform; blade extends anterior of platform a short distance.

Discussion: All three specimens illustrated by Ziegler and Sandberg (1990) from the same bed at Schmidt Quarry are typical *Pa. jamieae jamieae*, which suggests a restricted variability in the type population, which is stratigraphically younger than specimens from the supposed "*jamieae* Zone" at Martenberg. At Martenberg, we found one specimen with a rather narrow platform in strata corresponding to the type level but the typical subspecies is more common in equivalent beds at Beringhauser Tunnel (Saupe and Becker, in prep.). A typical feature of *Pa. jamieae jamieae* is the concave to near-straight anterior inner platform marked by a rim of raised nodes.

Following the refined diagnosis for *Pa. jamieae* of Klapper (2007) and based on the survey of all specimens illustrated in the literature and our re-sampling at Martenberg, three subspecies (*Pa. jamieae jamieae*, *Pa. jamieae savagei* n. ssp., *Pa. jamieae rosa* n. ssp.) and two related new species (*Pa. adorfensis* n. sp., *Pa. descendens* n. sp.) are named. Their distinction is useful to establish refined stratigraphical ranges. Additionally, two other

Table 2 Conodont biofacies based on genera at Martenberg

codonont biofacies	R	R-Q				Q		P
	top	base	8-14 b. t.	4.5-8 b. t.	bulk	base	18-30 a. b.	base
Ancyrodella	12.5%	9.3%	11.9%	5.6%	8.9%	0%	7.7%	9.9%
Ancyrognathus	3.1%	1.4%	3.4%	1.1%	2.2%	0%	3.5%	11.5%
Icriodus	10.9%	24.9%	10.7%	1.3%	6.0%	25%	0.4%	4.7%
Palmatolepis	18.8%	20.4%	35.9%	26.9%	50.1%	50%	57.5%	71.8%
Polygnathus	54.7%	44.1%	38.0%	65.1%	32.9%	25%	30.9%	2.2%

forms left here in open nomenclature have been identified in the literature as *Pa. jamieae*. Typical *Pa. jamieae* ssp. δ have a rather smooth platform apart from the margins, lack a distinctive outer posterior platform sinus, and the posterior carina is weakly curved inward (e.g. Ji and Ziegler 1993: pl. 27, Fig. 2; Çapkınoğlu 2005: p. 228, Figs. 5, 15; Ovnatanova and Kononova 2008: p. 1092, pl. 10, figs. 16–18; Huang and Gong 2016, fig. 6.20). The position of the central node projects laterally to the end of the platform lobe and the nodose anterior inner platform margin is slightly concave to straight, as in the typical subspecies. Another form, provisionally called *Palmatolepis* sp. ε, has a small, nodose platform, lacks an outer posterior sinus, and displays a well-developed, coarse posterior carina, which turns straight inwards without bending (e.g. Ovnatanova et al. 2017: p. 1084, pl. 35, Fig. 4). A weak development of the posterior outer sinus may also occur in some *Pa. jamieae jamieae* (one of the syntypes, Ziegler and Sandberg 1990, pl. 6, Fig. 9) and in *Pa. jamieae savagei* n. ssp. (e.g. Ovnatanova and Kononova 2008, pl. 11, Fig. 7, pl. 14, Fig. 10).

Stratigraphic and geographic range: *Pa. jamieae jamieae* is a rare (< 1 % of palmatolepids) to moderately common (1–5 % of palmatolepids) form in populations from its type locality, possibly from Frasnian Subzone 11b (Bed 21 with *Pa. semichatovae*, and Bed 22, Ziegler and Sandberg 1990, no specimen figured), from Frasnian Zone 12 (Bed 23 with *Ad. ioides*, type level, to Bed 26/5 with the FOD of *Ag. asymmetricus*, Lower Kellwasser Limestone), and possibly from the lower part of Frasnian Zone 13a (Beds 27/6 and 1/7, no specimen figured). According to our partly very rich samples, it is absent from the beds originally (Ziegler and Sandberg 1990) or later (Ziegler and Sandberg 2000) assigned to the *jamieae* Zone at Martenberg (Frasnian Zone 10 and Frasnian Subzone 11a), which confirms the revision of Ovnatanova and Kononova (2020). Records backed by illustrations from other regions are restricted to Frasnian Zone 12 (*winchelli* Zone) of the Ardennes (Tiènne du Lion backmound section, Belgium, Sample 85-BEL-120, Sandberg et al. 1992), the subsurface of Pomerania (Matyja 1993), the subsurface of the Holy Cross Mountains (Malec 2015), the Timan of northern Russia (Lyaiol River, Member 4 of Lyaiol Formation, Ovnatanova et al. 1999; Ovnatanova and Kononova 2008; compare age of the unit in House et al. 2000), the Rudnyi Altai of southern Siberia (Izokh et al. 2004, based on associated *Pa. rhenana* and *Pa. muelleri*), NW Thailand (Mae Sariang section, Bed D18-E with *Pa. khaensis,* a relative of *Pa. winchelli, Ad. ioides* M1, and *Pa.* aff. *bogartensis*, Savage 2013, 2019), and the Canning Basin of Western Australia (Horse Spring section, Klapper 2007). Occurrences of *Pa. jamieae jamieae* in Frasnian Subzone 11b (*nasuta* Subzone) and Frasnian Zone 13a (*bogartensis* Zone) require further documentation. In the Frasnian Zone 12 of the Timan, *Pa. jamieae jamieae* is proven to co-occur with *Pa. jamieae* ssp. δ and atypical *Pa. jamieae savagei* n. ssp. M2 that lack a posterior platform sinus.

Palmatolepis jamieae savagei n. ssp.
(M1: Figs. 8d, e, 10g–i; M2: Figs. 12q, s; ?M2: Figs. 10j, 12r)

e.p.	1992	*Palmatolepis hassi* – Lazreq, pl. 1, fig. 12 [only, = M1, variant with long, fine posterior carina].
e.p.	1993	*Palmatolepis jamieae* - Ji and Ziegler: pl. 27, fig. 1 [only, = M2; non fig. 2 = *Pa. jamieae* ssp. δ, fig. 3 = *Pa. winchelli*].
e.p.	1993	*Palmatolepis jamieae* - Ji: pl. 13, figs. 10–11 [only, = M1].
e p.	1994	*Palmatolepis jamieae* - Wang: p. 102, pl. 6, fig. 14 [only, = M2].
e.p.	2004	*Palmatolepis hassi* – Izokh et al., pl. 1, fig. 12 [only, = M2]
e.p.	2004	*Palmatolepis jamieae* – Galushin and Kononova, p. 38, fig. 8.5 [= M1, with smooth outer platform, giving a slight trend towards ssp. δ].
e.p.	2008	*Palmatolepis jamieae* – Ovnatanova and Kononova, p. 1092, pl. 11, fig. 7, pl. 14, fig. 10 [only, = M1, variants without posterior sinus]
	2010	*Palmatolepis jamieae* - Lang and Wang: p. 25, pl. 1, figs. 12, 13 [= M1, fig. 12 = elongated variant without posterior sinus].
?	2013	*Palmatolepis* aff. *jamieae* - Savage: p. 17, figs. 5.13–14 [resembling both M1 and *Pa. khaensis*].
e.p.	2016	*Palmatolepis jamieae* - Wang: p. 194, pl. D-5, fig. 8 [only, = M2, re-illustration of 1994 specimen].
??	2018	*Palmatolepis jamieae* - Komatsu et al.: fig. 7l [smooth form resembling M1].
?	2019	*Palmatolepis* aff. *Pa. jamieae* - Savage: p. 486, figs. 9.3–5 [= M1, re-illustration of 2013 specimen].

Derivation of name: In honour of Norman Savage (University of Oregon), in recognition of his major contributions to conodont research.

Material: Holotype GMM B9A.13-59 (Fig. 8e, M1), paratype GMM B9A.13-58 (Fig. 8d, M1), paratype GMM B9A.13-103 (Fig. 10g, M1), paratype GMM B9A.13-104 (Fig. 10h, M1), paratype GMM B9A.13-105 (Fig. 10i, M1), GMM B9A.13-157 (Fig. 12q, M2), GMM B9A.13-159 (Fig. 12s, M2), GMM B9A.13-106 (Fig. 10j, ?M2), GMM B9A.13-158 (Fig. 12r, ?M2); at least six more specimens of M1, three atypical M1 specimens, and six more specimens of M2 are known from seven other, partly distant regions/localities.

Type locality and level: Martenberg, eastern Rhenish Massif, Adorf Formation, Sample R-Q base, upper Frasnian, lower part of Frasnian Zone 10 (*plana* Zone).

Diagnosis: Outline of platform asymmetrically subtriangular, rather narrow and not bulbous in the posterior outer part around the central node; outer lobe rounded to subtriangular, moderately narrow, with variable position in relation to the central node, inner platform convex, arched; posterior sinus moderate to weak; carina weakly to moderately sigmoidal, bends anterior of central node towards the lobe; posterior carina weak and turns straight inwards, or not developed;

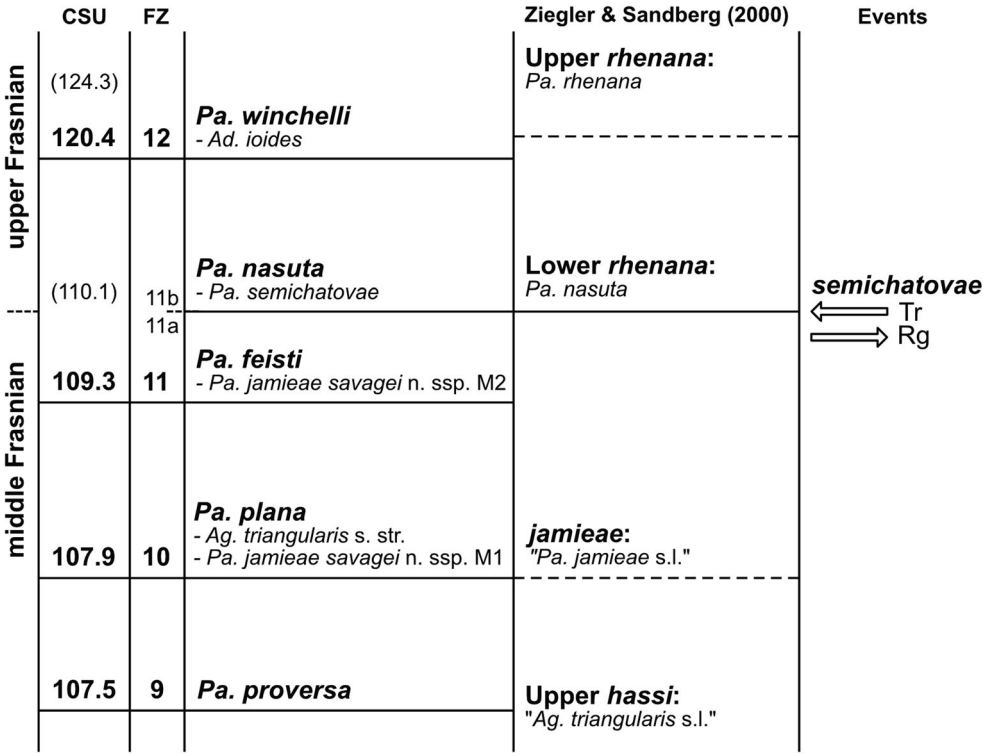

Fig. 14 Correlation of the conodont succession (sequence of important marker taxa), CSU units (Klapper et al. 1995; Klapper et al. 1996; Klapper and Kirchgasser 2016), Frasnian zones (FZ), and "standard zones" sensu Ziegler and Sandberg (1990) around the *semichatovae* Event and middle/upper Frasnian transition at Martenberg

marginal nodes or short ridges on inner side of platform usually present; blade extents anterior of platform a short distance.

Discussion: The new subspecies differs from *Pa. jamieae jamieae* in its rather narrow, more elongate platform, lacking a bulbous posterior outer platform around the central node, and, in typical forms, by the more convex, arched inner platform margin. The posterior sinus is moderately (in the holotype, Fig. 8e) to weakly developed (e.g. in paratype GMM B9A.13–103, Fig. 10g), and missing in extreme variants from northern Russia (Ovnatanova and Kononova 2008, pl. 11, Fig. 7, pl. 14, Fig. 10) and Inner Mongolia (Lang and Wang 2010, pl. 1, Fig. 12). *Palmatolepis jamieae* ssp. δ differs in its smooth inner platform (e.g. Ovnatanova and Kononova 2008, pl. 10, figs. 16–18, pl. 11, Fig. 3) and a straight to slightly concave anterior inner platform margin, as in *Pa. jamieae jamieae*.

We distinguish two morphotypes of *Pa. jamieae savagei* n. ssp. based on the position of the central node relative to the lobe. In Morphotype 1, which includes the holotype, the central node is located at the level of the apex of the lobe (Figs. 8d, e, 10g, i), while in Morphotype 2 (Figs. 12q, s; e.g. Ji and Ziegler 1993, pl. 27, Fig. 1; Wang 1994, pl. 6, Fig. 14; Izokh et al. 2004, pl. 1, Fig. 12), its position projects towards the posterior end of the lobe, as in typical *Pa. jamieae jamieae*. In median-sized Morphotype 1 specimens (Figs. 10g–i), the posterior carina is short to almost absent. One atypical Martenberg specimen, assigned questionably to Morphotype 2 (Fig. 10j), combines a moderately wide platform and rimmed, concave inner platform margin resembling *Pa. jamieae jamieae* but differs from the typical subspecies in its completely reduced posterior carina, while another one (Fig. 12r) is intermediate between Morphotype 1 and Morphotype 2 due to the position of the central node in relation to the platform.

Savage (2013, 2019) illustrated from much younger levels (upper part of Frasnian Zone 13a) of Mae Sariang, NW Thailand, an elongated specimen as *Pa.* aff. *jamieae* that resembles Morphotype 1. However, its lobe and central node sit in a very posterior position, as in other specimens assigned by him to *Pa. khaensis*. A typical feature of the latter is its long, straight carina anterior of the central node. In addition, we have the impression that the platform shapes of some Mae Sariang specimens are affected by distortion. A supposed *jamieae* specimen illustrated by Komatsu et al. (2018) from northern Vietnam is also significantly younger than typical *Pa. jamieae savagei* n. ssp. and differs by its smooth platform and a long, fine, posterior carina. The latter feature excludes it from *Pa. jamieae* ssp. δ.

Stratigraphic and geographic range: *Palmatolepis jamieae savagei* n. ssp. has a different, lower range than typical *Pa. jamieae* but its upper range overlaps with the typical subspecies. In the Rhenish Massif, Morphotype 1 was found from Frasnian Zone 10 (*plana* Zone) to Frasnian Subzone 11a

(*feisti* Subzone), Morphotype 2 in Frasnian Subzone 11a (records in Stichling et al., this vol.) and in the basal part of Frasnian Zone 12 (*winchelli* Zone). Elsewhere, Morphotype 1 occurs in the Frasnian Zone 10/ Frasnian Subzone 11a interval of the Moroccan Meseta (Lazreq 1992), Frasnian Subzone 11b (*nasuta* Subzone) to Frasnian Zone 12 (*winchelli* Zone) in South China (Ji 1993), at a similar level (regional Mendym Stage) in the Lemva River Basin of the Polar Urals (Ovnatanova et al. 2017), in the Volgograd region of the Russian Platform (Galushin and Kononova, 2004), and in the Rudnyi Altai (Izokh et al. 2004). The age of Morphotype 1 in Inner Mongolia (Heilongjiang Province, Niqiuhe Formation and Daminshan Formation, Lang and Wang 2010) cannot be clearly determined in a faunal association that represents the undivided Frasnian Zones 11–12 (*feisti* to *winchelli* Zone) interval. Morphotype 2 was found in South China in Frasnian Subzone 11b (*nasuta* Subzone, Sihongshan section, Sample CDC 372, Wang 1994, 2016) and Frasnian Zone 12 (*winchelli* Zone; Lali Section, Ji and Ziegler 1993, Bed 38 with *Pa. subrecta* = *winchelli*). Atypical specimens of Morphotype 2 without posterior platform sinus occur in the upper Frasnian Zone 12 (*winchelli* Zone) of the Timan (Ovnatanova and Kononova 2008).

Palmatolepis jamieae rosa n. ssp.
(Figs. 8a, 9l)

e.p.	1992	*Palmatolepis jamieae* - Helsen and Bultynck: pl. 3, fig. 7 [non fig. 6 = *Pa. wildungensis*].
	1994	*Palmatolepis jamieae* - Bai et al.: p. 172, pl. 7, figs. 10, 17, 18 [small specimens].
e.p.	2016	*Palmatolepis jamieae* – Huang and Gong, fig. 6.20 [only, smooth variant; non. fig. 4.14 = atypical ssp. δ].
e.p.	2017	*Palmatolepis jamieae* - Ovnatanova et al.: p. 1084, pl. 35, fig. 3 [only; non fig. 4 = *Palmatolepis* sp. ε, non pl. 41, fig. 1 = *Pa. jamieae savagei* n. ssp. M1].

Derivation of name: After the type locality, which in local folklore is referred to as "Rosenschlösschen", meaning small rose castle; *rosa* is Latin for rose.
Material: Holotype GMM B9A.13-89 (Fig. 9l), paratype GMM B9A.13-55 (Fig. 8a), and a third specimen from Sample P base. Six further specimens have previously been illustrated from three distant regions.
Type locality and level: Martenberg, Sample R-Q 8–14 cm below top, Frasnian Zone 10 (*plana* Zone), upper Frasnian.
Diagnosis: Outline of platform asymmetrically rhombic to slightly pyriform; broad, indistinctively delimited lobe with apex lying close to the position of the central node, bordered by near-straight anterior and posterior margins with weak to absent sini; carina sigmoidal, bends anterior of central node towards lobe side; posterior carina often thin, rather straight, ends before tip of platform; at maturity with rim of marginal nodes or short ridges on strongly convex inner side of platform; blade extents anterior of platform a short distance.
Discussion: The outline of the platform of the new subspecies lies between the pyriform shape of *Pa. jamieae jamieae* and the more broadly rhombic shape of *Pa. feisti*. The shape of the lobe is similar to *Pa. feisti* but is located in a more posterior position and the carina is more sigmoidal than in typical *Pa. feisti*. The arched inner platform margin differs from that in *Pa. jamiae jamieae* and agrees with that in the much narrower *Pa. jamieae savagei* n. ssp., which, again, differs clearly in its long, markedly concave anterior outer platform margin (compare Fig. 8e). In Chinese specimens, the platform is rather smooth, partly because of their small size, which indicates a transition towards *Pa. jamieae* ssp. δ that, however, also displays a long and strong anterior outer platform sinus. Due to its intermediate morphology and slightly earlier entry, it is likely that *Pa. jamieae rosa* n. ssp. was the ancestor of *Pa. feisti*.
Stratigraphic and geographic range: The new subspecies ranges in the Rhenish Massif from Frasnian Zone 10 (*plana* Zone) to the basal Frasnian Zone 12 (*winchelli* Zone). Elsewhere, it was found in Frasnian Zone 11 (*feisti* Zone) in Belgium (Nismes section, Neuville Formation, originally assigned to the *jamieae* Zone, Helsen and Bultynck 1992), in Frasnian Subzone 11b in South China (Nandong sections, specimens from above the FODs of *Pa. ederi* and *Pa. nasuta*, Bai et al. 1994), and in Frasnian Zone 12 (*winchelli* Zone) in Northeastern European Russia (Chernyshev Ridge: Shar`yu River, Vorota Formation, Ovnatanova et al. 2017, level with *Pa. gyrata*, compare its composite range in Klapper et al. 1996). A smooth variant occurs in Frasnian Zone 13a (*bogartensis* Zone) of South China (Huang and Gong 2016).

Palmatolepis adorfensis n. sp.
(Figs. 7b, r, s, 9i, j)

e.p.	1992	*Palmatolepis jamieae* - Lazreq: pl. 1, fig. 15 [only, non fig. 14 = ?].
	1998	*Palmatolepis jamieae* - Bultynck et al.: p. 58. pl. 1, fig. 13.
e.p.	1999	*Palmatolepis jamieae* - Lazreq: pl. 8., fig. 4. [only; non fig. 6 = *Pa. feisti*]
	2007	*Palmatolepis* aff. *Pa. jamieae* - Klapper: figs. 4.10–11.
	2014	*Palmatolepis jamieae* – Bardashev and Bardasheva, tab. 1.3, pl. 4, fig. 8.
e.p.	2016c	*Palmatolepis jamieae* - Becker et al., p. 226 [one specimen]
	2018	*Palmatolepis jamieae* – Bardashev, pl. 9. fig. 8 [reillustration from 2014].

Derivation of name: After the region of the type locality at Diemelsee-Adorf.
Material: Holotype GMM B9A.13-53 (Fig. 7r), paratypes GMM B9A.13-54 (Fig. 7s), GMM B9A.13-86 (Fig. 9i), GMM B9A.13-87 (Fig. 9j), and the slightly less typical GMM B9A.13-38 (Fig. 7b). Additional specimens occur in the Winsenberg

section near Adorf (Becker et al. 2016c) and in the Hönne Valley region (Stichling et al., this vol.). Five more specimens have previously been illustrated from four distant regions.

Type locality and level: Martenberg, Sample R-Q 8–14 cm below top, Frasnian Zone 10 (*plana* Zone), upper Frasnian.

Diagnosis: Outline of platform roughly subtriangular, wide in the centre and just anterior of central node; broad, well-rounded, lappet-like lobe ending in a position lateral to the central node; anterior and posterior sinus of lobe distinct; posterior outer platform margin straight or convexly arched; carina weakly sigmoidal, bends anterior of central node towards lobe; posterior carina fine or partly reduced, turns straight inwards with little to no bending; rim of marginal nodes or short ridges on inner side of platform; blade extents anterior of platform a short distance.

Discussion: There is no morphological intergradation with relatives of *Pa. jamieae*, which justifies the introduction of a new species. It differs from all subspecies of *Pa. jamieae* in its distinctive, well-defined, subsymmetric, broadly rounded and more anteriorly situated lobe bordered by marked anterior and posterior sini. In *Pa. feisti,* there are two weak posterior sini, instead of one pronounced one while *Pa. plana* is characterised by a strongly asymmetric side lobe with very pronounced to almost rectangular anterior sinus. *Palmatolepis amplificata* and the holotype of *Pa. manzuri* share a lappet-like side lobe but it is even wider and the posterior platform is distinctively longer, pointed and constricted at the end. In *Pa. unicornis*, the side lobe has a similar shape, but the platform bears very strong nodes and the free blade consists of a single large denticle. The specimen of Lazreq (1992) is rather atypical because of its coarse posterior carina.

Stratigraphic and geographic range: The new species ranges from Frasnian Zone 10 (*plana* Zone) of the Rhenish Massif to Frasnian Subzone 11a (*feisti* Subzone) in the Moroccon Meseta (Bou Ounebdou section near Mrirt, Lazreq 1992, Bed N34, between the FODs of *Pa. feisti* in Bed N33 and *Pa. nasuta* in Bed N35), and to Frasnian Subzone 11b (*nasuta* Subzone) in Belgium (Contournement à Frasnes section, Neuville Formation, above the FOD of *Pa. nasuta*, Bultynck et al. 1998), the Moroccan Meseta (Anajdam section, Lazreq 1999, Bed A33, just below the FOD of *Pa. subrecta* = *winchelli*), and Western Australia (Horse Spring succession, above FOD of *Pa. semichatovae*, Klapper 2007). The youngest Rhenish specimen comes from the basal part of the Usseln Limestone (Frasnian Zone 12 = *winchelli* Zone, Becker et al. 2016c).

Palmatolepis descendens n. sp.
(Figs. 10k, 12g, h)

2010 *Palmatolepis* sp. nov. B - Lang and Wang: p. 27, pl. 1, fig. 7.

Derivation of name: After the posterior direction of the lobe, from Latin *descendens* = to step down.

Material: Holotype GMM B9A.13-107 (Fig. 10k), paratypes GMM B9A.13-147 (Fig. 12g), GMM B9A.13-148 (Fig. 12h). A fourth specimen has been illustrated from the far distant region of Inner Mongolia (Lang and Wang 2010).

Type locality and level: Martenberg, Sample Q 18–30 cm above base, Frasnian Subzone 11b (*nasuta* Subzone), upper Frasnian.

Diagnosis: Outline of platform roughly subtriangular to pyriform; well-rounded, lappet-like, asymmetric, short lobe oriented posteriorly and ending slightly after the central node; anterior outer margin descending with a shallow sinus and with pronounced, subrectangular posterior sinus followed by an arched posterior margin; carina weakly to moderately sigmoidal, bends anterior of central node towards lobe; posterior carina pronounced or fine, turns straight inwards with little to no bending; rim of marginal nodes or short ridges on inner side of platform.

Discussion: Lang and Wang (2010) recognised *Pa. descendens* n. sp. as a new species but left it in open nomenclature. Its posteriorly arched and lapping (nose-like) outer lobe cannot be confused with the platform shape of any other Frasnian palmatolepid. A downlapping "nose" occurs also in the younger *Pa. khaensis* (see Savage 2019) but this species is very slender and its side lobe has a concave, not convex anterior margin.

Stratigraphic and geographic range: The new species was found in the Rhenish Massif in Frasnian Subzones 11a–b (*feisti* and *nasuta* Subzones). In Inner Mongolia (Heilongjiang Province, Niqiuhe to Daminshan formations, Lang and Wang 2010), its stratigraphical position cannot be determined in a faunal association of the Frasnian Zone 11–12 (*feisti–winchelli* zones) interval.

Palmatolepis ljaschenkoae Ovnatanova, 1976
(M1: Figs. 6d, g, 9r, 11m; M2: Figs. 5c, 8t, u, 11n; M3: Figs. 6j, 9d, 10a, b, 11o)

e.p. 1958 *Palmatolepis proversa* - Ziegler: p. 62–63, pl. 3, fig. 12 [= M3], pl. 4, figs. 1, 3–6 [= M3], fig. 8 [= M2] [non pl. 3, fig. 11, pl. 4, figs. 2, 7, 9–14 = *Pa. proversa*].

1971 *Palmatolepis proversa* - Szulczewski: p. 38, pl. 9, fig. 8, pl. 10, figs. 2, 3 [= M3].

* 1976 *Palmatolepis ljaschenkoae* - Ovnatanova: p. 216, pl. 9, figs. 6a–b [= M1].

1983 *Palmatolepis proversa* - Wang and Ziegler: pl. 4, fig. 2 [= M3].

e.p. 1987 *Palmatolepis proversa* - Fuchs: pl. 5, fig. 1 [= M2], fig. 2 [= M3], figs. 3a–b [=M1] [non figs. 4a–b = *Pa. proversa*].

1989 *Palmatolepis ljaschenkoae* - Klapper: pl. 2, figs. 12, 16 [= M3].

1989 *Palmatolepis ljaschenkoae* - Klapper and Lane: pl. 1, figs. 1, 2 [= M3].

1993 *Palmatolepis proversa* - Matyja: pl. 18, fig. 11 [= M1].

1993 *Palmatolepis ljaschenkoae* - Klapper and Foster Jr.: p. 8, figs. 8.5–7 [= M3], fig. 8.8 [= M2], figs. 8.9–10 [= M3], fig. 9.9 [= M3], fig. 9.10 [= M2], fig. 9.12 [= M3], figs. 10.5–10.8 [Pb elements]

e.p. 1994 *Palmatolepis proversa* - Wang: p. 103, pl. 2, figs. 6, 7 [= M2] [non fig. 2 = *Pa. proversa*].

1994 *Palmatolepis proversa* - Bai et al.: p. 172, pl. 7, fig. 15 [= M2], fig. 16 [= M3].

e.p. 1996 *Palmatolepis ljaschenkoae* - Klapper et al.: p. 147, figs. 10.9–10.10 [= M3], 10.12 [= M2].

1999 *Palmatolepis ljaschenkoae* – Ovnatanova et al.: pl. 1, fig. 26 [= M3], pl. 2, figs. 3 [= M1], 4 [= M3].

e.p. 2002 *Kielcelepis ljaschenkoae* - Dzik: p. 593, fig. 33B [= M3] [figs. 33C1-H = other elements, non fig. 33A = *Palmatolepis* sp. juv.].

2004 *Palmatolepis ljaschenkoae* – Galushin and Kononova, p. 38, 41, figs. 8.1 [= M2], 8.2 [= cf. M2].

2008 *Palmatolepis ljaschenkoae* - Ovnatanova and Kononova: p. 1094, pl. 5, fig. 12 [= M2], figs. 13–14 [= M1], figs. 16–17 [= M2].

non 2013 *Palmatolepis ljaschenkoae* - Tagarieva: fig. 6N [= *Pa.* cf. *winchelli*].

2013 *Palmatolepis ljaschenkoae* - Matveeva: pl. 1, fig. 1 [= M2].

2014 *Palmatolepis ljaschenkoae* – Bardashev and Bardasheva, tab. 1.3, pl. 3, fig. 13 [= M3].

2015 *Palmatolepis ljaschenkoae* - Mahboubi et al.: fig. 5k [= M3].

2017 *Palmatolepis ljaschenkoae* - Ovnatanova et al.: p. 1087, pl. 33, figs. 1 [= M1], 2 [= M2], 3 [= M1].

2017 *Palmatolepis proversa* - Ovnatanova et al.: p. 1104, pl. 39, fig. 1 [= M2].

2017 *Palmatolepis barba* - Ovnatanova et al.: p. 1067, pl. 32, fig. 7 [= M2].

2018 *Palmatolepis ljaschenkoae* - Soboleva et al.: pl. 6, fig. 11 [= M1].

2018 *Palmatolepis ljaschenkoae* – Bardashev: pl. 8, fig. 13 [= M3; re-illustration from 2014].

2019 *Palmatolepis ljaschenkoae* - Over et al.: fig. 6.4 [= M2]

2020 *Palmatolepis proversa* - Izokh et al.: fig. 3e [= M2]

Revised diagnosis: Platform elongate, with asymmetric, moderately wide, anteriorly clearly demarcated lobe directed to the side, positioned well anterior of central node, margin posterior to platform lobe without any sinus, with a constricted, pointed tip, or with an additional weak to distinctive sinus defining the posterior lobe; short free blade and carina first straight, then slightly sigmoidal, fine (with three to seven nodes) after the central node, directed straight or kinked inwards, shortened or reaching the platform tip; platform weakly to moderately ornamented, small nodes arranged along platform margins may form a denticulated margin especially in anterior part.

Discussion: Specimens identified in the literature as *Pa. ljaschenkoae* display a large variability of platform shape and ornamentation. This supposed large variability contrasts with narrower taxonomic concepts in other Frasnian palmatolepids. As a step towards refinement, three morphotypes are distinguished, mostly based on the different shape of the posterior outer platform. Since they co-occur in several Martenberg beds, we do not suggest a subspecies differentiation.

Morphotype 1, which includes the holotype, is characterised by an asymmetrically arched platform margin, without any sinus, from the tip of the lobe to the posterior end. The lateral lobe and the round posterior part of the platform are, therefore, very weakly defined. The surface of the platform is rather smooth apart from nodes at the interior anterior margin in the holotype.

Morphotype 2 lacks a clear sinus delimiting the posterior end of the lobe but has a constricted and pointed posterior platform tip. Marginal nodes and fewer nodes inside the platform are typical.

Morphotype 3 has a pronounced sinus directly after the lobe and also mostly a constricted and pointed tip. The ornament resembles M2 but can be even stronger in some specimens.

Palmatolepis ljaschenkoae resembles *Pa. proversa* because of the partially (slightly) anteriorly oriented lobe. However, the angle of the anterior sinus is significantly more acute in *Pa. proversa* and its platform is stronger ornamented. Matveeva and Zhuravlev (2014) showed that juveniles of *Pa. proversa* may resemble morphotypes 1 and 2 of *Pa. ljaschenkoae*. Morphotype 1 of *Pa. ljaschenkoae* approaches *Pa. simpla*, which, however, differs by an extended, wider and anteriorly longer platform.

Stratigraphic and geographic range: The species ranges from higher parts of Frasnian Zone 8 (*housei* Zone) to within Frasnian Subzone 11b (*nasuta* Subzone; compare composite range in Klapper 1997) and occurs in Western Canada, the Illinois Basin, the Rhenish Massif (Germany), Montagne Noire (France), the Timan-Pechora Region (northern Russia), western Urals, and Canning Basin (Western Australia). Tagarieva (2013) illustrated a much younger (*linguiformis* Zone) supposed *Pa. ljaschenkoae* from the southern Urals, which possesses a more posteriorly situated side lobe, at the level of the central node. We regard it as a *Pa. winchelli* with weak posterior platform sini.

Palmatolepis proversa Ziegler, 1958
(M1: Figs. 6p, 9e, f; M2: Figs. 6o, 11q)

*e.p. 1958 *Palmatolepis proversa* - Ziegler: p. 62-63, pl. 3, fig. 11 [= M1], pl. 4, figs. 2, 7, 9–11 [= M1], figs. 12, 14 [= M2], fig. 13 [non pl. 3, fig. 12, pl. 4, figs. 1, 3–6, 8 = *Pa. ljaschenkoae*].

e.p. 1987 *Palmatolepis proversa* - Fuchs: pl. 5, figs. 4a, b [= M2] [non figs. 1-3b = *Pa. ljaschenkoae*].

non 1971 *Palmatolepis proversa* - Szulczewski: p. 38, pl. 9, fig. 8, pl. 10, figs. 2, 3 [= *Pa. ljaschenkoae*], pl. 10, figs. 1, 4 [= *Pa. housei*].

1979 *Palmatolepis proversa* - Puchkov: pl. 1, fig. 2 [= M1].

non 1983 *Palmatolepis proversa* - Wang and Ziegler: pl. 4, fig. 2 [= *Pa. ljaschenkoae*].

1989 *Palmatolepis proversa* - Klapper: pl. 2, figs. 14, 15.

	1989	*Palmatolepis proversa* - Klapper and Lane: pl. 1, figs. 3, 4.
	1990	*Palmatolepis proversa* - Ziegler and Sandberg: p. 46–47, pl. 4, figs. 1–2, pl. 5, fig. 7.
*	1990	*Palmatolepis barba* - Ziegler and Sandberg: p. 48, pl. 4, figs. 3–4, 8.
	1991	*Palmatolepis proversa* - Irwin and Orchard: pl. 2, fig. 14.
non	1993	*Palmatolepis proversa* - Matyja: pl. 18, fig. 11 [= *Pa. ljaschenkoae*].
	1993	*Palmatolepis proversa* - Klapper and Foster: p. 12, figs. 8.1–2, 9.1–8, 10.1–4.
e.p.	1994	*Palmatolepis proversa* - Wang: p. 103, pl. 2, fig. 2 [non figs. 6, 7 = *Pa. ljaschenkoae*].
non	1994	*Palmatolepis proversa* - Bai et al.: p. 172, pl. 7, figs. 15, 16 [= *Pa. ljaschenkoae*].
e.p.	2002	*Mesotaxis*? *proversa* - Dzik: p. 593, fig. 32A [fig. 32B = Pb-element].
	2007	*Palmatolepis proversa* - Klapper: p. 527, figs. 2.10–12.
	2013	*Palmatolepis proversa* - Matveeva: pl. 1, fig. 2.
	2013	*Palmatolepis barba* - Matveeva: pl. 1, fig. 10.
e.p.	2017	*Palmatolepis proversa* - Ovnatanova et al.: p. 1104, pl. 34, figs. 6–7, pl. 38, fig. 14, pl. 39, fig. 2 [pl. 33 fig. 13 missing, non pl. 39, fig. 1 = *Pa. ljaschenkoae*].
e.p.	2017	*Palmatolepis barba* - Ovnatanova et al.: p. 1067, pl. 32, figs. 9–14 [non fig. 7 = *Pa. ljaschenkoae*, fig. 8 = *Pa.* cf. *redana*].
non	2020	*Palmatolepis proversa* - Izokh et al.: fig. 3e [= *Pa. ljaschenkoae*].

Revised diagnosis: Subtriangular platform, moderately to strongly ornamented, anterior part usually with rostrum, posterior part asymmetrically constricted, pointed and bent down; free blade and carina anterior to central node straight to slightly curved; carina posterior to central node straight, fine, approaching posterior tip; narrow side lobe strongly anteriorly oriented, with acute anterior sinus and distinct notch, located anterior of central node; underside of lobe with keel (Morphotype 1) or without (Morphotype 2).

Discussion: The initial German description by Ziegler (1958) contained details omitted in the revised diagnosis by Ziegler and Sandberg (1990). These points are considered in the present revised diagnosis and contribute to the assignment of two morphotypes, which are established in order to provide a base to establish possible different distributions in time, space, and facies. **Morphotype 1** has a keel on the aboral side of the lobe, which runs towards the centre of growth at an angle of ca. 45° in relation to the longitudinal keel, **Morphotype 2** lacks the keel. In general, we follow the synonymy of Klapper and Foster Jr. (1993), which is not repeated, but add recent records and supply older references that showed lower views, where the morphotype affiliation is clear.

This species resembles *Pa. ljaschenkoae* in which the angle of the anterior sinus is significantly wider (> 90°), with the lobe oriented to the side, and its platform is usually weaker ornamented. Juveniles of both species may be similar (Matveeva and Zhuravlev 2014). Klapper and Foster Jr. (1993) synonymized *Pa. barba* Ziegler and Sandberg, 1990 and *Pa. redana* Irwin and Orchard, 1991. The latter is an extreme variant with a spine-like side lobe oriented at < 45° to the carina and with a reduced posterior carina. Such forms are currently unknown from Europe. Therefore, it qualifies as a palaeogeographically restricted form, either as a regional full species or subspecies.

Stratigraphic and geographic range: The species ranges from Frasnian Zone 9 (*proversa* Zone) to Frasnian Subzone 11b (*nasuta* Subzone) and can be found in the Canadian Rocky Mountains, Iowa (USA), Belgium, Rhenish Massif (Germany), Montagne Noire (southern France), Morocco, Holy Cross Mountains, Pomerania (both Poland), Timan-Pechora Region (northern Russia), South China, and Canning Basin (Western Australia).

Palmatolepis amplificata Klapper, Kuz'min and Ovnatanova, 1996
(Figs. 5f, 7l, 11d–e, r; cf.: Figs. 7l, 9m)

Discussion: Specimens with a markedly curved carina, with fine denticles after the central node, and raised, strongly ornamented inner margin, but without a rostrum on the platform (Figs. 5f, 7l, 11d), are intermediate towards *Pa. manzuri* Bardashev, 2009 (see Fig. 6k), in the sense of its holotype, but were part of the type series (Klapper et al. 1996, fig. 7.4). Specimens with only a few coarser nodes at the margin supports intergradation between the two species but they partly lack the posterior carina (Figs. 11e, r). Because of the close similarity, Klapper and Kirchgasser (2016) placed *Pa. manzuri* in synonymy with *Pa. amplificata*. Since rostra or raised anterior platform margins were not documented in the Asian populations (Bardashev 2009), we decided to report both forms until variabilities are better understood based on larger collections. Specimens identified as *Pa.* cf. *amplificata* (Figs. 7l, 9m) differ in an only weakly sinuous carina consisting after the central node of one or a few coarser, partly irregular, merged nodes. The platform is not flat but has raised margins both on the outer and inner side, including the side lobe, which bears a short side carina. Klapper and Kirchgasser (2016, fig. 12.15) included a somewhat different variant with weakly bent, coarse and shortened carina in *Pa. amplificata*. Further material is required to define subspecies or morphotypes within *Pa. amplificata* and to establish their ranges in space and time.

Stratigraphic and geographic range: Frasnian Zone 10 (*plana* Zone) to Frasnian Zone 12 (*winchelli* Zone) of the Canadian Rocky Mountains, Iowa, New York State, Texas, SW England (Devon), eastern Rhenish Massif, Holy Cross Mountains, and the Timan (Russia). The cf. specimens from Martenberg extend the range to Frasnian Zone 9 (*proversa* Zone).

Palmatolepis aff. *feisti*
(Figs. 7q, 12a-b)

?	1999	*Palmatolepis jamieae* - Lazreq: p. 69–70, pl. 8, fig. 4.

Description: Outline of platform moderately wide, triangular. Relatively broad, laterally directed lobe with shallow to moderately developed posterior sinus. Carina nearly straight, with slight curvature anterior of central node and posteriorly either fine, short, or missing.
Discussion: Specimens identified as *Pa.* aff. *feisti* differ from typical *Pa. feisti* in their comparatively narrower platform and their posterior carina, which is finer, short, or completely missing. In contrast to *Pa. jamieae rosa* n. ssp., their outer anterior platform is strictly concave, as in *Pa. feisti*. Lazreq (1999, pl. 8, fig. 4) identified a somewhat similar specimen as *Pa. jamieae* with a relatively pronounced sinus of the posterior platform margin.
Stratigraphic and geographic range: Frasnian Zone 11a (*feisti* Zone) in the eastern Rhenish Massif. The Moroccan specimen is probably from the base of Frasnian Zone 12 (*winchelli* Zone).

Microfacies

On the basis of the nomenclature of Dunham (1962), Hartenfels (2011) defined 19 modified microfacies types for outer shelf settings, which can be assigned to the standard facies zones (1B to 4) of Flügel (2004) and can be divided into two facies series, MF-A: facies below storm wave base, MF-B: facies supposedly within the influence of storm waves or bottom currents. According to Hartenfels (2011), this modification is necessary because hemipelagic or neritic carbonates cannot be classified with sufficient differentiation in the classic microfacies zone model of Wilson (1975) and its critical review by Flügel (2004). However, it should be noted that current-induced sedimentation in the subphotic, pelagic realm may originate from contourites rather than from storms. In the Rhenish Massif, the modified classification sensu Hartenfels (2011) was successfully applied by Lüddecke et al. (2017) on the Upper Ballberg Quarry, a middle Famennian hemipelagic seamount section. Since the Martenberg section was deposited on top of a drowned volcanic seamount, an older but comparable depositional setting is assumed to interprete the microfacies (Fig. 13).

In the micrite-saturated, partly micro-sparitized matrix of the reddish to reddish-brown, flaser-bedded wackestones (MF-A4 / MF-B1) of the top of Bed R (Fig. 13a) and the base of Bed R-Q (Fig. 13b), the proportion of skeletal hard parts varies between 10 and 30 % (compare Hartenfels 2011). The matrix is heavily churned due to bioturbation of unknown origin, which causes a partly nodular texture (Fig. 13a). Poorly preserved dacryoconarids occur isolated or as small packstone nests (Fig. 13a1) together with ostracods of Thuringian and "Entomozoacean" ecotypes. There are iron encrustations at the pressure solution seams and some dispersed aggregates with small, *Frutexites*-type microstromatolites (Fig. 13a2). The lower part of Bed R-Q differs from the top of Bed R by two minor erosion horizons (Figs. 13b1, 13b2), which subdivide the interval. Above undulating truncation levels, there are thin accumulations of angular to subangular, small-sized white iron-mineralized extraclasts, probably partly volcaniclasts, within a micrite-saturated, partly micro-sparitized matrix.

"Sheet 1" (Fig. 13c) is a well-sorted, fine-grained, partly chloritized (Fig. 13c1), calcareous, volcaniclastic packstone without any fossils. It resembles hyaloclastite matrix described from the region by Sunkel (1990). Dark iron minerals and clay minerals form the flaser seams, which represent diagenetic dissolution fronts. "Sheet 2" (Fig. 13d) consists of several layers, layers 1-5. Layer 1 consists of a very fine, recrystallized tuffite with some chlorite in its greenish to greenish-brown micro-sparitic matrix. It is followed by an undulating discontinuity surface that is partly enhanced by a thin, sparitic sheet crack, Layer 2 (Fig. 13d1). Layer 3 is a thin band of grey, clotted micrite, partly with tube-like, meandering internal structures (Fig. 13d1). It contains some fine, angular clasts, more frequent subrounded intraclasts derived from the lowermost layer, partly with dark rims and minute hematite crystals, and greenish, angular to irregular, partly slightly larger, altered (chloritized) volcaniclastics. The upper boundary of the grey band is sharp, rippled, and followed by an interval of coarse, light-grey to white orthosparite, Layer 4 (Figs. 13d, 13d1). Angular, moderately sorted, often cavernous volcaniclasts, partly associated with iron minerals, and a small amount of fine white clasts, float isolated in the sparite, mostly at the base (Fig. 13d). Layer 5 is the upper part of the thick sparite seam and characterised by a high number of floating, mostly chloritic volcaniclasts. Some of the white clasts represent crinoidal detritus since a few small crinoid ossicles were found in the barren conodont residue.

The flaser-bedded "Sheet 3" interval (Fig. 13e) consists mostly of a reddish, micritic mudstone with a small amount of small angular, white extraclasts. At the base (Fig. 13e3) and the top (Fig. 13e1), there are, again, thin volcaniclastic layers, combined with iron-mineralized dissolution seams. The volcanic particles differ from those in "Sheet 1 and 2" and contain packed, small, spherical, chloritized aggregates (Fig. 13e2). In the middle of the unit, there are a few larger lumps of these microlapilli (Fig. 13e4). Distinctive is the almost lack of identifiable skeletal remains and the lack of microfauna. Bed Q begins with a last greenish volcaniclast layer (Fig. 13f3), overlain by reddish-brown, partly micro-sparitized, flaser-bedded, micritic cephalopod limestone (Fig. 13f) with fragmentary or complete goniatites that include *Ponticeras* and *Manticoceras* (see House and Ziegler 1977), ostracods, fragmented, partly ribbed bivalves, and rare last microlapilli (Fig. 13f2). Some goniatites show horizontal, geopetal filling (Fig. 13f1) with very fine micrite and orthosparite.

Discussion

Facies development across the *semichatovae* Event

The middle-upper Frasnian palaeogeographic setting of the volcanic Martenberg seamount can be characterised as constantly shallow pelagic and below the euphotic zone. This is in accord with the rich conodont assemblages and macrofaunas (e.g. Holzapfel 1882; Paeckelmann 1936; House and Ziegler 1977) that are dominated by cephalopods associated with specialised, subphotic benthic faunal elements, such as buchiolid and other bivalves, rare gastropods, very rare proetid trilobites, and small-sized, deeper-water solitary rugose corals. The fauna and microfacies of Bed R represent MF A4 sensu Hartenfels (2011), which suggests calm and slow deposition below the photic zone and storm wave base. Based on the strong bioturbation, the sea-floor was fully oxic. Microstromatolites (Fig. 13a2) are typical for such condensed pelagic sedimentation (compare Préat et al. 2008; Hartenfels 2011; Hartenfels and Becker 2016). Dacryoconarid nests may stem from the burrowing (Fig. 13a1).

The minor erosion horizons of Bed R-Q indicate brief episodes of discontinuous sedimentation with iron mineralizations (Fig. 13b1), episodic winnowing/scouring (Fig. 13b2), and fine extraclast (volcaniclast) influx caused by bottom currents, either by distal storms or contourites. A characteristic feature of such MF-B1 wackestones (sensu Hartenfels 2011) is the combined occurrence of components of different provenance. The episodically increased bottom turbulence suggests a minor regressive trend in the terminal middle Frasnian. It is recorded in the conodont biofacies by a dominance of *Polygnathus* and partially *Icriodus* (Table 2), which persists from Sample R top to Sample R-Q 4.5–8 cm below top (Frasnian Zone 9 = *proversa* Zone to Frasnian Subzone 11a = *feisti* Subzone). This trend is briefly interrupted in Sample R-Q 8–14 cm below top by a small resurge of *Palmatolepis* (Table 2).

The top of the middle Frasnian, recorded in the thin "Sheets 1–3" interval, is marked by a further increase of bottom turbulence, early lithification, minor reworking, several phases of non-sedimentation, a complete perturbation of the fossil succession, at a time with resumed local volcanism. Previously, the youngest pyroclastic eruptions of the region were known until the lower/middle Frasnian transition (e.g. Bottke 1965; Sunkel 1990). It is remarkable that the significant changes of deposition were not recognised during the initial bed-by-bed surveys of the section (e.g. Ziegler 1958, 1971), perhaps because of the lateral unconformities increasing on the "classic" eastern face of the cliff. Klapper and Becker (1999) noted the layered interval with sheet cracks at the base of Bed Q but, due to macroscopic similarity, did not separate crinoidal bioclasts from the volcaniclasts.

The partly chloritic clasts of "Sheet 1" (Fig. 13c1) resemble the fine crystalline matrix of tuffites that are poor in degassing structures as described from the region by Sunkel (1990). There is some sorting but no grading or cross-bedding, as typical for epiclastites that are commonly redeposited on volcanic slopes. Since there are no coarse lapilli or volcanic breccias, it is not likely that the Martenberg was re-activated as an eruption centre. Due to the partial good sorting in "Sheets 1 and 2", the volcaniclasts may represent distal fallout from one of the many other volcanoes of the region. Layer 1 of "Sheet 2" consists of even finer (Fig. 13d1), probably more distal fallout mixed with carbonate mud. The overlying fine sheet crack (Layer 2) indicates a depositional interruption due to increased bottom water agitation. The overlying clotted micrite (Layer 3, Fig. 13d1), especially in combination with *Stromatactis*-type sheets (Fig. 13d), is typical for a microbial origin (e.g. Zhou and Pratt 2019). Therefore, we relate the short, diffuse tubular structures also to microbial biomineralization. Minor bottom currents led to the re-deposition of reworked and coated tuffite clasts within Layer 3 and an influx of microlapilli that were later chloritized (Fig. 13d1). The sharp, rippled surface of Layer 3 provides further evidence for weak bottom currents. This culminated in a longer phase of non-deposition marked by the thick second sheet crack (Figs. 13d, 13d1). Since chloritized microlapilli float in its late diagenetic, blocky orthosparite, there must have been an original microbial mat in the space of layers 4–5. Fine volcaniclastic and biogenic detritus was washed in by episodic currents and could not sink in the growing organic layer. This "volcaniclastic bindstone" is a rather unique type of sediment that lies outside the normal microfacies classification scheme. In the overlying "Sheet 3", pelagic micritic limestone deposition resumed but the fossil content remained very sparse (Fig. 13e) and the influx of fine volcaniclastics (Figs. 13e1–4) continued episodically.

The biotic perturbation at the end of the middle Frasnian includes a strong local decline of planktonic dacryoconarids, which proliferate in general under eutrophic conditions. The absence of conodonts in all three sheet samples, especially in the micritic "Sheet 3", suggests a phase of poor living conditions. As noted in the chapter on conodont stratigraphy, several taxa disappeared or declined locally at the top of Bed R-Q (e.g. *Ag. amplicavus, Ag. coeni, Pa. amplificata, Pa. domanicensis, Pa. jamieae savagei* n. ssp.). Microbial mats develop as typical opportunists in crisis times, especially when there are no grazers and during strong oligotrophy (e.g. Prieto-Barajas et al. 2018). In other Rhenish successions, zebra and *Stromatactis* limestones yield very rich pelagic conodont faunas (Becker et al. 2016a, c). It is not likely that the regionally youngest volcanic episode caused directly the local ecosystem crisis. The Givetian lapilli tuffites at the base of the Martenberg cliff are characterised by a highly diverse fauna of benthos and nekton.

The onset of the transgressive *semichatovae* Event is placed above the last thin, sorted, and current-induced volcaniclastic layer right at the base of Bed Q (Fig. 13f3). This is supported

by the initial appearance of *Pa. semichatovae* and *Pa. nasuta* (Frasnian Subzone 11b / *nasuta* Subzone) and by a conodont biofacies shift to dominant *Palmatolepis* (Table 2). Although our Sample Bed Q base is not diagnostic due to the very small number of conodonts, this trend can be observed well in the higher samples of Bed Q (18–30 cm above base). It is noteworthy, that no new specimens of *Pa. semichatovae* were found during resampling. As shown by the onset of micritic cephalopod floatstones (Fig. 13f), the basal upper Frasnian environmental conditions at Martenberg were too pelagic; the species prefers more neritic facies, as in the Ardennes or North America. The deepening trend is supported by a sudden bloom of goniatites (e.g. Wedekind 1913; House and Ziegler 1977) and pelagic bivalves, but the dacryoconarid population did not recover. The spread of *Stilleoceras* (= *Maternoceras*) and entry of *Playfordites* within Wedekind´s do Iß characterise UD I-I, as part of a global, rapid, basal upper Frasnian goniatite radiation (e.g. Becker and House 1993, 1997). It should be noted that the position of Iß is incorrectly marked in House and Ziegler, 1977, Fig. 2); the true level of rich *Stilleoceras* faunas is given in the bed-by-bed goniatite record. After the volcaniclastic influx had faded very gradually in the main part of Bed Q (Fig. 13f2), the hemipelagic, subphotic, and calm deposition continued in Bed P. Upsection, its cephalopod floatstones with *Manticoceras* were increasingly altered by late diagenetic dolomitisation, resulting in yellow to pink weathering colours and poor preservation of macrofaunas (compare Wedekind 1913; House and Ziegler 1977).

Conodont zonation and the middle/upper Frasnian boundary

The problem of the precise correlation of the *jamieae* Zone in its type locality with the Frasnian zonation has been briefly outlined above. It has to be emphasised that the Martenberg was designated as the reference section for the zone and that it is, therefore, critical to reach a refined understanding and to clarify if it is a useful biostratigraphic unit at all. As shown below in detail, the zone has been uncritically used by many authors on a global scale. Therefore, we are aware that it will not be easy to delete it from the future literature.

Ziegler and Sandberg (1990) assigned beds R and R-Q and laterally equivalent samples (samples VI′/12-10, VI/12a) to the Upper *hassi* Zone, Bed Q (samples VI′/9-6, VI/11b-11a) to the *jamieae* Zone, and Bed P (samples VI′/5, VI/10e) to the Lower *rhenana* Zone (Figs. 3 and 14). However, no *Pa. jamieae* was figured from the *jamieae* Zone and due to their wide concept of the species, including *Pa. feisti* and forms placed by us in separate species/subspecies, the Martenberg level of *Pa. jamieae* sensu its holotype remained undocumented. Klapper and Becker (1999) correlated Bed R-Q with Frasnian Zone 10 (*plana* Zone), Bed Q, the supposed *jamieae* Zone, with Frasnian Zone 11 (*feisti* Zone), and Bed P, the assumed basal Lower *rhenana* Zone, with the lower part of the Frasnian Zone 12 (*winchelli* Zone). This created a contrast with the Lion Quarry section of Sandberg et al. (1992), where the Lower *rhenana* Zone falls in Frasnian Zone 11, not in Frasnian Zone 12. This stimulated faunal revisions and corrections by Ziegler and Sandberg (2000), who re-assigned the "upper part of Bed R" (VI'/10), which refers to Bed R-Q, to the *jamieae* Zone, because of a rare occurrence of supposed *Pa. jamieae,* Bed Q (Sample VI/11b) to the Lower *rhenana* Zone, and Bed P to the Upper *rhenana* Zone. The *jamieae* Zone shifted completely its position and became very thin. This resulted in a new correlation of the Frasnian Zone 10 with the assumed *jamieae* Zone, of Frasnian Zone 11 with the lower part of the Lower *rhenana* Zone, as at Lion, and of Frasnian Zone 12 with the basal Upper *rhenana* Zone. As in 1990, it remained unknown, which form included in *Pa. jamieae* (here "*Pa. jamieae* auct.") does occur in the new *jamieae* Zone level. Clarification was partly provided by the revision of original collections by Ovnatanova and Kononova (2000), who did not find any true *Pa. jamieae* in beds R-Q and Q, only in Bed P, which equals the type level of the species (and subspecies) at Schmidt Quarry. Consequently, the justification for the *jamieae* Zone as a separate biostratigraphic unit was denied.

Our new samples enable a further clarification of the problem. We can confirm that no typical *Pa. jamieae*, *Pa. jamieae jamieae* of our revised taxonomy, occur in beds R to Q. We also did not find any among the 1763 new Pa elements from the middle part of Bed Q. This suggests that it is locally a very rare form with random occurrences that is NOT suitable as a zonal index taxon. The recognition of *Pa. jamieae savagei* n. ssp., *Pa. jamieae rosa* n. ssp., and *Pa. adorfensis* n. sp. in the lower/middle part of Bed R-Q explains the Ziegler and Sandberg (2000) *jamieae* record from this bed and supports the implied revised correlation with Frasnian Zone 10 (*plana* Zone). However, our new taxa are rare and *Pa. plana*, represented by 50 specimens in our two samples, is a distinctive, much better zonal index form. We follow Ovnatanova and Kononova (2000) and postulate to abandon the *jamieae* Zone completely. If authors do not wish to apply the Montagne Noire zonation, they should replace the *jamieae* Zone by the *plana* Zone, which has the big advantage to enable a straight forward correlation of both zonation schemes. Based on data in Sandberg et al. (1992), the entry of *I. praealternatus praealternatus* predates in Belgium the entry of *Pa. plana*, but not at Martenberg. *Ancyrognathus triangularis* is an additional Frasnian Zone 10 marker but becomes much more common in the overlying zones.

As explained above, the Frasnian Zone 11 (*feisti* Zone) is subdivided into Frasnian Subzone 11a (*feisti* Subzone) and Frasnian Subzone 11b (*nasuta* Subzone). The first begins just before the probably eustatically controlled regression preceding the *semichatovae* Transgression and may have been a short interval. However, this view is based on the reduced thickness at Martenberg, which is perhaps distorted by times of non-deposition. Based on the successions of the Timan from Member 1 (TP-

VIIb Assemblage of Ovnatanova and Kononova 2020) and basal part of Member 2 of the Lyaiol Formation (basal TP-VIII Assemblage of Ovnatanova et al. 1999), and the Canning Basin (Klapper 2007), *Pa. elegantula, Pa. ederi*, *Pa. timanensis,* and *Pa. brevis* also occur in Frasnian Subzone 11a (*feisti* Subzone) but may partly enter slightly earlier than *Pa. feisti* (compare composite range for *Pa. ederi* in Klapper et al. 1996 and range charts in Ovnatanova and Kononova 2008, 2020). Therefore, there is not a precise correlation with the regional, northern Russian *elegantula-semichatovae* Zone of Ovnatanova and Kononova (2008), which ranges from the top of Frasnian Zone 10 (*plana* Zone) to the top of Frasnian Subzone 11b (*nasuta* Subzone).

The *semichaetovae* Transgression or *semichatovae* Event s.str. characterises the base of Frasnian Subzone 11b, with *Pa. nasuta* as index species (as for the Lower *rhenana* Zone). It is important to distinguish *Pa. nasuta* correctly from the morphologically somewhat similar, partly older, partly overlapping *Pa. mucronata* and from the younger *Pa. boogardi* (see Klapper et al. 1996, p. 147: focus on the carina curvature and orientation). Auxiliary index forms are *Pa. semichatovae* (index of the shallow-water *semichatovae* Subzone of Morrow and Sandberg 2008 and of Alberta Zone 5 of Klapper and Lane 1989) and *Po. lodinensis* (compare Klapper 2007 and Narkiewicz and Bultynck 2011; but see an alleged lower range predating the entry of *Pa. plana* in the Polar Urals, Sobolev and Soboleva 2018). In northern Russia and Australia, *Pa. anzhelae* and *Pa. playfordi* are further guide species (see Klapper 2007; Ovnatanova and Kononova 2020); in the Timan probably also *Po. siratchoicus* and *Pa. lyaiolensis* (Ovnatanova and Kononova 2008; Ovnatanova et al. 2017; Sobolev and Soboleva 2018). In New York State and Iowa, *Po. unicornis* and *Tortodus deformis* enter with *Pa. semichatovae* (Klapper and Kirchgasser 2016; Day and Witzke 2017). *Palmatolepis eureka* appears in Belgium at the same level as *Pa. nasuta* (Ziegler and Sandberg 1990; Sandberg et al. 1992). In the shallow-water regions of the Russian Platform, *Pa. semichatovae* provides a correlation with the *Polygnathus subincompletus* Zone of Ovnatanova and Kononova (2008).

The combined FADs of palmatolepids, polygnathids, and species of other genera give an optimal correlation potential. Therefore, **we propose to place the future base of a formal upper Frasnian substage at the base of Frasnian Subzone 11b** (base *nasuta* Subzone = base Lower *rhenana* Zone = base *semichatovae* Subzone), which conforms with the original proposal of Ziegler and Sandberg (1997). The so defined substage would be easily recognisable in ammonoid biostratigraphy by the onset of UD I-I faunas and in sequence stratigraphy by the TST base. Detailed chemostratigraphic work is required. The final ending of basaltic phreatomagmatic volcanism at Martenberg may be a coincidence; elsewhere in the northern Rhenish Massif, last "Diabas" lava flows were found up to the highest Frasnian (e.g, at Wuppertal-Barmen, Paeckelmann 1928b).

Previous regional records of supposed *Pa. jamieae* and the *jamieae* Zone

In the light of the new knowledge, previous records of the *jamieae* Zone and supposed regional *Pa. jamieae* occurrences are reviewed, giving the relevant literature for further reading. This is an essential precondition to revise former age identifications, international correlations, and an important step towards a correct substage recognition in many regions.

In the Great Basin of the **Western United States**, at Devils Gate, Nevada, Ziegler and Sandberg (1990) showed the supposed position of the *jamieae* Zone but without any record of its index form above the FOD of *Pa. plana* and below the FOD of *Pa. nasuta*. A supposed specimen from the top of the "Early *rhenana* Zone" was re-assigned by Klapper (2007) to *Pa. uyenoi*. There is also no faunal record of the *jamieae* Zone at Tempiute Mountain (Morrow 2000), where not-figured "*jamieae* auct." were first recorded with *Pa. nasuta*, which is Frasnian Subzone 11b (*nasuta* Subzone). In the chert facies at Whiterock Canyon (Morrow 2000), there is no record of "*Pa. jamieae* auct." in the noted *jamieae* Zone, as at Devils Gate; only *Pa. proversa* and *Pa. simpla* were found, which suggests Frasnian zones 9/10 (*proversa*/*plana* zones).

Levman and Bitter (2002) illustrated as *Pa. jamieae* a specimen from the Long Rapids Formation of northern **Ontario** (Canada), which combines the platform shape of *Pa. feisti* with an ornament as in *Pa. winchelli*. This homoeomorphic new form comes from the top of Frasnian Zone 13a (top *bogartensis* Zone) and has nothing to do with *Pa. jamieae jamieae*, nor with the older *Pa. feisti*. This is probably also true for three further not figured specimens and for another one from the subsequent basal Frasnian Zone 13b (*linguiformis* Zone). The region has no *jamieae* Zone record but Frasnian Zone 10 (*plana* Zone) was distinguished by Klapper et al. (2004).

Helsen and Bultynck (1992; compare Bultynck et al. 1998) identified the *jamieae* Zone in the Nismes section of the **Ardennes** and showed it questionably in the Mariembourg section in the southern flank of the Dinant Syncline. However, both Nismes specimens illustrated are not *Pa. jamieae jamieae*, but *Pa. jamieae rosa* n. ssp. (their pl. 3, fig. 7) and *Pa. wildungensis* (their pl. 3, fig. 6). The first comes from high in Member 2 of the Neuville Formation (Bed C10B) and from well above the level of the *semichatovae* Event, suggesting Frasnian Subzone 11b, the second from the higher part of Member 3 (Bed C13B), above the FOD of *Ad. ioides* (in Bed C12) and above the FOD of *Pa. winchelli* (in Bed C12c; identified by Bultynck et al. 1998, pl. 2, fig. 7 as *Pa. gigas*), therefore, from Frasnian Zone 12 (*winchelli* Zone). The listed (not figured) oldest "*Pa. jamieae* auct." enter at Nismes with *Ag. triangularis* and above the first *Pa. plana* in Bed C1. Therefore, they come from Frasnian zones 10 to 11 (*plana* to *feisti* zones); which gives a good match with the Martenberg. Younger "*Pa. jamieae* auct." from the Upper

rhenana Zone (Frasnian Zone 12) may have included typical specimens. The specimen from the Frasnes-W section illustrated by Bultynck et al. (1998) does not represent *Pa. jamieae jamieae* but *Pa. adorfensis* n. sp. (pl. 1, Fig. 13). As the not figured "*jamieae* auct." specimens from below (Sample CFrW 2), it comes from Frasnian Subzone 11b (*nasuta* Subzone); the *jamieae* Zone was not recognised in that section, nor at Neuville and Lessive, where not figured "*Pa. jamieae* auct." occur in the Upper *rhenana* Zone.

Sandberg et al. (1992) reported *Pa. jamieae* from the Lion Quarry access road section and the north side of the Tiènne du Lion section and used it to determine the local lower limits of the *jamieae* Zone. One of the two specimens of *Pa. jamieae* shown is *Pa. feisti* (their pl. 3, fig. 5). It was found at a level (Sample 85-BEL-118) above the entry of *Pa. nasuta* (85-BEL-115), *Pa. winchelli* (= *subrecta*) and *Ad. ioides* (both in 85-BEL-116), therefore, in Frasnian Zone 12 (*winchelli* Zone). The other figured specimen is *Pa. jamieae jamieae*. It is even younger (85-BEL-120, their pl. 3, fig. 3) and was associated with *Pa. rhenana*, as in the Kellerwald type level. The not figured "*Pa. jamieae* auct." enter with (Tiènne du Lion) or above (access road section, base of Boussou-en-Fagne Member) *Pa. plana* in Frasnian Zone 10, which gives another good fit with Martenberg. In the railroad cut west of the Lion Quarry and in the section at the south end, the *jamieae* Zone was not recognised but Frasnian Zone 10 (*plana* Zone) is recognisable by its index species, near the base of the Boussou-en-Fagne Member. Therefore, the Lion successions underline the usefulness of the *plana* Zone. In summary, no early member of the *Pa. jamieae* Group has ever been figured in the Ardennes from time equivalents of the supposed *jamieae* Zone at Martenberg. The typical subspecies occurs regionally at its type-level while the precise affinities of even younger specimens, from the lower part of the Matagne Formation, are currently unknown.

In the eastern **Rhenish Massif**, the *jamieae* Zone was recognised by Ziegler and Sandberg (1990) in the Heimberg section, which still exists but the middle-upper Frasnian transition lies at a very steep slope above an old quarry and is dangerous to access. Only some beds have been sampled so far. The *jamieae* Zone was recognised above the entry of *Pa. plana* and *Ag. triangularis* (Frasnian Zone 10 / *plana* Zone) and below the entry of *Pa. nasuta* (Frasnian Subzone 11b / *nasuta* Subzone). None of the "*jamieae* auct." specimens were illustrated and *Pa. feisti* or early *Pa. jamieae* subspecies would be expected between the two recognised levels. The section has potential but resampling is required. Pas et al. (2013) showed the *jamieae* Zone in the Burgberg section situated on a drowned volcano south of the Brilon Reef. They referred to conodont data of Stritzke (1990), who did not report any *Pa. jamieae*, and to their own samples, which results were not given.

At Benner near Bicken in the southern Rhenish Massif (Lahn Syncline), the middle-upper Frasnian transition shown in the section log by Ziegler and Sandberg (1990) is condensed. The more than 3 m thick interval from the supposed base of the Lower *rhenana* Zone to the base of the Lower Kellwasser level does not correlate well with the more detailed log of Schindler (1990), who noted that older beds became inaccessible after flooding by a fish pond, including strata up to the middle Frasnian (Schülcke 1995). Ziegler and Sandberg´s not figured "*Pa. jamieae* auct." enter jointly with *Pa. plana*, as at Martenberg, and range into faunas with *Pa. rhenana* and *Pa. winchelli* (= *subrecta*) from just below the Lower Kellwasser level (higher Frasnian Zone 12 = *winchelli* Zone). The latter specimens may have included typical *Pa. jamieae*. The local supposed *jamieae* Zone (beds 59–60), here re-assigned to the *plana* Zone/*feisti* Subzone interval, was thin (ca. 25 cm); it needs to be restudied.

In the **Carnic Alps**, Spalletta and Perri (1998) recognised the *jamieae* Zone based on the entry of *Pa. foliacea*, which, however, enters later (high in Frasnian Zone 11, Klapper and Kirchgasser 2016) than the supposed *jamieae* Zone levels at Martenberg. In France and Spain, the *jamieae* Zone has not been identified although the term was used unspecifically by Sanz-López (2002) in a discussion of the Pyrenees Frasnian.

In the Mrirt region of the **Moroccan Meseta**, the *jamieae* specimens illustrated by Lazreq (1992, 1999) do not belong to *Pa. jamieae jamieae*. At Bou Ounebdou (= Gara d´Mrirt), a representative from the rich fauna of the supposed *jamieae* Zone of Bed N33 (1999: pl. 8, Fig. 4) is a *Pa. feisti*, while a specimen from the next higher Bed N34 (1992: pl. 1, Fig. 15) falls in *Pa. adorfensis* n. sp. A specimen from Bed N32 identified as *Pa. hassi* (1992: pl. 1, Fig. 12) is close to *Pa. jamieae savagei* n. ssp. M1. Not figured *Ad. ioides* (s.l.) from these beds indicate the Frasnian Zone 11/12 interval and a condensed succession starting with Frasnian Zone 10 (*plana* Zone; see review of Becker et al. 2020b) that requires refinements. A supposed younger *jamieae* specimen from Bed N41 (1992: pl. 1, Fig. 14) falls already in Frasnian Zone 13a (*bogartensis* Zone) and does not belong to a named species. Further not-figured "*Pa. jamieae* auct." were reported from the same succession by Hüneke (2001) and should be revised.

The situation seems similar in Lazreq´s Anajdam section, in the south of Mrirt, where not figured "*Pa. jamieae* auct." enter in the solid beds 31–31c, again jointly with not figured *Ad. ioides* (s.l.). Resampling produced a typical fauna from the upper Frasnian Zone 10 (*plana* Zone, Becker et al. 2020b: their Bed 33c). Strangely, Lazreq´s Fig. 10 showed a higher start of the *jamieae* Zone with her Bed 32. The only figured *Pa. jamieae* from Anajdam (Lazreq 1999, pl. 8, Fig. 4) is a *Pa.* aff. *feisti* from her Bed 33, which also yielded "*Pa. gigas gigas*" and which just predates the entry of *Pa. winchelli* (= *subrecta*) in her Bed 34. An even younger Anajdam specimen illustrated as *Palmatolepis* ?n. sp. by Becker et al. (2020b, fig. 18.19), from just below the Lower Kellwasser Limestone (Frasnian Zone 12), resembles vaguely *Pa. jamieae rosa* n. ssp. but is rotund, not subrhombic in shape.

In the more southern part of the Mrirt region, at Tougguiou-Allal (see map in Becker et al. 2020b), the *jamieae* Zone was again recognised by Lazreq (1999) in beds with *Ag. ioides* (s.l.), above the FOD of *Ag. triangularis* and below the FOD of *Pa. semichatovae*, which suggests the Frasnian Zone 10/Frasnian Subzone 11a interval, as at Martenberg. However, no specimen was figured. From Mrirt far to the northwest, in the northern El Hamam Zone, the *jamieae* Zone was recognised by Lazreq (1999) at Bou Alzaz North and Aïn Azza in the same position; again, the affinities of not figured "*Pa. jamieae* auct." are unclear. Re-sampling is required, also to clarify whether the repeated early *Ag. ioides* records of the Meseta refer to *Ag. ioides* M1 sensu Klapper (2021) that enters in the Rhenish Massif in Frasnian Subzone 11a (*feisti* Subzone, Stichling et al., this vol.).

Matyja and Narkiewicz (1995) described the *jamieae* Zone from the Janczyce I borehole section (at 373.3 m depth) in the eastern **Holy Cross Mountains** (Poland) and pictured in a slightly oblique view one of their two oldest specimens, which is probably *Pa. jamieae* n. ssp. δ. Associated are mostly polygnathids, *I. praealternatus praealternatus*, and *Pa. simpla*, which suggests Frasnian Zone 10 (*plana* Zone). A locally youngest, not-figured "*Pa. jamieae* auct." was found in the same level as *Pa. nasuta* (at 347 m depth), indicating Frasnian Subzone 11b. In the Pagow IG 1 borehole of the Malopolska Massiv, Malec (2015) illustrated specimens close to *Pa. kireevae* as supposed *Pa. jamieae* from an interval with *Pa. proversa* and *Pa. ederi*, which was assigned to the *jamieae*-Lower *rhenana* Zone interval. A *Pa. jamieae jamieae* from a level with numerous *Pa. subrecta* (= *winchelli*; Frasnian Zone 12) was identified as "*Pa.* cf. *rotunda*".

The *jamieae* specimens found by Çapkınoğlu, 2005, figs. 5.15–16) in the Ayineburnu Formation section (Istanbul Zone, **Turkey**) are smooth and lack a marked posterior platform sinus. Therefore, they are assigned to *Pa. jamieae* ssp. δ and come from Frasnian Zone 13a (*bogartensis* Zone). Not figured "*Pa. jamieae* auct." occur lower down, above *Po. lodinensis*, which indicates Frasnian Subzone 11b (*nasuta* Subzone) at the section base.

In the **southern Timan** of the northern Russian Platform, *Pa. jamieae jamieae* is restricted to the regional TP-IX assemblage of Ovnatanova et al. (1999), which occurs in the upper part of Member 3 and Member 4 of the Lyaiol Formation (Ovnatanova and Kononova 2008) that falls in Frasnian Zone 12 (e.g. Klapper et al. 1996; House et al. 2000). *Palmatolepis jamieae* ssp. δ and an atypical variant of *Pa. jamieae savagei* n. ssp. M2 without posterior platform sinus are associated; no *jamieae* Zone was regionally distinguished. In the **northern Timan/Subpolar Urals** region, Savage and Yudina (2001) illustrated a specimen as *Pa. jamieae*, which is a typical *Pa. feisti*. Therefore, their *jamieae* Zone, recognised in Sample 87-2/83 in the Syv`yu River section, falls in Frasnian Subzone 11a (*feisti* Subzone). Their younger (Sample 87-2/98) *Pa.* cf. *jamieae* includes a probable *Pa. nasuta* with short side lobe and a *Pa.* ?*hassi*, suggesting a Frasnian Subzone 11b age (*nasuta* Subzone). Our revisions agree with Ovnatanova et al. (2017, tab. 4), who did not recognise any *Pa. jamieae* (s.str.) in their extensive samples from the same section and why they questioned the regional meaning of the *jamieae* Zone, which previously, however, was used by Tsyganko (2011). In the adjacent Shar´yu River section, not illustrated "*Pa. jamieae* auct." of Ovnatanova et al. (2017) occur within the Vorota Formation with *Pa. semichatovae* and *Pa. nasuta* in the Frasnian Subzone 11b (*nasuta* Subzone). Slightly younger specimens (Ovnatanova et al. 2017, pl. 35, Figs. 3 and 4, Sample 217) are re-assigned to *Pa. jamieae rosa* n. ssp. and *Palmatolepis* sp. ε; they co-occurred with *Pa. gyrata*, indicating Frasnian Zone 12 (see Klapper et al. 1996). From the Bol´shaya Sa´uyga River, there are only cf. records of "*Pa. jamieae* auct." associated with *Pa.* cf. *semichatovae* (Ovnatanova et al. 2017, Table 2). In the Kozhim River section of the same region, Matveeva (2013) recognised the *jamieae* Zone above the FOD of *Pa. plana* and below the FODs of *Pa. nasuta*, correlating with the higher FZ 10 and FZ 11a interval, but the reported palmatolepid fauna lacks any *Pa. jamieae* records. For the Lemna River Basin of the **Polar Urals**, Ovnatanova et al., 2017, pl. 41, Fig. 1) documented a *Pa. jamieae* that represents ssp. δ. Details of its assemblage and precise level at Nadota River are unknown. In summary, the available date don´t justify a *jamieae* Zone below equivalents of Frasnian Subzone 11b in all of northern Russia.

In the **Tatarstan** region west of the Urals, *Pa. jamieae* ssp. δ was documented by Ovnatanova and Kononova, 2008, pl. 11, Fig. 3) from probable beds of Frasnian Zone 13a (*bogartensis* Zone). Not figured "*Pa. jamieae* auct." range lower, probably into Frasnian Zone 12 levels; no *jamieae* Zone was recognised. In the western **South Urals**, not figured "*Pa. jamieae* auct." were reported with *Pa. plana* and the endemic *Pa. triquetra* from within the regional "Domanik Horizon" of the Gabdyukovo section (Artyushkova et al. 2011), therefore, from within Frasnian Zone 10 (*plana* Zone). In the much more densely sampled Ryauzyak section, the *jamieae* Zone was based on the entry of not figured "*Pa. jamieae* auct." just before the FOD of *Pa. plana,* well below the very closely spaced successive entries of *Pa. semichatovae, Pa. nasuta,* and *Pa. bogartensis* (= *rotunda*) in the overlying Mendym Horizon (Artyushkova et al. 2011). Alleged *jamieae* specimens range very high in the Upper *rhenana* Zone (Frasnian Zone 13a). From the subsurface of the **Volgograd region** of the Russian Platform, *Pa. jamieae savagei* n. ssp. M1 was illustrated from an interval in borehole 96-Kamyshiiskoj that also contained *Pa. lyaiolensis, Pa. foliacea,* and *Pa. subrecta* (= *winchelli*), indicating Frasnian Zone 12. Not figured "*Pa. jamieae* auct." enter already below, at a level with *Po. lodinensis* and *Pa. lyaiolensis*, indicating Frasnian Subzone 11b (*nasuta* Subzone), and at an unspecified level of Frasnian zones 11–13 in a second borehole (14-Pamsiatno-Sasovskoj).

In the **Rudny Altai** of southern Siberia, the *jamieae* Zone was recognised by Izokh et al. (2004) based on occurrences of the typical subspecies. However, these come from well above the entry of UD I-I ammonoid faunas (unpublished material collected by RTB in 2005), indicative of Frasnian Subzone 11b, and are obviously associated with *Pa. rhenana, Pa. muelleri,* and *Pa. jamieae savagei* n. ssp. M2, suggesting a Frasnian Zone 12 (*winchelli* Zone) age for figured specimens. The supposed occurrence of *Pa. jamieae* in the Tien Shan of **Uzbekistan** is based on an atypical specimen closer to *Pa. foliacea* than to *Pa. jamieae* (Erina in Kim et al. 2007). A *jamieae* specimen from **Tadzhikistan** (Bardashev and Bardasheva 2014; Bardashev 2018) is very close to our *Pa. adorfensis* n. sp.

Ji and Ziegler (1993) assigned in the Lali section of **Guangxi**, **South China**, their Bed 33 to the *jamieae* Zone but did not illustrate any specimen from this level, which contained *Pa. plana*, suggesting Frasnian Zone 10 (*plana* Zone). A not figured cf. *jamieae* specimen was reported from the level of *Pa. proversa* (Frasnian Zone 9 = *proversa* Zone) in the bed below. The overlying Frasnian Subzone 11b with *Pa. nasuta* yielded not figured "*Pa. jamieae* auct." (beds 34 and 36) and *Pa. jamieae* ssp. δ (pl. 27, fig. 2, Bed 37). Supposed *jamieae* specimens, re-assigned to *Pa. jamieae savagei* n. ssp. M2 (pl. 27, Fig. 1) and *Pa. winchelli* (pl. 27, Fig. 3), come from the overlying beds 38 and 39 with *Pa. subrecta* (= *winchelli*), proving Frasnian Zone 12. Zhang et al. (2019) did not recognise the *jamieae* Zone in their new Lali section, which is not the same as the now covered section of Ji and Ziegler (1993).

Among the *jamieae* specimens of Ji (1993), collected from the Yangti (= Yangdi or Fuhe) section, Guangxi (compare Ji 1992), one is *Pa. jamieae* ssp. δ (pl. 13, Fig. 12), while two others belong to *Pa. jamieae savagei* n. ssp. M1 (pl. 13, Figs. 10 and 11). They range from Frasnian Subzone 11b (*nasuta* Subzone, Sample YT-21), just above cherts of the Lazhutai Formation (the local *semichatovae* Event Interval), to Frasnian Zone 12 (*winchelli* Zone, Sample YT-26). The two *jamieae* specimens from Frasnian Zone 13a (*bogartensis* Zone) shown by Huang and Gong (2016) are atypical. One (fig. 4.14) is an extreme variant of ssp. δ with very posteriorly positioned, triangular side lobe, one (fig. 6.20) is a smooth form with the platform shape of *Pa. jamieae rosa* n. ssp.

Wang (1994, with re-illustrations in Wang 2016) identified the *jamieae* Zone in the Dongcun and Sihongshan sections in Guangxi. The figured specimens are not *Pa. jamieae jamieae*, but *Pa. plana* (pl. 2, Fig. 10: top Frasnian Zone 12; pl. 6, Fig. 13, Frasnian Subzone 11b with *Pa. nasuta*), *Pa. uyenoi* (pl. 6, Figs. 11 and 12), and *Pa. jamieae savagei* n. ssp. M2 (pl. 6, Fig. 14, from Frasnian Subzone 11b with *Pa. nasuta*; the sample number clearly indicates the Sihongshan section, not the Longmen section as said in the plate explanation). Specimens from the supposed *jamieae* Zone were not figured: at Dongcun, oldest, not figured "*Pa. jamieae* auct." were found between *Pa. simpla*, indicative at Martenberg for Frasnian Zone 10 (*plana* Zone), and the first *Pa. nasuta*, therefore, probably in equivalents of Frasnian Subzone 11a (*feisti* Subzone). At Sihongshan, they were reported from the same level, just below a single sample with *Pa. semichatovae*. Zhang et al. (2008) vaguely noted the *jamieae* Zone in their section log of the Bancheng section, southeastern Guangxi, but without any conodont record. There are further not figured Guangxi records of "*Pa. jamieae* auct." from Frasnian Zone 13a (*bogartensis* Zone, based on *Pa. rotunda* = *bogartensis*) of the Liujing section (Du et al. 2008) and from the Frasnian Subzone 11a with *Pa. nasuta* to lower Frasnian Zone 13a (*bogartensis* Zone, based on *Pa. rotunda*) of the Nandong section (Huang et al. 2018).

In the Shetianqiao section of **Hunan**, Ma et al. (2004) and Ma and Zong (2010) assigned a conodont-free interval below *Pa.* cf. *semichatovae* to the *jamieae* Zone. In summary, from all of South China, no *jamieae* specimen has ever been figured from time equivalents of the supposed *jamieae* Zone at Martenberg. From higher beds, there is no proven record of *Pa. jamieae jamieae* but of the three other subspecies. Additional forms seem to characterise Frasnian Zone 13a and require further work. The *jamieae* specimens from **Inner Mongolia** shown by Lang and Wang (2010, pl. 1, Figs. 12 and 13) are elongate variants of *Pa. jamieae savagei* n. ssp. M1 and come from a unit with mixed faunas.

Savage (2013, 2019) described *Pa. jamieae jamieae* jointly with *Ad. ioides*, close relatives of *Pa. subrecta* (= *winchelli*; named as *Pa. khaensis* in 2019) and "*Pa.* aff. *rotunda*" from the upper part of Frasnian Subzone 12 (*winchelli* Zone) of **Northwestern Thailand.** A specimen named as *Pa.* aff. *jamieae* resembles *Pa. jamieae savagei* n. ssp. Morphotype 1 (Savage 2013: figs. 5, 13 and 14 = 2019: figs. 9, 3, 4 and 5) but may have been elongated by tectonic deformation. It is much younger than the Martenberg specimens and comes from the upper part of Frasnian Zone 13a (*bogartensis* Zone). Ta et al. (2021) recognised in **Central Vietnam** a *jamieae* Zone between an *Ag. triangularis* Zone below, beginning well above the FOD of *Pa. plana*, and a *Pa. rhenana nasuta* Zone above, therefore from the upper Frasnian Zone 10 to Frasnian Subzone 11a interval, as at Martenberg. However, none of the supposed *Pa. jamieae* from four beds have been illustrated, which prevents a re-interpretation. The same applies to "*Pa. jamieae* auct." noted in the range chart of Matsuo et al. (2020) for their Frasnian-Famennian boundary section (stratotype of the Xom Nha Formation) in the same region, which were noted between the FODs of *Pa. rhenana* and *Pa. boogardi*, therefore in Frasnian Zone 12 (*winchelli* Zone).

Klapper (2007) described *Pa. jamieae jamieae* from Frasnian Zone 12 (*winchelli* Zone), the type level, and a cf. specimen from Frasnian Subzone 11b (*nasuta* Subzone, regionally identified by the entry of *Pa. semichatovae*) of the

Horse Spring section (Canning Basin, **Western Australia**). Below, as at Martenberg, there are no *Pa. jamieae* sensu the holotype in Frasnian Zone 10 (*plana* Zone) or Frasnian Subzone 11a (*feisti* Subzone).

This summary underlines the very heterogeneous nature of previous literature records of *Pa. jamieae* and local versions of the *jamieae* Zone. Various oldest records fall in the globally recognisable Frasnian Zone 10 (*plana* Zone), as at Martenberg, but there is no evidence that a precisely correlated time interval was meant in the many different regions. *Palmatolepis feisti* has not been recorded widely but it may be hidden among "*Pa. jamieae* auct." specimens that were not illustrated. We expect that the *feisti* Zone/Subzone will be recognised in pelagic successions of more regions in the future.

Potential basal upper Frasnian GSSP sections

The northern slope of the protected Martenberg section currently has potential as a future GSSP for the base of a formal upper Frasnian substage. Geochemical work would have to be added to the data on conodont and ammonoid biostratigraphy, sedimentology/microfacies, and sequence stratigraphy. The extreme rarity of zircons in Rhenish basaltic volcanites strongly delimits the options for an absolute dating of the thin volcaniclastic layers. The closest zircon-bearing distal fallout layer belong to the Pegasus Group of the tephrostratigraphic correlation of Winter (2015). They lie a third up in the Lower *rhenana* Zone at Benner (Lahn Syncline), in the Lion Quarry of Belgium, and in the upper Oos Formation (in the supposed *jamieae* Zone) of the Prüm area, Eifel Mountains (Grimm and Rothausen 1992).

On a global scale, very few other sections with a sufficient bed-by-bed record of conodont faunas, especially of the top Frasnian Zone 9 (*proversa* Zone) to Frasnian Subzone 11b (*nasuta* Subzone) interval, and more specifically around the regressive-transgressive phases around the *semichatovae* Event, have been published. One exception is Devils Gate in Nevada (Ziegler and Sandberg 1990), which includes a small unconformity between the entries of *Pa. nasuta* (Sample 10) and of rare *Pa. semichatovae* (Sample 9B), and which lacks other biostratigraphic markers, such as goniatites. There are other sections with potential for detailed correlation that should be re-investigated at finer detail before any GSSP decision. We omit from a short compilation sections that are very difficult to access (e.g. in the Russian Far East or in the military zone at the Moroccan-Algerian border), temporary (boreholes, filled trenches, e.g. at La Serre, southern France, overgrown, e.g. the original Lali section of Ji and Ziegler 1993; active quarries, such as Kowala in the Holy Cross Mountains), characterised by long siliciclastic intervals without conodonts (e.g. Appalachian Foreland, Tafilalt Basin, pelagic shelf basin facies of Germany), with extreme condensation or significant unconformities (e.g. central Tafilalt Platform), outcrop gaps (e.g. southern Timan river sections), or deposited in shallow-water facies (e.g. Pomerania, Russian Platform, Iran). This leaves the following sections:

1. Heimberg section, eastern Rhenish Massif (see Ziegler and Sandberg 1990): dense re-sampling of interval from samples 420 to 449 required.
2. Nismes section, Dinant Syncline, Belgium (Helsen and Bultynck 1992; Bultynck et al. 1998): outcrop conditions difficult (folding and faulting), sampling gaps, faunas not very diverse, no recognition of *feisti* Subzone, *Pa. nasuta* enters above *Ad. ioides* and "*Pa. gigas*".
3. Pramosio 327 section, Italian Carnic Alps (Spalletta and Perri 1998): only preliminary data are published.
4. Coumiac, Upper Quarry, Montagne Noire (Klapper 1989): Frasnian Zone 11 subdivision not yet known; no *Pa. semichatovae*.
5. Col du Puech de la Suque, Section H, Montagne Noire (Klapper 1989): Frasnian Zone 11 subdivision not yet known; no *Pa. semichatovae*.
6. Luscar Mountain, Alberta, Canada (Klapper and Lane 1989): no published section log, no record of *Pa. feisti* and *Pa. plana* below *Pa. semichatovae*.
7. Mount Houltain, Alberta, Canada (Klapper and Lane 1989): no published section log, no record of *Pa. feisti* and *Pa. plana* below *Pa. semichatovae*.
8. Sivyu River section, northern Timan, northern Russia (Savage and Yudina 2001): detailed conodont record not yet published and no correlation with the discontinuous Section 5302 of Ovnatanova et al. (2017).
9. Shar`yu River section, Subpolar Urals (Ovnatanova et al. 2017): interval below first record of *Pa. nasuta* not yet sampled.
10. Kozhim River section, northern Timan/Subpolar Urals (Matveeva 2013; Soboleva 2017): FOD of *Pa. semichatovae* postdates significantly the FODs of *Pa. nasuta* and of *Pa. lyaiolensis;* more documentation of faunas and microfacies required.
11. Malaya Usa River section, Subpolar Urals (Sobolev and Soboleva 2018): higher resolution of conodont sampling required; the currently known FODs of *Pa. semichatovae* and *Pa. nasuta* postdate the FOD of *Pa. eureka* at the base of a deepening interval taken as *semichatovae* Event Interval.
12. Gabdyukova section, western slope of South Urals (Artyushkova et al. 2011): large sampling gap between levels of *Pa. plana* (Sample 6226) and of *Pa. nasuta, Pa. semichatovae*, and *Pa. winchelli* (= *subrecta*; Sample 7131 and just above).
13. Ryauzyak section, western slope of southern Urals (Artyushkova et al. 2011): the detailed conodont succession requires photo documentation, especially around the local Domanik/Mendym boundary.

14. Bou Alzaz North, Moroccan Meseta (Lazreq 1999): Small sampling gap, unclear affinities of "*Pa. jamieae* auct." below *Pa. semichatovae*, no records of *Pa. plana* and *Pa. nasuta*; re-sampling required.
15. Anajdam, Mrirt region, Moroccan Meseta (Lazreq 1999; Becker et al. 2020b): condensed, re-sampling of the interval from Bed 33c (Laz 31-31c) to Bed 37 (= Laz 34) required.
16. Bou Ounebdou, Mrirt region (Lazreq 1999; Becker et al. 2020b): condensed, re-sampling of basal part of Submember 2 of Mrirt Member required since *Pa. nasuta* shows a delayed FOD and *Pa. semichatovae* has not yet been found.
17. Touggui-ou-Allal, Mrirt region, Moroccan Meseta (Lazreq 1999): revision of ranges below the local entry of *Pa. semichatovae* (beds 100–104) required.
18. Bou Tchrafine, Tafilalt, southern Morocco (Becker and House 2000; Becker et al. 2018; and unpublished data by G. Klapper): full documentation of faunas from around the base of black Kellwasser-type facies required.
19. Dongcun section, Guangxi, South China (Wang 1994): more detailed, less schematic section log, with even closer sampling and microfacies data required.
20. Sihongchan section, Guangxi, South China (Wang 1994): additional documentation of conodonts and microfacies data required.
21. New Lali section of Zhang et al. (2019): more extensive documentation of conodont faunas from Frasnian zones 10/11 required.
22. Horse Spring, Canning Basin, Western Australia (e.g. Becker and House 2009; Klapper 2007): condensed and with a locally delayed FOD of *Pa. feisti* in relation to the FODs of *Pa. ederi, Pa. brevis, Pa. semichatovae*, and *Po. lodinensis*; rich in goniatites and with other fauna.

Several regions have the potential for further suitable sections, e.g. Nevada, the Rhenish Massif (e.g. some of the sections of Stritzke 1990, sections in western parts), Pyrenees, Cantabrian Mountains, Tafilalt, Holy Cross Mountains, Urals, and South China.

Conclusions

1. The conodont-rich Martenberg section exposures currently the best record for faunas across the middle-upper Frasnian transition and of sedimentary changes associated with the global *semichatovae* Event, which has been recognised so far in ca. 20 regions/basins of North America, Europe, North Africa, Asia, and Australia.
2. Based on a review of specimens depicted in the literature, our new faunas, and building on the narrow species concept of Klapper (2007), it could be demonstrated that the originally widely defined *Pa. jamieae* includes several subspecies and partly new species that can be clearly distinguished from forms close to its holotype.
3. The new faunas in combination with the revision of original collections by Ovnatanova and Kononova (2020) show that no typical *Pa. jamieae* (= *jamieae jamieae*) occur in the beds (beds R-Q and Q) that were originally (Ziegler and Sandberg 1990) or later (Ziegler and Sandberg 2000) assigned to the *jamieae* Zone. However, they contain *Pa. jamieae savagei* n. ssp., *Pa. adorfensis* n. sp., *Pa. jamieae rosa* n. ssp., and *Pa. descendens* n. sp. in association with *Pa. plana*, which explain the original zone recognition. The *jamieae* holotype comes at Schmidt Quarry from a higher level with *Ag. ioides*, which indicates the basal Frasnian Zone 12 (*winchelli* Zone).
4. All taxa close to or formerly included in *Pa. jamieae* s.l. are rare, show rather variable global ranges, and are not suitable as zonal index forms. Therefore, we fully agree with the conclusion of Ovnatanova and Kononova (2020) to completely abandon the *jamieae* Zone. Instead, the FAD of *Pa. plana*, index species of Frasnian Zone 10, is a globally recognisable correlation level and the *plana* Zone should replace the *jamieae* Zone irrespective of the use of the Frasnian zonation (FZ). It includes the oldest *Ag. triangularis* s.str.
4. The subsequent Frasnian Zone 11 (*feisti* Zone) can be subdivided into Frasnian Subzone 11a (*feisti* Subzone), based on the FAD of *Pa. feisti*, and Frasnian Subzone 11b (*nasuta* Subzone), based on the FADs of *Pa. nasuta*, index species of the Lower *rhenana* Zone sensu Ziegler and Sandberg (1990), and *Pa. semichatovae*, index species of the more shallow-water *semichatovae* Subzone. There are further auxiliary marker palmatolepids and polygnathids (e.g. *Po. lodinensis, Po. subincompletus*) with more restricted distribution.
5. At Martenberg, the eustatic *semichatovae* Event/Transgression coincides with the base of Frasnian Subzone 11b (*nasuta* Subzone) and is associated with a significant goniatite radiation marking UD I-I (do Iß faunas of House and Ziegler 1977). It is preceded in Frasnian Subzone 11a by a partly overlooked thin regressive interval with unconformities, microbial layers, sheet cracks, and volcaniclastics deposited by currents. An earlier, minor re-transgression couplet is indicated by carbonate microfacies and conodont biofacies within Frasnian Zone 10 (*plana* Zone).
6. Following the original proposal by Ziegler and Sandberg (1997), we recommend to define a formal upper Frasnian substage by the base of Frasnian Subzone 11b and the global *semichatovae* Event (Fig. 14). This level can be correlated with the terrestrial miospore record (Streel et al. 1974).

7. Despite its condensed nature, the highly fossiliferous Martenberg section would be suitable as a future upper Frasnian GSSP section. Trace element and isotope stratigraphy data and magnetic susceptibility studies are still lacking. A global literature survey identified 22 further conodont sections that expose the middle/upper Frasnian transition but in most of them research is still at an early stage, with required revisions, re-sampling, closure of sampling gaps, full documentation of faunas, microfacies and chemostratigraphy studies.

Acknowledgements We thank D. Jeffrey Over (SUNY, Geneseo) and one anonymus reviewer for their helpful reviews. Gilbert Klapper (Earth and Planetary Sciences, Northwestern University, Evanston, IL) has thankfully given us critical advice on *Palmatolepis* taxonomy. We are also grateful to guest editors Christoph Hartkopf-Fröder (University of Cologne) and Sven Hartenfels (Geologischer Dienst NRW, Krefeld) for their comments on the manuscript. Traudel Fährenkemper assisted with some of the graphics, Davina Mathijssen and Lukas Afhüppe processed conodont samples, Rike Zimmermann and her team helped with the preparation of thin sections, and Till Söte took new photos of the outcrop (all University of Münster). Hanna Cieszynski (University of Cologne) thankfully photographed some additional conodonts in the scanning electron microscope.

Funding Open Access funding enabled and organised by Projekt DEAL.

Data availability statement All data generated or analysed during this study are included in this published article.

Declarations

Conflict of interests The authors declare that they have no conflict of interest.

References

Aboussalam, Z. S. (2003). Das "Taghanic-Event" im höheren Mitteldevon von West-Europa und Marokko. *Münstersche Forschungen zur Geologie und Paläontologie*, *97*, 1–332.

Aboussalam, Z. S., & Becker, R. T. (2016). A lower Frasnian reef drowning episode at Walheim (Aachen region, Inde Syncline, NW Rhenish Massif). *Münstersche Forschungen zur Geologie und Paläontologie*, *108*, 14–28.

Aboussalam, Z. S., Becker, R. T., Richter, J., Hartenfels, S., El Hassani, A., & Eichholt, S. (2020). The unique Devonian of Immouzer-du-Kandar (Middle Atlas basement) – biostratigraphy, faunas, and facies development. *Frontiers in Science and Engineering, Earth, Water and Ocean, Environmental Studies, 10*(1), 127–173.

D'Archiac, V., & De Verneuil, M. E. (1842). On the Fossils of the Older Deposits in the Rhenish Provinces; preceded by a general Survey of the Fauna of the Palaeozoic Rocks, and followed by a Tabular List of the Organic Remains of the Devonian System in Europe. *Transactions of the Geological Society of London, second series, 6*, 303–410 + pls. 25–38.

Artyushkova, O. V., Maslov, V. A., Pazukhin, V. N., Kulagina, E. I., Tagarieva, R. C., Mizenz, L. I., & Mizenz, A. G. (2011). *Devonian and Lower Carboniferous type sections of the western South Urals.* Pre-Conference Field Excursion Guidebook (pp. 1–91). Ufa: Kollektiv Avtorov.

Bai, S.-L., Bai, Z.-Q., Ma, X.-P., Wang, D.-R., & Sun, Y.-L. (1994). *Devonian events and biostratigraphy of South China* (pp. 1–303 + 45 pls.). Beijing: University Press.

Bardashev, I. A. (2009). New Frasnian conodonts of the Genus *Palmatolepis* from the Central Tajikistan. *Paleontologicheskiy Zhurnal*, *2009*(3), 61–66. [published in English in Paleontological Journal, *43*(3), 300–305.]

Bardashev, I. A. (2018). *Stratigrafia i konodontiy devona Tadzhikistana.* (pp. 1–316). Dushanbe: "Donish" Publishing House.

Bardashev, I. A., & Bardasheva, N. P. (2012). *Platform conodonts from the Givetian-Frasnian boundary (Middle-Upper Devonian)* (pp. 1–90). Dushanbe: "Donish" Publishing House.

Bardashev, I. A., & Bardasheva, N. P. (2014). The conodonts and detailed stratigraphy of the Frasnian of Tajikistan. In *Modern problems of geological and seismological studies of Tajikistan. Materials of the Republic Science Conference on the 80th anniversary of Manzur R. Djalilov, Academician of the Tajik Academy of Science, Doctor of Geological and Mineralogical Sciences.* (pp. 12–36, 6 pls.) Dushanbe. [in Russian]f

Bartzsch, K., Blumenstengel, H., & Weyer, D. (2002). Stratigraphie des Oberdevons im Thüringischen Schiefergebirge, Teil 2: Berga-Antiklinorium. *Beiträge zur Geologie von Thüringen, Neue Folge*, *8*, 303–327. [imprint 2001]

Becker, R. T. (1984). *Die Geologie des Gebietes nördlich von Adorf zwischen Rhenetal und R3487 (MBL 4618 Adorf)* (pp. 1–70, 1 map). Unpublished Diplom Mapping Thesis, Ruhr University Bochum.

Becker, R. T. (2002). Frasnian goniatites from the Boulonnais (France) as indicators of regional sealevel changes. *Annales de la Société Géologique du Nord, 2ème série, 9*, 129–140.

Becker, R. T., & House, M. R. (1993). New early Upper Devonian (Frasnian) goniatite genera and the evolution of the "Gephuroceratoceae". *Berliner geowissenschaftliche Abhandlungen*, *E9*, 111–133.

Becker, R. T., & House, M. R. (1994). Kellwasser Events and goniatite successions in the Devonian of the Montagne Noire with comments on possible causations. *Courier Forschungsinstitut Senckenberg, 169*, 45–77.

Becker, R. T., & House, M. R. (1997). Sea-level changes in the Upper Devonian of the Canning Basin, Western Australia. *Courier Forschungsinstitut Senckenberg*, *199*, 129–146.

Becker, R. T., & House, M. R. (1998). Proposal for an international substage subdivision of the Frasnian. *SDS Newsletter*, *15*, 17–22.

Becker, R. T., & House, M. R. (2000). Late Givetian and Frasnian ammonoid succession at Bou Tchrafine (Anti-Atlas, Southern Morocco). *Notes et Mémoires du Service géologique*, *399*, 27–36.

Becker, R. T., & House, M. R. (2009). Devonian ammonoid biostratigraphy of the Canning Basin. In P. E. Playford, R. M. Hocking & A. E. Cockbain (Eds.), *Devonian Reef Complexes of the Canning Basin, Western Australia. Geological Survey of Western Australia Bulletin, 145*, 415–439.

Becker, R. T., House, M. R., & Kirchgasser, W. T. (1993). Devonian goniatite biostratigraphy and timing of facies movements in the Frasnian of the Canning Basin, Western Australia. In E. A. Hailwood, & R. B. Kidd (Eds.), *High Resolution Stratigraphy*. *Geological Society, London, Special Publications*, *70*, 293–321.

Becker, R. T., House, M. R., & Klapper, G. (1997). Event-Sequence and Sealevel Changes in the Upper Givetian and Frasnian of the Tafilalt (Southern Morocco). In *The Amadeus Grabau Symposium: International Meeting on Cyclicity and Bioevents in the Devonian System, Program and Abstracts, 18*. University of Rochester.

Becker, R. T., Aboussalam, Z. S., Bockwinkel, J., Ebbighausen, V., El Hassani, A., & Nübel, H. (2004). The Givetian and Frasnian at Oued Mzerreb (Tata region, weastern Dra Valley). In A. El Hassani (Ed.), Devonian neritic-pelagic correlation and events in the Dra Valley (western Anti-Atlas, Morocco). *Documents de l'Institute Scientifique*, *19*, 29–43.

Becker, R. T., Aboussalam, Z. S., Hartenfels, S., Nowak, H., Juch, D., & Drozdzewski, G. (2016a). Drowning and sedimentary cover of Velbert Anticline reef complexes (Northwestern Rhenish Massif). *Münstersche Forschungen zur Geologie und Paläontologie*, *108*, 76–101.

Becker, R. T., Aboussalam, Z. S., Stichling, S., May, A., & Eichholt, S. (2016b). The Givetian-Frasnian Hönne Valley Reef Complex (northern Sauerland) – an outline of stratigraphy and facies development. *Münstersche Forschungen zur Geologie und Paläontologie*, *108*, 126–140.

Becker, R. T., Piecha, M., Gereke, M., & Spellbrink, K. (2016c). The Frasnian/Famennian boundary in shelf basin facies north of Diemelsee-Adorf. *Münstersche Forschungen zur Geologie und Paläontologie, 108*, 220–231.

Becker, R. T., Aboussalam, Z. S., Hartenfels, S., El Hassani, A., & Baidder, L. (2018). Bou Tchrafine – central Tafilalt reference section for Devonian stratigraphy and cephalopod successions. *Münstersche Forschungen zur Geologie und Paläontologie, 110*, 158–187.

Becker, R. T., Marshall, J. E. A., Da Silca, A.-C., Agterberg, F. P., Gradstein, F., & Ogg, J. G. (2020a). The Devonian Period. In F. Gradstein, J. G. Ogg, M. D. Schmitz & G. M. Ogg (Eds.), *Geological Time Scale 2020*, Volume 2. (pp. 733–810). Amsterdam: Elsevier.

Becker, R. T., Aboussalam, Z. S., El Hassani, A., Hartenfels, S., & Hüneke, H. (2020b). Devonian and basal Carboniferous of an allochthonous nappes at Mrirt (eastern part of Western Meseta) – review and new data. *Frontiers in Science and Engineering, Earth, Water and Ocean, Environmental Studies, 10*(1), 87–126.

Bender, P., Hörmann, S., Lottmann, J., Sandberg, C. A., Schindler, E., Walliser, O. H., & Ziegler, W. (1988). Field Trip B (29.-31. July 1988), Rhenish and Harz Mountains. *Courier Forschungsinstitut Senckenberg*, *102*, 157–224.

Bernauer, F. (1890). *Beschreibung der Bergreviere Arnsberg, Brilon und Olpe, sowie der Fürstenthümer Waldeck und Pyrmont* (pp. 1–250). Bonn: Königliches Oberbergamt.

Beyrich, E. (1837). *Beiträge zur Kenntnis der Versteinerungen des Rheinischen Übergangsgebirges* (pp. 1–44 + pls. 1–2). Berlin: Druckerei der Königlichen Akademie der Wissenschaften.

Bischoff, G. (1956). Oberdevonische Conodonten (toIδ) aus dem Rheinischen Schiefergebirge. *Notizblatt des Hessischen Landesamtes für Bodenforschung*, *84*, 115–137.

Bischoff, G., & Ziegler, W. (1956). Das Alter der Urfer Schichten im Marburger Hinterland nach Conodonten. *Notizblatt des Hessischen Landesamtes für Bodenforschung*, *84*, 138–169.

Bischoff, G., & Ziegler, W. (1957). Die Conodontenchronologie des Mitteldevons und des tiefsten Oberdevons. *Abhandlungen des Hessischen Landesamtes für Bodenforschung*, *22*, 1–136.

Bottke, H. (1962). Der Roteisenstein des östlichen Sauerlandes und seine Beziehungen zur Stratigraphie und Fazies des oberen Givets und der Adorf-Stufe. *Roemeriana*, *6*, 17–96.

Bottke, H. (1965). Die exhalative-sedimentären devonischen Roteisensteinlagerstätten des Ostsauerlandes. *Beihefte zum Geologischen Jahrbuch, 63*, 1–147 + 9 pls.

Boulvain, F., Bultynck, P., Coen, M., Coen-Aubert, M., Lacroix, D., Laloux, M., Casier, J.-G., Dejonghe, L., Dumoulin, V., Ghysel, P., Godefroid, J., Helsen, S., Mouravieeff, N. A., Sartenaer, P., Touneur, G., & Vanguestaine, M. (1999). Les formations du Frasnien de la Belgique. *Memoirs of the Geological Survey of Belgium*, *44*, 1–125.

Branson, E. B., & Mehl, M. G. (1934). Conodonts from the Grassy Creek shale of Missouri. *University of Missouri Studies*, *8*, 171–259.

Branson, E. B., & Mehl, M. G. (1938). The conodont genus *Icriodus* and its stratigraphic distribution. *Journal of Paleontology*, *12*(2), 156–166.

Buch, L. von (1832). (A) Über Ammoniten. über ihre Sonderung in Familien, über die Arten, welche in den älteren Gebirgsschichten vorkommen, und (B) über Goniatiten insbesondere. *Abhandlungen der Königlichen Akademie der Wissenschaften zu Berlin, Physikalische Klasse, 1830*, 159–187 + pls. 1–2.

Buchholz, P., Luppold, F. W., & Stoppel, D. (2001). Conodontenstratigraphie und Sedimentologie der Cephalopodenkalke im Langestal (Eifelium-Frasnium, Oberharz). *Braunschweiger geowissenschaftliche Arbeiten*, *24*, 103–124.

Bultynck, P., Helsen, S., & Hayduckiewich, J. (1998). Conodont succession and biofacies in upper Frasnian formations (Devonian) from the southern and central parts of the Dinant Synclinorium (Belgium) - (Timing of facies shifting and correlation with late Frasnian events). *Bulletin de l'Institut Royal des Sciences Naturelles de Belgique, Sciences de la Terre*, *68*, 25–75.

Çapkınoğlu, Ş. (2005). Upper Devonian (Upper Frasnian-Lower Famennian) conodont biostratigraphy of the Ayineburnu Formation (Istanbul Zone, NW Turkey). *Geologica Carpathica*, *56*(3), 223–236.

Coen-Aubert, M., & Lacroix, D. (1979). Le Frasnien dans la partie orientale du bord sud du Synclinorium de Namur. *Annales de la Société géologique de Belgique*, *101*, 269–279.

Da Silva A.-C., Yans J., & Boulvain F. (2010). Early-Middle Frasnian (early Late Devonian) sedimentology and magnetic susceptibility of the Ardennes area (Belgium): Identifications of severe and rapid sea-level fluctuations. *Geologica Belgica*, *13*(4), 319–332.

Day, J., & Witzke, B. J. (2017). Upper Devonian Biostratigraphy, Event Stratigraphy, and Late Frasnian Kellwasser Extinction Bioevents in the Iowa Basin: Western Euramerika. In M. Montenari (Ed.), *Stratigraphy & Timescales, Vol. 2* (pp. 243–332). Burlington: Academic Press.

Denayer J., & Poty, E. (2010). Facies and palaeoecology of the upper member of the Aisemont Formation (Late Frasnian, S. Belgium): an unusual episode within the Late Frasnian Crisis. *Geologica Belgica*, *13*(3), 197–212.

Denckmann, A. (1895). Zur Stratigraphie des Oberdevon im Kellerwald und in einigen benachbarten Devon-Gebieten. *Jahrbuch der Königlichen Preußischen geologischen Landesanstalt und Bergakademie, 15*, 8–64 + 2 pl. [for 1894].

Denckmann, A. (1903). Über die untere Grenze des Oberdevon im Lennetal und im Hönnetal. *Zeitschrift der deutschen geologischen Gesellschaft*, *55*, 393–402 + pl. 18.

Dopieralska, J., Belka, Z., & Walczak, A. (2015). Nd isotope composition of conodonts; An accurate proxy of sea-level fluctuations. *Gondwana Research, 34*, 284–295.

Du, Y.-S., Gong, Y.-M., Zeng, X.-W., Huang, H.-W., Yang, J.-J., Zhang, Z., & Huang, Z.-Q. (2008). Devonian Frasnian-Famennian transitional event deposits of Guangxi, South China and their possible tsunami origin. *Science in China, Series D, Earth Sciences, 51*(11), 1570–1580.

Dunham, R. J. (1962). Classification of carbonate rocks according to depositional texture. *American Association of Petroleum Geologists, Memoir*, *1*, 108–121.

Dzik, J. (2002). Emergence and collapse of the Frasnian conodont and ammonoid communities in the Holy Cross Mountains, Poland. *Acta Palaeontologica Polonica*, *47*(4), 565–650.

Dzik, J. (2006). The Famennian "Golden Age" of conodonts and ammonoids in the Polish part of the Variscan sea. *Palaeontologica Polonica*, *63*, 1–359.

Emde, A. (1965). Der Bergbau im Adorfer Raum. *Geschichtsblätter für Waldeck, 57*, 36–87.

Feist, R. (1985). Devonian stratigraphy of the Southeastern Montagne Noire (France). In W. Ziegler, & R. Werner (Eds), Devonian Series boundaries - results of worldwide studies. *Courier Forschungs-institut Senckenberg, 75*, 331–352.

Flügel, E. (2004). *Microfacies of carbonate rocks: analysis, interpretation and application* (pp. 1–976). Berlin, Heidelberg: Springer Science & Business Media.

Fuchs, A. (1987). Conodont biostratigraphy of the Elbingerode reef complex, Harz Mountains. *Acta Geologica Polonica*, *37*(1–2), 33–50.

Galushin, G. A., & Kononova, L. I. (2004). Upper Frasnian and lower Famennian biostratigraphy of Volgograd Povolzhie on conodonts. *Biulleten` Moskovskogo obshchestva ispytatelei prirody, otdel geologicheskii, 79*(1), 33–47. [in Russian]

García-López, S., & Sanz-López, J. (2002). Devonian to Lower Carboniferous conodont biostratigraphy of the Bernesga Valley section (Cantabrian Zone, NW Spain). *Cuadernos del Museo Geominero*, *1*, 163–205.

Gatley, S. S. (1983). *Frasnian (Upper Devonian) goniatites from southern Belgium* (pp. 1–375). Unpublished Ph.D. Thesis, University of Hull.

Gereke, M. (2007). Die oberdevonische Kellwasser-Krise in der Beckenfazies von Rhenohercynikum und Saxothuringikum (spätes Frasnium/frühestes Famennium, Deutschland). *Kölner Forum für Geologie und Paläontologie, 17*, 1–228.

Goolaerts, S., & Gouwy, S. (2015). The Lahonry quarry at Lompret, Belgium: an extraordinary new site to study Upper Frasnian cephalopods during the onset of anoxia in the Dinant Basin. *Strata, série 1: communications*, *16*, 61–62.

Gouwy, S., & Bultynck, P. (2000). Graphic correlation of Frasnian sections (Upper Devonian) in the Ardennes, Belgium. *Bulletin de l´ Institut royal des Sciences naturelles Belgique, Sciences de la Terre, 70*, 25–52.

Grimm, M. C., & Rothausen, K. (1992). Fossilinhalt und Biostratigraphie des Oos-Plattenkalks (Frasnium, Büdesheimer Mulde, Eifel, Deutschland). *Mainzer geowissenschaftliche Mitteilungen, 21*, 41–54.

Grimm, M. C., Piecha, M., Prick, R., & Joachimski, M. M. (2008). Höheres Mitteldevon und Oberdevon der Prümer Mulde (Givetium bis tiefes Famennium/Eifel). *Schriftenreihe der Deutschen Gesellschaft für Geowissenschaften*, *52*, 375–391.

Gutschick, R. C., & Sandberg, C. A. (1991). Upper Devonian biostratigraphy of Michigan Basin. *Geological Society of America Special Paper*, *256*, 155–179.

Hartenfels, S. (2011). Die globalen *Annulata*-Events und die Dasberg-Krise (Famennium, Oberdevon) in Europa und Nord-Afrika: hochauflösende Conodonten-Stratigraphie, Karbonat-Mikrofazies, Paläoökologie und Paläodiversität. *Münstersche Forschungen zur Geologie und Paläontologie*, *105*, 17–527.

Hartenfels, S., & Becker, R. T. (2016). Age and correlation of the transgressive *Gonioclymenia* Limestone (Famennian, Tafilalt, eastern Anti-Atlas, Morocco). *Geological Magazine, 155*(3), 586–629.

Hartenfels, S., Becker, R. T., Aboussalam, Z. S., El Hassani, A., Baidder, L., Fischer, T., & Stichling, S. (2013). The Upper Devonian at El Khraouia (southern Tafilalt). *Documents de l´Institut Scientifique, Rabat, 27*, 41–50.

Hartenfels, S., Becker, R. T., & Aboussalam, Z. S. (2016). Givetian to Famennian stratigraphy, Kellwasser, *Annulata* and other events at Beringhauser Tunnel (Messinghausen Anticline, eastern Rhenish Massif). *Münstersche Forschungen zur Geologie und Paläontologie*, *108*, 196–219.

Hauser, J., & Hauser, A. (2002). *Oberdevonische Echinodermen aus den Dolomit-Steinbrüchen von Wallersheim-Loch (Rheinisches Schiefergebirge, Prümer Mulde; Eifel)* (pp. 1–69 and 1–14). Bonn: privately published.

Heckel, P. H. & Witzke, B. J. (1979). Devonian world palaeogeography determined from distribution of carbonates and related lithic palaeoclimatic indicators. In M. R. House, C. T. Scrutton, and M. G. Bassett (Eds), *The Devonian System. Special Papers in Palaeontology, 23*, 99–123.

Helsen, S., & Bultynck, P. (1992). Conodonts and megafauna from two sections at Nismes and Mariembourg (Frasnian of the southern flank of the Dinant Synclinorium, Belgium). *Annales de la Société Géologique de Belgique*, *115*(1), 145–157.

Holzapfel, E. (1882). Die Goniatiten-Kalke von Adorf in Waldeck. *Palaeontographica*, *28*, 225–261 + pls. 44–49.

Holzapfel, E. (1895). Das obere Mittel-Devon (Schichten mit *Stringocephalus burtini* und *Maeneceras terebratum*) im Rheinischen Schiefergebirge. *Abhandlungen der Preußischen geologischen Landesanstalt, neue Folge*, *16*, 1–459.

House, M. R., & Kirchgasser, W. T. (1993). Devonian goniatite biostratigraphy and timing of facies movements in the Frasnian of eastern North America. In E. A. Hailwood, & R. B. Kidd (Eds.), *High Resolution Stratigraphy. Geological Society, London, Special Publications, 70*, 267–292.

House, M. R., & Ziegler, W. (1977). The goniatite and conodont sequence in the early Upper Devonian at Adorf, Germany. *Geologica et Palaeontologica*, *11*, 69–108.

House, M. R., Menner, V. V., Becker, R. T., Klapper, G., Ovnatanova, N. S., & Kuz´min, V. (2000). Reef episodes, anoxia and sea-level changes in the Frasnian of the southern Timan (NE Russian platform). – In E. Insalaco, P. W. Skelton & T. J. Palmer (Eds.), *Carbonate Platform Systems: components and interactions. Geological Society, London, Special Publications*, *178*, 147–176.

Huang, C., & Gong, Y. (2016). Timing and patterns of the Frasnian–Famennian event: Evidences from high-resolution conodont biostratigraphy and event stratigraphy at the Yangdi section, Guangxi, South China. *Palaeogeography, Palaeoclimatology, Palaeoecology*, *448*, 317–338.

Huang, C., Song, J.-J., Shen, J., & Gong, Y.-M. (2018). The influence of the Late Devonian Kellwasser events on deep-water ecosystems: Evidence from palaeontological and geochemical records from South China. *Palaeogeography, Palaeoclimatology, Palaeoecology, 504*, 60–74.

Huddle, J. W. (1970). Revised descriptions of some Late Devonian polygnathid conodonts. *Journal of Paleontology*, *44*(6), 1029–1040.

Hüneke, H. (2001). *Gravitative und strömungsinduzierte Resedimente devonischer Karbonatabfolgen im marokkanischen Zentralmassif (Rabat-Tiflet-Zone, Decke von Ziar-Mrirt)* (pp. 1–230). Unpublished Habilitation Thesis, Ernst-Moritz-Arndt University Greifswald.

Irwin, S. E. B., & Orchard, M. J. (1991). Upper Devonian-Lower Carboniferous conodont biostratigraphy of the Earn Group and overlying units, northern Canadian Cordillera. In M. J. Orchard & A. D. McCracken (Eds.), Ordovician to Triassic Conodont Paleontology of the Canadian Cordillera. *Geological Survey of Canada Bulletin*, *417*, 185–213.

Izokh, N. G., Yolkin, E. A., & Bakharev, N. K. (2004). Early Frasnian conodonts from the Rudny Altai (West Siberia). *Geologiya I Geofizika, Supplement, News on Paleontology and Stratigraphy, 6/7*, 89–101. [in Russian with English summary]

Izokh, N. G., Erina, M. V., Obut, O. T., Abdiev, N. H., Kim, A. I., & Rakhmonov, U. D. (2020). Pozdnedevonskie konodonty zeravšano-

gissarskoj gornoj oblasti (Uzbekistan). *Paleontologicheskiy Zhurnal*, *2020*(2), 56–64.

Jaglarz, P., Rychliński, T., Filipiak, P., Uchman, A., & Vainorius, J. (2021 online). Sedimentary environments and stratigraphy of the Stipinai Formation (Upper Frasnian, northern Lithuania): a sedimentary record of sea-level changes in the Main Devonian Field of the East European Platform. *Geological Quarterly, 65*(52), https://doi.org/10.7306/gq.1621, 15 pp.

Ji, Q. (1992). On the Frasnian-Famennian Mass Extinction Event in South China. *Courier Forschungsinstitut Senckenberg, 117*, 275–301.

Ji, Q. (1993). On the Frasnian-Famennian extinction event in South China as viewed in the light of conodont study. *Professional Papers of Stratigraphy and Palaeontology*, *24*, 79–107.

Ji, Q., & Ziegler, W. (1993). The Lali section: an excellent reference section for Upper Devonian in South China. *Courier Forschungsinstitut Senckenberg*, *157*, 1–183.

Johnson, J.G., Klapper, G., & Sandberg, C.A. (1985). Devonian eustatic fluctuations in Euramerica. *Geological Society of America Bulletin*, *96*, 567–587.

Kim, A. I., Salimova, F. A., Kim, I. A., & Meshchankina, N. A. (Eds., 2007). *Palaeontological Atlas of Phanerozoic faunas and floras of Uzbekistan, Volume I, Palaeozoic* (pp. 1-420 + 142 pls). Tashkent.

Kirilishina, E. M., & Kononova, L. I. (2004). Konodontovyie biofacii vo franskom basseine úgo-zapada Moskovskoi sineklizyi. *Vestnik Moskovskogo Instituta, Seriya 4, Geologia, 2004*(2), 32–40.

Klapper, G. (1989). The Montagne Noire Frasnian (Upper Devonian) Conodont Succession. In N. J. McMillan, A. F. Embry, & D. J. Glass (Eds.), Devonian of the World. *Canadian Society of Petroleum Geologists, Memoir, 14* (III), 449–468 [imprint 1988].

Klapper, G. (1990). Frasnian Species of the Late Devonian Conodont Genus *Ancyrognathus*. *Journal of Paleontology*, *64*(6), 998–1025.

Klapper, G. (1997). Graphic correlation of Frasnian (Upper Devonian) sequences in Montagne Noire, France, and western Canada. *Special Papers of the Geological Society of America*, *321*, 113–130.

Klapper, G. (2007). Frasnian (Upper Devonian) conodont succession at Horse Spring and correlative sections, Canning Basin, Western Australia. *Journal of Paleontology*, *81*(3), 513–537.

Klapper, G. (2021). Revision of the Frasnian Late Devonian conodont genus *Ancyrodella*. *Bulletin of Geosciences*, *96*(3), 295–325.

Klapper, G., & Becker, R. T. (1998). Comparison of Frasnian (Upper Devonian) conodont zonations. In G. Bagnoli (Ed.), *ECOS VII, Seventh International Conodont Symposium held in Europe, Abstracts,* 53–54.

Klapper, G., & Becker, R. T. (1999). Comparison of Frasnian (Upper Devonian) conodont zonations. *Bolletino della Società Paleontologica Italiana*, *37*(2–3), 339–348.

Klapper, G., & Foster Jr, C. T. (1986). Quantification of outlines in Frasnian (Upper Devonian) platform conodonts. *Canadian Journal of Earth Sciences*, *23*(8), 1214–1222.

Klapper, G., & Foster Jr., C. T. (1993). Shape analysis of Frasnian species of the Late Devonian conodont genus *Palmatolepis*. *Journal of Paleontology, Memoir*, *32*, 1–35.

Klapper, G., & Kirchgasser, W. T. (2016). Frasnian Late Devonian conodont biostratigraphy in New York: graphic correlation and taxonomy. *Journal of Paleontology, 90*(3), 525–554.

Klapper, G., & Lane, H. R. (1985). Upper Devonian (Frasnian) Conodonts of the *Polygnathus* Biofacies, N.W.T., Canada. *Journal of Paleontology*, *59*(4), 904–951.

Klapper, G., & Lane, H. R. (1989). Frasnian (Upper Devonian) conodont sequence at Luscar Mountain and Mount Haultain, Alberta Rocky Mountains. In N. J. McMillan, A. F. Embry, & D. J. Glass (Eds.), Devonian of the World. *Canadian Society of Petroleum Geologist, Memoir*, *14*(III), 469–478. [imprint 1988].

Klapper, G., Kirchgasser, W. T., & Baesemann, J. F. (1995). Graphic correlation of a Frasnian (Upper Devonian) composite standard. *SEPM Special Publications*, *53*, 177–184.

Klapper, G., Kuz'min, A. V., & Ovnatanova, N. S. (1996). Upper Devonian conodonts from the Timan-Pechora region, Russia, and correlation with a Frasnian composite standard. *Journal of Paleontology*, *70*, 131–152.

Klapper, G., Uyeno, T. T., Armstrong, D. K., & Telford, P. G. (2004). Conodonts of the William Island and Long Rapids Formations (Upper Devonian, Frasnian-Famennian) of the Onakawana B Drillhole, Moose River Basin, northern Ontario, with a revision of Lower Famennian species. *Journal of Paleontology*, *78*(2), 371–387.

Kleinebrinker, G. (1992). Conodonten-Stratigraphie, Mikrofazies und Inkohlung im Mittel- und Oberdevon des Bergischen Landes. *Sonderveröffentlichung Geologisches Institut, Universität zu Köln*, *85*, 1–101.

Komatsu, T., Urakawa, R., Inada, T., Yamauchi, K., Maekawa, T., Takashima, R., Williams, M., Nguyen, P. D., Doan, H. D., Nguyen, M. T., Niko, S., Tanaka, G. & Yamaguchi, T. (2018). The Kellwasser events in the Upper Devonian Frasnian to Famennian transition in the Toc Tat Formation, northern Vietnam. *Island Arc*, *28*(1), 1–17.

Kononova, L. I., Alekseev, A. S., Barskov, I. S., & Reimers, A. N. (1996). New species of Polygnathid assemblages from the Frasnian Stage of the Moscow Syneclise. *Paleontologicheskiy Zhurnal*, *3*, 94–99.

Korn, D. (2021a). Revision of *Tornoceras frechi* Wedekind, 1918 and consequences for the Late Devonian ammonoid stratigraphy. *Neues Jahrbuch für Geologie und Paläontologie, 300*(3), 291–302.

Korn, D. (2021b). Revision of *Tornoceras typus* (Sandberger & Sandberger, 1851) – an iconic Devonian ammonoid of a clade with slow morphological evolution. *Neues Jahrbuch für Geologie und Paläontologie, 302*(2), 147–167.

Kralick, J. A. (1994). The conodont genus *Ancyrodella* in the middle Genesee Formation (Lower Upper Devonian, Frasnian), western New York. *Journal of Paleontology*, *68*, 1384–1395.

Kullmann, J., & Ziegler, W. (1970). Conodonten und Goniatiten von der Grenze Mittel-/Oberdevon aus dem Profil am Martenberg (Ostrand des Rheinischen Schiefergebirges). *Geologica et Palaeontologica*, *4*, 73–75.

Lang, J.-B., & Wang, C.-Y. (2010). Two Devonian conodont faunas from Onor area in the Great Xing'an Range of Inner Mongolia, China. *Acta Micropalaeontologica Sinica*, *27*(1), 13–27.

Lazreq, N. (1992). The Upper Devonian of M'rit (Morocco). *Courier Forschungsinstitut Senckenberg*, *154*, 107–123.

Lazreq, N. (1999). Biostratigraphie des conodontes du Givétien au Famennien du Maroc central – Biofaciès et événement Kellwasser. *Courier Forschungsinstitut Senckenberg, 214*, 1–111.

Levman, B. G., & Bitter, P. H. V. (2002). The Frasnian-Famennian (mid-Late Devonian) boundary in the type section of the Long Rapids Formation, James Bay Lowlands, northern Ontario, Canada. *Canadian Journal of Earth Sciences*, *39*(12), 1795–1818.

Liao, J.-C., & Valenzuela-Ríos, J. I. (2012). Upper Givetian and Frasnian (Middle and Upper Devonian) conodonts from Ampriú (Aragonian Pyrenees, Spain): global correlations and palaeogeographic relations. *Palaeontology, 55*(4), 819–842.

Lüddecke, F., Hartenfels, S., & Becker, R. T. (2017). Conodont biofacies of a monotonous middle Famennian pelagic carbonate succession (Upper Ballberg Quarry, northern Rhenish Massif). In B. Mottequin, L. Slavík, & P. Königshof (Eds.) *Climate change and biodiversity patterns in the mid-Palaeozoic. Palaeobiodiversity and Palaeoenvironments*, *97*(3), 591–613.

Lys, M., & Serre, B. (1957). Études micropaléontologiques dans le Paléozoique de la Montagne Noire (Foraminifères, Conodontes,

etc.). *Revue de l'Institut Français du Pétrole et Annales des Combustibles Liquides*, *16*, 783–833.

Ma, X.-P., & Bai, S.-L. (2002). Biological, depositional, microspherule, and geochemical records of the Frasnian/Famennian boundary beds, South China. *Palaeogeography, Palaeoclimatology, Palaeoecology, 181,* 325–346.

Ma, X.-P., & Zong, P. (2010). Middle and Late Devonian brachiopod assemblages, sea level change and paleogeography of Hunan, China. *Science China, Earth Sciences, 53*(10), 1849–1863.

Ma, X.-P., Sun, Y-L., Bai, Z.-Q., & Wang, S.-Q. (2004). New advances in the study of the Upper Devonian Frasnian strata of the Shetianqiao section, Central Hunan. *Journal of Stratigraphy*, *28*(4), 369–374. [in Chinese with English summary]

Ma, X.-P., Liao, W.-H., & Wang, D.-M. (2009). The Devonian System of China, with a discussion on sea-level change in South China. In Königshof, P. (Ed.), *Devonian Change: Case Studies in Palaeogeography and Palaeoecology*. *Geological Society, London, Special Publications*, *314*, 241–262.

Ma, X.-P., Wang, H.-H., & Zhang, M.-Q. (2017). Devonian event succession and sea level change in South China – with Early and Middle Devonian carbon and oxygen isotopic data. *SDS Newsletter*, *32*, 17–24.

Mahboubi, A., Feist, R., Cornée, J.-J., Ouali Mehadji, A., & Girard, C. (2015). Frasnian (Late Devonian) conodonts and environments at the northern margin of the Algerian Sahara platform: the Ben Zireg section. *Geological Magazine*, *152*(5), 844–857.

Mahboubi, A., Cornée, J.-J., Feist, R., Camps, P., & Girard, C. (2019). Frasnian (Upper Devonian) integrated facies analysis, magnetic susceptibility and sea-level fluctuations in the NW Algerian Sahara. *Geological Magazine*, *156*(8), 1295–1310.

Malec, J. (2015). Biostratygrafia utworów dewonu i karbonu z centralnej części masywu Malopolskiego na podstawie konodontów. *Buletyn Państwowego Instytutu Geologicznego*, *462*, 41–82.

Masling, K. (1911). Die Erzlagerstätten des Fürstenthum Waldeck. *Zeitschrift für praktische Geologie, 19*, 361–377.

Matern, H. (1929). Die Gliederung der Adorf-Stufe. Zugleich ein Beitrag zur Nomenklatur von *Gephuroceras* HYATT (Ceph.). *Senckenbergiana*, *11*(3), 142–152.

Matsuo, R., Komatsu, T., Matsuda, H., Maekawa, T., Inada, T., Takashima, R., Yamada, T., Williams, M., Nguyen, P. D., Doan, H. D., Nguyen, H. B., & Nguyen, M. T. (2020). The Kellwasser Events in the Upper Devonian Xom Nha Formation, Central Vietnam. *Journal of the Sedimentological Society of Japan, 78*(2), 55–75. [in Japanese with English abstract]

Matveeva, M. A. (2013). Conodont characteristic of the Frasnian deposits of the Kozhym River section (Subpolar Urals). *Vesihnuk*, *2013*(7), 17–22.

Matveeva, M. A., & Zhuravlev, A. V. (2014). The ontogenetic changes of platform elements of the *Palmatolepis proversa* Ziegler, 1958 (Conodonta) from the Frasnian deposits of the Kozhym River (Subpolar Urals). *Litosfera, 2014*(5), 117–121 [in Russian with short English summary].

Matyja, H. (1993). Upper Devonian of Western Pomerania. *Acta Geologica Polonica*, *43*(1–2), 27–94.

Matyja, H., & Narkiewicz, M. (1995). Conodont stratigraphy of the Upper Devonian in the Janczyce I borehole section, eastern Holy Cross Mts. *Geological Quarterly*, *39*(2), 177–206.

McLean, R. A., & Klapper, G. (1998). Biostratigraphy of Frasnian (Upper Devonian) strata in western Canada, based on conodonts and rugose corals. *Bulletin of Canadian Petroleum Geology, 46*(4), 515–563.

Mertmann, D. (2017). Das Rosenschlösschen bei Adorf – Typuslokalität der Adorf-Stufe. *Fossilien, Journal für Erdgeschichte, Sonderheft GrenzWelten,* 41–43.

Morrow, J. R. (2000). Shelf-to-Basin Lithofacies and Conodont Paleoecology across Frasnian-Famennian (F-F, mid-late Devonian) Boundary, Central Great Basin (Western U.S.). *Courier Forschungsinstitut Senckenberg*, *219*, 1–57.

Morrow, J. R., & Sandberg, C. A. (2008). Evolution of Devonian carbonate-shelf margin, Nevada. *Geosphere*, *4*(2), 445–458.

Mottequin, B. & Poty, E. (2016). Kellwasser horizons, sea-level changes and brachiopod-coral crises during the late Frasnian in the Namur-Dinant Basin (southern Belgium): a synopsis. In R. T. Becker, P. Königshof & C. E. Brett (Eds.), *Devonian Climate, Sea Level and Evolutionary Events*. *Geological Society, London, Special Publications*, *423*, 235–250.

Mouravieff, A. N. (1982). Conodont stratigraphic scheme of the Frasnian of the Ardennes. *Geological Survey of Belgium, Papers on the Frasnian-Givetian boundary*, 101–118.

Müller, K. J. (1956). Zur Kenntnis der Conodonten-Fauna des europäischen Devons, 1; Die Gattung *Palmatolepis*. *Abhandlungen der Senckenbergischen Naturforschenden Gesellschaft*, *494*, 1–70.

Müller, K. J., & Müller, E. (1957). Early Upper Devonian (Independence) conodonts from Iowa, Part 1. *Journal of Paleontology*, *31*(6), 1069–1108.

Narkiewicz, M. (1989). Turning points in sedimentary development in the Late Devonian in southern Poland. In N. J. McMillan, A. F. Embry, & D. J. Glass (Eds.), *Devonian of the World. Canadian Society of Petroleum Geologists, Memoirs*, *14*(II), 619–635. [imprint 1988]

Narkiewicz, K., & Bultynck, P. (2010). The upper Givetian (Middle Devonian) *subterminus* conodont zone in North America, Europe and North Africa. *Journal of Paleontology*, *84*(4), 588–625.

Narkiewicz, K., & Bultynck, P. (2011). Biostratygrafia konodontowa dewonu Górnego Lubelszczyzny. *Prace Państwowego Instytutu Geologicznego*, *196*, 193–254.

Over, D. J., Hauf, E., Wallace, J., Chiarello, J., Over, J.-S., Gilleaudeau, G. J., Song, Y., & Algeo, T. J. (2019). Conodont biostratigraphy and magnetic susceptibility of Upper Devonian Chattanooga Shale, eastern United States: Evidence for episodic deposition and disconformities. *Palaeogeography, Palaeoclimatology, Palaeoecology*, *524*, 137–149.

Ovnatanova, N. S. (1969). Novye verkhnedevonskie konodonty tsentral'nykh rayonov Russkoy Platformy i Timana. *Trudy Vsesoyuznyy Nauchno-Issledovatel'skiy Geologorazvedochnyy Neftyanoy Institut, 93*, 139–141.

Ovnatanova, N. S. (1976). New Late Devonian conodonts of the Russian Platform. *Paleontological Journal, 1976*(2), 210–219.

Ovnatanova, N. S., & Kononova, L. I. (2008). Frasnian conodonts from the eastern Russian Platform. *Paleontological Journal*, *42*(10), 997–1166.

Ovnatanova, N. S., & Kononova, L. I. (2020). Taxonomic problems of some zonal species of the genus *Palmatolepis* and the correlation of the Frasnian of the East European Platform with conodont zonations. *Acta Geologica Polonica*, *70*(1), 107–124.

Ovnatanova, N. S., & Kuz'min, A. V. (1991). Konodonty tipovykh razrezov Domanikovoy svity na yuzhnom Timane. *Izvestiya Akademii Nauk SSSR, Seriya Geologicheskaya*, *1991*(3), 37–50.

Ovnatanova, N. S., Kuz'min, A. V., & Menner, V. V. (1999). The succession of Frasnian conodont assemblages in the type sections of the southern Timan-Pechora Province (Russia). *Bollettino della Società paleontologica italiana*, *37*(2–3), 349–360.

Ovnatanova, N. S., Kononova, L. I., Kolesnik, L. S., & Gatovsky, Y. A. (2017). Upper Devonian conodonts of northeastern European Russia. *Paleontological Journal*, *51*(10), 973–1165.

Paeckelmann, W. (1928a). Der geologische Bau des Gebietes zwischen Bredelar, Marsberg und Adorf am Nordostrande des Rheinischen Schiefergebirges. *Jahrbuch der Königlich Preussischen geologischen Landesanstalt und Bergakademie zu Berlin*, *49*, 370–412.

Paeckelmann, W. (1928b). Blatt Barmen, Nr. 2721. *Erläuterungen zur Geologischen Karte von Preußen und benachbarten deutschen*

Ländern, Lieferung 263 (pp. 1–99 + pl. 1). Berlin: Preußische Geologische Landesanstalt.

Paeckelmann, W. (1936). *Erläuterungen zu Blatt Adorf Nr. 2660. – Geologische Karte von Preußen und benachbarten deutschen Ländern,* Lieferung 341 (pp. 1–66). Berlin: Preußische Geologische Landesanstalt.

Pas, D., Da Silva, A. C., Cornet, P., Bultynck, P., Königshof, P., & Boulvain, F. (2013). Sedimentary development of a continuous Middle Devonian to Mississippian section from the fore-reef fringe of the Brilon Reef Complex (Rheinisches Schiefergebirge, Germany). *Facies*, *59*(4), 969–990.

Pölsler, P. (1969). Conodonten aus dem Devon der Karnischen Alpen (Findenigkofel, Österreich). *Jahrbuch der geologischen Bundesanstalt*, *112*, 399–440.

Poty, E., & Chevalier, E. (2007). Late Frasnian phillipsastreid biostromes in Belgium. In J. J. Alvaro, M. Aretz, F. Boulvain, A. Munnecke, D. Vachard, & E. Vennin (Eds.), *Palaeozoic Reefs and Bioaccumulations: Climatic and Evolutionary Controls. Geological Society, London, Special Publications, 275*, 143–161.

Préat, A., El Hassani, A., & Mamet, B. (2008). Iron bacteria in Devonian carbonates (Tafilalt, Anti-Atlas, Morocco). *Facies, 54*, 107–120.

Prieto-Barajas, C. M., Valencia-Cantero, E., & Santoyo, G. (2018). Microbial mat ecosystems: Structure types, functional diversity, and biotechnological application. *Electronic Journal of Biotechnology, 21*, 48–56.

Puchkov, V. N. (1979). Rekomendacii po poiskam i obrabotke konodontov na poverkhnostjakh sloistosti beskarbonatnykh porod. In Papulov, G. N., & Puchkov, V. N. (Eds.), *Konodonty urala i ikh stratigraficheske znachenie. Trudy Instituta Geologii i Geokhimii*, *145*, 132–144).

Ree, C. (1953). Zur Stratigraphie und Tektonik des Roteisensteinvorkommens bei Adorf im östlichen Sauerland. *Notizblatt des hessischen Landesamtes für Bodenforschung*, *81*, 236–242.

Reissner, B. (1990). *Stratigraphische und fazielle Untersuchungen im Mittel- und Oberdevon des Aachener Raumes, Nordeifel, Rheinisches Schiefergebirge* (pp. 1–179). Unpublished Ph.D. Thesis, Technische Hochschule Aachen.

Sandberg, C. A., & Dreesen, R. (1984). Late Devonian icriodontid biofacies models and alternate shallow-water conodont zonation. *Geological Society of America, Special Paper*, *196*, 143–178.

Sandberg, C. A., & Ziegler, W. (1998). Comments on Proposed Frasnian and Famennian Subdivisions. *SDS Newsletter, 15*, 43–46.

Sandberg, C. A., Ziegler, W., & Bultynck, P. (1989a). New standard conodont zones and early *Ancyrodella* phylogeny across Middle-Upper Devonian boundary. *Courier Forschungsinstitut Senckenberg*, *110*, 195–230.

Sandberg, C. A., Poole, F. G., & Johnson, J. G. (1989b). Upper Devonian of Western United States. In N. J. McMillan, A. F. Embry, & D. J. Glass (Eds.), Devonian of the World. *Canadian Society of Petroleum Geologists, Memoir*, *14*(I), 183–220. [imprint 1988]

Sandberg, C. A., Ziegler, W., Dreesen, R., & Butler, J. L. (1992). Conodont Biochronology, Biofacies, Taxonomy, and Event Stratigraphy around Middle Frasnian (F2h), Frasnes, Belgium. *Courier Forschungsinstitut Senckenberg*, *150*, 1–87.

Sandberg, C. A., Morrow, J. R., & Ziegler, W. (2002). Late Devonian sea-level changes, catastrophic events, and mass extinctions. *Geological Society of America, Special Papers*, *356*, 473–488.

Sandberg, C. A., Morrow, J. R., Poole, F. G., & Ziegler, W. (2003). Middle Devonian to Early Carboniferous event stratigraphy of Devils Gate and Northern Antelope Range sections, Nevada, U.S.A. *Courier Forschungsinstitut Senckenberg, 242*, 187–207.

Sandberger, G., & Sandberger, F. (1850-1856). *Die Versteinerungen des Rheinischen Schichtensystems in Nassau* (I-XIV, 1–564, pls. 1–41). Wiesbaden: Kreidel und Niedner Verlagshandlung.

Sannemann, D. (1955). Beitrag zur Untergliederung des Oberdevons nach Conodonten. *Neues Jahrbuch für Geologie und Paläontologie, Abhandlungen*, *100*, 324–331.

Sanz-López, J. (2002). Devonian and Carboniferous pre-Stephanian rocks from the Pyrenees. *Cuadernos del Museo geominero*, *1*, 367-389.

Savage, N. M. (2013). *Late Devonian conodonts from northwestern Thailand* (pp. 1–48). Eugene: Bourland Printing.

Savage, N. M. (2019). Frasnian-Famennian transition in western Thailand: conodonts, biofacies, eustatic changes, extinction. *Journal of Paleontology*, *93*(3), 476–495.

Savage, N. M., & Yudina, A. B. (2001). Late Devonian (Frasnian) conodonts from the Timan-Pechora Basin, Russia. *Journal of the Czech Geological Society*, *46*(3-4), 287–298.

Schindler, E. (1990). Die Kellwasser-Krise (hohe Frasne-Stufe, Ober-Devon). *Göttinger Arbeiten zur Geologie und Paläontologie*, *46*, 1–115.

Schindler, E., Brocke, R., Becker, R. T., Buchholz, P., Jansen, U., Luppold, F.-W., Nesbor, H.-D., Salamon, M., Weller, H., & Weyer, D. (2018). The Devonian in the Stratigraphic Table of Germany 2016. *Zeitschrift der Deutschen Gesellschaft für Geowissenschaften, 168*(4), 447–463.

Schlüter, H. (1927). Das Mitteldevon im oberen Diemelgebiet und der geologische Bau des Martenberges bei Adorf. *Jahrbuch der Preußischen geologischen Landesanstalt, 48*, 175–214 + 1 pl.

Schülcke, I. (1995). Evolutive Prozesse bei *Palmatolepis* in der frühen Famenne-Stufe (Conodonta, Ober-Devon). *Göttinger Arbeiten zur Geologie und Paläontologie, 67*, 1–108.

Schwab, M., & Hüneke, H. (2008). Devon. In G. H. Bachmann, B.-C. Ehling, R. Eichner & M. Schwab (Eds.), *Geologie von Sachsen-Anhalt* (pp. 87–109). Stuttgart: Schweizerbart.

Sobolev, D. B., & Soboleva, M. A. (2018). Reflection of global events, Frasnian epoch, in the section of the western slope Polar Urals. *Lithosphere, 18*(3), 341–362.

Soboleva, M. A. (2017). Novye ridy zona *Palmatolepis* (konodonty) iz franskikh otloszhenii pripoliaznogo i poliaznogo Urala. *Trudy Instituta Geologii*, *130*, 40–50.

Soboleva, M. A., Sobolev, D. B., & Matveeva, N. A. (2018). Litologiâ i biostratigrafiâ razreza franskogo ârusa i pogranič nyh otloženij na r. Kos'û (Pripolârnyj Ural). *Stratigrafiâ i litologiâ v neftânoj geologii*, *43*, 1–30.

Söte, T., & Becker, R. T. (2021). Upper Frasnian ammonoids and gastropods from Boudouda (Benahmed region, Moroccan Meseta). In R. T. Becker, A. El Hassani & Z. S. Aboussalam (Eds.), *Devonian to Lower Carboniferous stratigraphy and facies of the South-Western Moroccan Meseta: Implications for paleogeography and structural interpretation. Frontiers in Science and Engineering, Earth, Water and Oceans, Environmental Sciences, 10*(2), 75–102.

Söte, T., Becker, R. T., Herd, K. J., & Bockwinkel, J. (2021). Upper Frasnian Tornoceratidae (Ammonoidea) from the Sand Formation (Bergisch Gladbach-Paffrath Syncline, Rhenish Massif). *Paläontologische Zeitschrift, 95*(2), 237–273.

Spalletta, C., & Perri, M. C. (1998). Stop 2.1B – Givetian and Frasnian conodonts from the Pramosio 327 section (Carnic Alps, Italy). *Gionale di Geologia, serie 3*, *60*, 190–197.

Stauffer, C. R. (1938). Conodonts of the Olentangy Shale. *Journal of Paleontology*, *12*, 411–443.

Stichling, S., Becker, R. T., Hartenfels, S., Aboussalam, Z. S., & May, A. (in press). Drowning, extinction, and subsequent facies development of the Devonian Hönne Valley Reef Complex (northern Rhenish Massif, Germany). *Palaeobiodiversity and Palaeoenvironments 102*(3), https://doi.org/10.1007/s12549-022-00539-x. [this issue]

Streel, M., Bless, M., Bouckaert, J., Coen, M., Coen-Aubert, M., Conil, R., Dreesen, R., Dusar, M., Mouravieff, N., & Thorez, J. (1974). Chief micropaleontological limits in the Belgian Upper Devonian. In J. Bouckaert, & M. Streel (Eds.), *Namur 1974, International*

Symposium on Belgian micropaleontological limits, from Emsian to Visean, September 1st to 10th. *Geological Survey of Belgium Publications, 19*, 1–30.

Stritzke, R. (1990). Die Karbonatsedimentation im Briloner Vorriffbereich. *Geologisches Jahrbuch*, *D95*, 253–315.

Sunkel, G. (1990). Devonischer submariner Vulkanismus im Ostsauerland (Rheinisches Schiefergebirge): Vulkanaufbau, Magmenzusammensetzung und Alteration. *Bochumer Geologische und Geotechnische Arbeiten*, *34*, 1–250.

Szulczewski, M. (1971). Upper Devonian conodonts, stratigraphy and facial development in the Holy Cross Mts. *Acta Geologica Polonica*, *21*(1), 1–130.

Ta, H. P., Königshof, P., Ellwood, B. B., Nguyen, T. C., Luu, P. L. T., Doan, D. H., & Munkhjargal, A. (2021). Facies, magnetic susceptibility and timing of the Late Devonian Frasnian/Famennian boundary interval (Xom Nha Formation, Central Vietnam). *Palaeobiodiversity and Palaeoenvironments, 102*(1), 129–146.

Tagarieva, R. C. (2013). Conodont biodiversity of the Frasnian-Famennian boundary interval (Upper Devonian) in the Southern Urals. *Bulletin of Geosciences*, *88*(2), 297–314.

Teeke, M. (1953). Das Eisenerzvorkommen der Grube Christiane bei Adorf im Vergleich zu den Eisenerzen im Lahn-Dillgebiet. *Zeitschrift der deutschen geologischen Gesellschaft, 104*, 287–288.

Tsyganko, V. S. (2011). *Devon zapadnogo sklona severa Urali i Pai-Khoya (stratigrafiya, printsipy raschlerneniya, korrelyatsiya)*. Ekaterinburg: Ural Otdel. Rossja Academia Nauk.

Ulrich, E. O., & Bassler, R. S. (1926). A classification of the toothlike fossils, conodonts, with descriptions of American Devonian and Mississippian species. *United States National Museum Proceedings*, *68*(12), 1–63.

Wang, C.-Y. (1994). Application of the Frasnian Standard Conodont Zonation in South China. *Courier Forschungsinstitut Senckenberg*, *168*, 83–129.

Wang, C.-Y. (2016). *Conodont Biostratigraphy in China* (pp. 1–379). Beijing: Zehjiang University Press.

Wang, C.-Y., & Ziegler, W. (1983). Devonian conodont biostratigraphy of Guangxi, South China, and its correlation with Europe. *Geologica et Palaeontologica, 17*, 75–107

Wedekind, R. (1913). Die Goniatitenkalke des unteren Oberdevons von Martenberg bei Adorf. *Sitzungsberichte der Gesellschaft Naturforschender Freunde zu Berlin*: 23–77.

Wedekind, R. (1918). Die Genera der Palaeoammonoidea (Goniatiten). *Palaeontographica*, *62*, 85–184, pls. 14-22.

Wendt, J. (2021). Middle and Late Devonian sea-level changes and synsedimentary tectonics in the eastern Anti-Atlas (Morocco). *Journal of African Earth Sciences, 182*(104247), 16 pp.

Wendt, J., & Belka, Z. (1991). Age and depositional environment of Upper Devonian (early Frasnian to early Famennian) black shales and limestones (Kellwasser facies) in the eastern Anti-Atlas, Morocco. *Facies*, *25*, 51–89.

Wilson, J. L. (1975). *Carbonate facies in geologic history* (pp. 1–492). Berlin, Heidelberg: Springer Science & Business Media.

Winter, J. (2015). Vulkanismus und Kellwasser-Krise – Zirkon-Tephrostratigraphie, Identifizierung und Herkunft distaler Fallout-Aschelagen (Oberdevon, Synklinorium von Dinant, Rheinisches Schiefergebirge, Harz). *Zeitschrift der Deutschen Gesellschaft für Geowissenschaften, 166*(3), 227–251.

Yolkin, E. A., Bakharev, N. K., Izokh, N. G., Gratsianova, R. T., Kipriyanova, T. P., & Obut, O. T. (2005). *Devonian sequences of Salair, Rudny & Gorny Altai, Field Excursion Guidebook, International Conference "Devonian terrestrial and marine Environments from Continent to Shelf" (IGCP 499 Project/SDS joint field meeting), Novosibirsk, Russia, July 25 – August 9, 2005 (pp. 1–79)*. Novosibirsk: Publishing House of SB RAS, "Geo" Branch.

Youngquist, W. L. (1945). Upper Devonian conodonts from the Independence shale (?) of Iowa. *Journal of Paleontology*, *19*, 355–367.

Youngquist, W. L. (1947). A new Upper Devonian conodont fauna from Iowa. *Journal of Paleontology*, *21*, 95–112.

Zhang, N., Xia, W.-C., Dong, Y.-X., & Shang, H.-J. (2008). Conodonts and radiolarians from pelagic cherts of the Frasnian–Famennian boundary interval at Bancheng, Guangxi, China: Global recognition of the upper Kellwasser event. *Marine Micropaleontology*, *67*(1–2), 180–190.

Zhang, X., Over, D. J., Ma, K., & Gong, Y. (2019). Upper Devonian conodont zonation, sea-level changes and bio-events in offshore carbonate facies Lali section, South China. *Palaeogeography, Palaeoclimatology, Palaeoecology*, *531*, 109219.

Zhou, K., & Pratt, B. R. (2019). Composition and origin of stromatactis-bearing mud-mounds (Upper Devonian, Frasnian), southern Rocky Mountains, western Canada. *Sedimentology, 66*(6), 2455–2489.

Ziegler, W. (1958). Conodontenfeinstratigraphische Untersuchungen an der Grenze Mitteldevon/Oberdevon und in der Adorf-Stufe. *Notizblatt des Hessischen Landesamtes für Bodenforschung*, *87*, 7–77.

Ziegler, W. (1962). Taxionomie und Phylogenie Oberdevonischer Conodonten und ihre stratigraphische Bedeutung. *Abhandlungen des Hessischen Landesamtes für Bodenforschung*, *38*, 1–166.

Ziegler, W. (1971). *Symposium on Conodont Taxonomy, A field trip guidebook, Post-symposium Excursion, Sept. 15-18, 1971 to Rhenish Slate Mountains and Harz Mountains* (pp. 1–47). Marburg: Phillips Universität.

Ziegler, W. (1975). *Catalogue of Conodonts – Volume 2* (pp. I–VI, 1–403). Stuttgart: E. Schweizerbart'sche Verlagsbuchhandlung.

Ziegler, W., & Sandberg, C. A. (1984). *Palmatolepis*-based revision of upper part of standard Late Devonian conodont zonation. *Geological Society of America Special Paper*, *196*, 179–194.

Ziegler, W., & Sandberg, C. A. (1990). The Late Devonian Standard Conodont Zonation. *Courier Forschungsinstitut Senckenberg*, *121*, 1–115.

Ziegler, W., & Sandberg, C. A. (1997). Proposal of boundaries for a late Frasnian Substage and for subdivision of the Famennian Stage into three Substages. *SDS Newsletter*, *14*, 11–12.

Ziegler, W., & Sandberg, C. A. (2000). Utility of Palmatolepids and Icriodontids in recognising Upper Devonian Series, Stage, and possible Substage boundaries. *Courier Forschungsinstitut Senckenberg*, *225*, 335–347.